

12 DEC 2000

**EFFECTS OF STEVIOSIDE AND STEVIOL ON  
P-AMINOHIPPURATE TRANSPORT BY ISOLATED  
PERFUSED RABBIT RENAL PROXIMAL TUBULE**

**PROMSUK JUTABHA**  
/

**A THESIS SUBMITTED IN PARTIAL FULFILLMENT  
OF THE REQUIREMENTS FOR  
THE DEGREE OF DOCTOR OF PHILOSOPHY (PHYSIOLOGY)  
FACULTY OF GRADUATE STUDIES  
MAHIDOL UNIVERSITY**

**2000**

**ISBN 974-664-734-2**

**COPYRIGHT OF MAHIDOL UNIVERSITY**

TH  
P9652  
2000 46211

Thesis

entitled

**EFFECTS OF STEVIOSIDE AND STEVIOL ON  
P-AMINOHIPPURATE TRANSPORT BY ISOLATED  
PERFUSED RABBIT RENAL PROXIMAL TUBULE**

*Promsuk Jutabha*  
.....  
Miss Promsuk Jutabha  
Candidate

*Varanuj Chatsudthipong*  
.....  
Assoc.Prof.Varanuj Chatsudthipong,  
Ph.D.  
Major-advisor

*Chaivat Toskulkao*  
.....  
Prof.Chaivat Toskulkao, D.V.M., Ph.D.  
Co-advisor

*Samaisukh Sophasan*  
.....  
Assoc.Prof.Samaisukh Sophasan, Ph.D.  
Co-advisor

*Chumpol Pholpramool*  
.....  
Assoc.Prof.Chumpol Pholpramool, Ph.D.  
Co-advisor

*Liangchai Limlomwongse*  
.....  
Prof.Liangchai Limlomwongse, Ph.D.  
Dean  
Faculty of Graduate Studies

*Pawinee Piyachaturawat*  
.....  
Assoc.Prof.Pawinee Piyachaturawat,  
Ph.D.  
Chairman  
Doctor of Philosophy Programme in  
Physiology  
Faculty of Science

Thesis

entitled

**EFFECTS OF STEVIOSIDE AND STEVIOL ON  
P-AMINOHIPPURATE TRANSPORT BY ISOLATED  
PERFUSED RABBIT RENAL PROXIMAL TUBULE**

was submitted to the Faculty of Graduate Studies, Mahidol University  
for the degree of Doctor of Philosophy (Physiology)

on

September 18, 2000

*Promsuk Jutabha*

.....  
Miss Promsuk Jutabha  
Candidate

*Varanuj Chatsudthipong*

.....  
Assoc.Prof. Varanuj Chatsudthipong,  
Ph.D.  
Chairman

*Samaisukh Sophasan*

.....  
Assoc.Prof. Samaisukh Sophasan, Ph.D.  
Member

*Chaivat Toskulkao*

.....  
Prof. Chaivat Toskulkao, D.V.M., Ph.D.  
Member

*Narongsak Chaiyabutr*

.....  
Prof. Narongsak Chaiyabutr, D.V.M.,  
Ph.D.  
Member

*Chumpol Pholpramool*

.....  
Assoc. Prof. Chumpol Pholpramool, Ph.D.  
Member

*Liangchai Limlomwongse*

.....  
Prof. Liangchai Limlomwongse, Ph.D.  
Dean  
Faculty of Graduate Studies  
Mahidol University

*Amaret Bhumiratana*

.....  
Prof. Amaret Bhumiratana, Ph.D.  
Dean  
Faculty of Science  
Mahidol University

## ACKNOWLEDGEMENTS

I would like to express my thanks and deep appreciation to my principal advisor, Assoc. Prof. Dr. Varanuj Chatsudthipong, for her considerable guidance, supervision, valuable advice and encouragement throughout my study to bring this work to the final goal. Without her sympathy, this work would never have been completed. She was never lacking in kindness and support. I could not find appropriate words to express her precious advice. I also wish to express my sincere gratitude and appreciation to Prof. William H. Dantzler, Chairman of Dept. of Physiology, College of Medicine, University of Arizona, who gave me an opportunity for training in the *in vitro* microperfusion technique and valuable suggestions during the work.

I also wish to express my thanks to my co-advisors and the examination committee, Dr. Chaivat Toskulkao, Dr. Chumpol Pholpramool, Dr. Samaisukh Sophasan, as well as an external examiner, Dr. Narongsak Chaiyabutr, for their valuable criticism and correction of this thesis. I also wish to extend my appreciation to Dr. Surawat Jariyawat who taught me the isolation of proximal tubular segments under the microscope, Mr. Sirichai Kositarat for his guidance regarding the HPLC instrument, and Dr. Pawinee Piyachaturawat for her valuable advice, sympathy and sincere encouragement. I also thank Mrs. Umaporn Udomsubpayakul at the Statistical Unit, Research Center, Ramathibodi Hospital, for her guidance in statistical analysis, as well as Miss Chonlada Sapeeya for her excellent typing of this manuscript.

I am particularly indebted to the Dept. of Physiology, Fac. of Science, Mahidol University for access to all laboratory facilities, and the Institutional Strengthening Program of the Faculty of Science, Mahidol University and to the National Science and Technology Development Agency of Thailand (NSTDA) for the scholarship which enabled me to undertake this study.

Finally, I would like to express my deep appreciation to my beloved parents and my sisters who encouraged me to carry out this study. They gave me understanding and kindness throughout the period of study and all the time of my life.

Promsuk Jutabha

3836180 SCPS/D : MAJOR : PHYSIOLOGY ; Ph.D. (PHYSIOLOGY)

KEY WORDS : STEVIOSIDE / STEVIOL / PAH /  $\text{Na}^+\text{-K}^+$  ATPase / RENAL PROXIMAL TUBULE / *IN VITRO* MICROPERFUSION / CELL ATP

PROMSUK JUTABHA : EFFECTS OF STEVIOSIDE AND STEVIOL ON P-AMINOHIPPURATE TRANSPORT BY ISOLATED PERFUSED RABBIT RENAL PROXIMAL TUBULE. THESIS ADVISORS: VARANUJ CHATSUDTHIPONG, Ph.D., CHAIVAT TOSKULKAO, D.V.M., Ph.D., SAMAISUKH SOPHASAN Ph.D., CHUMPOL PHOLPRAMOOL, Ph.D. 199 p. ISBN 974-664-734-2.

Stevioside is a non-caloric natural sweetener which has been used widely as a sugar substitute in many countries. It is a major component isolated from the *Stevia rebaudiana* leaves. There are several reports suggesting stevioside and its major metabolite, steviol, to have some influences on renal function, but little is known about their effects on renal tubular function. Therefore, the present study was designed to explore the direct effect of stevioside and steviol on transepithelial transport of p-aminohippurate ( $J_{\text{PAH}}$ ) in the isolated  $S_2$  segment of rabbit renal proximal tubules by using an *in vitro* microperfusion technique. Addition of stevioside at a concentration of 0.45 mM to either the tubular lumen or bathing medium or both at the same time had no effect on  $J_{\text{PAH}}$ . Similarly, a concentration of 0.7 mM when present in the lumen had no effect on  $J_{\text{PAH}}$ . However, this concentration in the bathing medium inhibited PAH transport significantly by approximately 25-30%. The inhibitory effect of stevioside was abolished after it was removed from the bath. To further examine this phenomenon, 0.7 mM stevioside was added to both lumen and bathing medium at the same time; there was no added inhibitory effect from that observed with bath addition alone. Addition of steviol (0.01-0.25 mM) to the bathing medium significantly depressed  $J_{\text{PAH}}$  (50-90%). The inhibitory effect was of dose-dependent manner and reached maximum at a concentration of 0.05 mM. Steviol at a low concentration (0.01 mM) permanently reduced  $J_{\text{PAH}}$ , but had no effect when present in the lumen. However, increasing the concentration of steviol in the lumen to 0.05 mM inhibited  $J_{\text{PAH}}$  by about 70%. The reduction of  $J_{\text{PAH}}$  after 0.7 mM stevioside or 0.01 and 0.05 mM steviol treatment occurred without the alterations of  $\text{Na}^+\text{-K}^+$  ATPase activity and cell ATP content. The kinetic studies indicate that both stevioside and steviol inhibit transepithelial transport of PAH by interfering with the basolateral entry step, the rate-limiting step for transepithelial transport at the PAH transporter. The results from the present study suggest that stevioside does not harm the renal tubule, whereas steviol does.

3836180 SCPS/D : สาขาวิชา: สรีรวิทยา; ปร.ด. (สรีรวิทยา)

พร้อมสุข ชูตาภา: ผลของสารสตีวิโอไซด์และสตีวียอลต่อการขนส่งพาราอะมิโนฮิปปูเรตโดยหลอดไตส่วนต้นของกระต่าย (EFFECTS OF STEVIOSIDE AND STEVIOL ON P-AMINOHIPPURATE TRANSPORT BY ISOLATED PERFUSED RABBIT RENAL PROXIMAL TUBULE) คณะกรรมการควบคุมวิทยานิพนธ์: วรนุช ฉัตรสุทธิพงษ์, Ph.D., ชัยวัฒน์ ต่อสกุลแก้ว, สพ.บ., ปร.ด., สมัยศึก โสภาสรรค์, Ph.D., ชุมพล ผลประมูล, Ph.D., 199 หน้า ISBN 974-644-734-2

สตีวิโอไซด์เป็นสารหวานที่ปราศจากพลังงานสกัดได้จากใบของต้นหญ้าหวาน และได้นำมาใช้ทดแทนน้ำตาลกันอย่างแพร่หลายในหลายประเทศ มีรายงานระบุว่า สตีวิโอไซด์และสตีวียอลซึ่งเป็นสารอนุพันธ์ของสตีวิโอไซด์มีผลเปลี่ยนแปลงการทำงานของไต แต่การรายงานเกี่ยวกับผลของสารดังกล่าวที่มีต่อการทำงานของหลอดไตยังมีอยู่น้อยมาก ดังนั้นในการวิจัยครั้งนี้จึงมีวัตถุประสงค์เพื่อตรวจสอบผลของสตีวิโอไซด์และสตีวียอลต่อการขนส่ง PAH โดยหลอดไตส่วนต้นโดยใช้เทคนิค *in vitro* microperfusion ในการศึกษาดังกล่าว พบว่าสตีวิโอไซด์ความเข้มข้น 0.45 มิลลิโมลาร์ เมื่อให้เข้าไปในสารละลายที่ไหลผ่านหลอดไตหรือสารละลายที่อยู่รอบนอกของหลอดไตไม่มีผลเปลี่ยนแปลงการขนส่ง PAH ผ่านเซลล์หลอดไต สตีวิโอไซด์ความเข้มข้น 0.7 มิลลิโมลาร์มีผลลดการขนส่ง PAH อย่างมีนัยสำคัญทางสถิติประมาณ 25-30 เปอร์เซ็นต์ เมื่อให้เข้าไปในสารละลายที่อยู่รอบนอกของหลอดไต และผลดังกล่าวสามารถฟื้นคืนได้เมื่อเปลี่ยนสารละลายรอบนอกหลอดไตใหม่โดยไม่มีสตีวิโอไซด์ปะปนอยู่ นอกจากนี้การให้สตีวิโอไซด์ไปพร้อมๆกันในสารละลายที่ไหลผ่านหลอดไตและสารละลายที่อยู่รอบนอกไม่พบการเปลี่ยนแปลงที่เพิ่มขึ้นอย่างมีนัยสำคัญทางสถิติ เมื่อเทียบกับการให้สารดังกล่าวในสารละลายรอบนอกหลอดไตเพียงอย่างเดียว ส่วนสตีวียอลที่มีความเข้มข้นในช่วง 0.01-0.25 มิลลิโมลาร์เมื่อใส่เข้าไปในสารละลายรอบนอกหลอดไต มีผลลดการขนส่ง PAH อย่างมีนัยสำคัญทางสถิติประมาณ 50-90 เปอร์เซ็นต์ การยับยั้งดังกล่าวเพิ่มขึ้นตามความเข้มข้นของสตีวียอลที่ใช้และพบว่าการขนส่ง PAH ลดลงมากที่สุดเมื่อเพิ่มความเข้มข้นของสตีวียอลเป็น 0.05 มิลลิโมลาร์ จากการตรวจสอบฤทธิ์ของสารสตีวียอลที่ความเข้มข้น 0.01 มิลลิโมลาร์ พบว่าผลการยับยั้งการขนส่ง PAH ไม่สามารถฟื้นคืนสู่ปกติเมื่อกำจัดสตีวียอลออกจากสารละลายรอบนอกหลอดไต ในทางตรงข้ามเมื่อให้สตีวียอลความเข้มข้น 0.01 มิลลิโมลาร์เข้าไปในสารละลายที่ไหลผ่านหลอดไต ไม่มีผลยับยั้งการขนส่ง PAH ผ่านเซลล์ แต่เมื่อเพิ่มความเข้มข้นของสตีวียอลเป็น 0.05 มิลลิโมลาร์มีผลยับยั้งการขนส่ง PAH ประมาณ 70 เปอร์เซ็นต์ นอกจากนี้ยังพบว่าสารละลายสตีวิโอไซด์ขนาด 0.7 มิลลิโมลาร์และสารละลายสตีวียอลขนาด 0.01 และ 0.05 มิลลิโมลาร์ซึ่งมีผลยับยั้งการขนส่ง PAH ผ่านเซลล์หลอดไตส่วนต้นนั้น ไม่เปลี่ยนแปลงการทำงานของเอนไซม์  $\text{Na}^+ - \text{K}^+$  ATPase และปริมาณ ATP ภายในเซลล์ นอกจากนี้ยังพบว่าทั้งสตีวิโอไซด์และสตีวียอลยับยั้งการขนส่ง PAH ผ่านหลอดไตส่วนต้นโดยการออกฤทธิ์ที่กระบวนการขนส่ง PAH เข้าเซลล์ทางด้าน basolateral โดยเฉพาะอย่างยิ่งออกฤทธิ์โดยตรงต่อโปรตีนขนส่ง PAH ซึ่งมีบทบาทสำคัญต่อกระบวนการขนส่ง PAH ผ่านเซลล์หลอดไต การศึกษานี้แสดงให้เห็นว่าสตีวิโอไซด์ไม่มีอันตรายต่อหลอดไตแต่สตีวียอลมีพิษต่อการทำงานของหลอดไต

## CONTENTS

	<b>Page</b>
<b>ACKNOWLEDGEMENTS</b>	<b>iii</b>
<b>ABSTRACT (ENGLISH)</b>	<b>iv</b>
<b>ABSTRACT (THAI)</b>	<b>v</b>
<b>LIST OF FIGURES</b>	<b>viii</b>
<b>LIST OF ABBREVIATIONS</b>	<b>xii</b>
<b>CHAPTER</b>	
<b>I INTRODUCTION</b>	<b>1</b>
<b>II LITERATURE REVIEW</b>	<b>4</b>
<b>I. THE KIDNEY AND THE EXCRETION OF             XENOBIOTICS</b>	<b>4</b>
<b>II. THE RENAL PROXIMAL TUBULE AND THE P-             AMINOHIPPURATE TRANSPORT SYSTEM</b>	<b>6</b>
<b>III. SODIUM AND POTASSIUM-DEPENDENT             ADENOSINE TRIPHOSPHATASE (Na<sup>+</sup>-K<sup>+</sup>             ATPase)</b>	<b>23</b>
<b>IV. STEVIA PLANT, STEVIOSIDE AND STEVIOL</b>	<b>31</b>
<b>III MATERIALS AND METHODS</b>	<b>66</b>
<b>IV RESULTS</b>	<b>89</b>
<b>V DISCUSSION</b>	<b>119</b>
<b>VI CONCLUSION</b>	<b>141</b>
<b>REFERENCES</b>	<b>143</b>

## CONTENTS (CONT.)

	<b>Page</b>
<b>APPENDIX</b>	<b>178</b>
<b>BIOGRAPHY</b>	<b>198</b>



## LIST OF FIGURES

Figure	Page
1. The model for organic anion (PAH) secretion by proximal renal tubules.	23
2. The chemical structures of stevioside and steviol.	34
3. Diagram of substances from stevioside hydrolysis by $H^+$ or $OH^-$ or enzyme.	35
4. The perfusion of an isolated tubule.	70
5. Apparatus for perfusing an isolated tubule fragments.	71
6. Timing diagram of changing perfusate and bathing medium, as well as the time for sample collections.	78
7. Control transepithelial secretory transport of p-aminohippurate (PAH), $J_{PAH}$ in isolated proximal tubules perfused and bathed with a bicarbonate-buffered medium.	90
8. The effect of 0.45 mM stevioside (a) in perfusate, (b) in a bath, and (c) in both a bath and perfusate on $J_{PAH}$ in tubules perfused and bathed with a bicarbonate-buffered medium.	92
9. The effect of 0.1 mM probenecid addition to the bathing medium at the end of the recovery period of 0.45 mM stevioside treatment in (a) perfusate, (b) bath, and (c) both bath and perfusate on $J_{PAH}$ .	94
10. The effects of various concentrations (0.45, 0.5, 0.6 and 0.7 mM) of stevioside in a bath on $J_{PAH}$ of isolated proximal tubules after incubation periods of 10 and 20 minutes.	95

**LIST OF FIGURES (CONT.)**

	<b>Page</b>
11. The effect of 0.7 mM stevioside (a) in perfusate, (b) in a bath, and (c) in both a bath and perfusate on $J_{PAH}$ in the tubules perfused and bathed with a bicarbonate-buffered medium.	97
12. Control transepithelial secretory transport of p-aminohippurate (PAH), $J_{PAH}$ in isolated proximal tubules perfused with a bicarbonate-buffered medium and bathed with a medium containing 0.125% (v/v) dimethylsulfoxide (DMSO).	99
13. The effects of various concentrations (0.005, 0.010, 0.015, 0.025, 0.05, 0.10 and 0.25 mM) of steviol in a bath on $J_{PAH}$ of isolated proximal tubules after incubation periods of 10 and 30 minutes.	100
14. The effect of 0.01 mM steviol (a) in perfusate, (b) in a bath, and (c) in both a bath and perfusate on $J_{PAH}$ in tubules perfused and bathed with a bicarbonate-buffered medium containing 0.005% (v/v) DMSO.	102
15. The effect of 0.05 mM steviol in the perfusate on $J_{PAH}$ in tubules perfused and bathed with a bicarbonate-buffered medium containing 0.025% (v/v) DMSO.	104
16. The effects of 0.7 mM stevioside and various concentrations (0.01, 0.05 and 2.0 mM) of steviol on $Na^+K^+$ ATPase activity in rabbit renal proximal tubule suspension after a 20-minute treatment.	106

**LIST OF FIGURES (CONT.)**

	<b>Page</b>
17. The effects of 0.7 mM stevioside and various concentrations (0.01, 0.05 and 2.0 mM) of steviol on cell ATP content extracted from rabbit renal proximal tubule suspensions after a 20-minute treatment.	108
18. The effects of 0.7 mM stevioside and various concentrations (0.01, 0.05 and 2.0 mM) of steviol on cell ATP content extracted from rabbit renal proximal tubule suspensions after a 20-minute treatment.	109
19. The effects of 0.7 mM stevioside and various concentrations (0.01, 0.05 and 2.0 mM) of steviol on cell AMP content extracted from rabbit renal proximal tubule suspensions after a 20-minute treatment.	110
20. The effects of 0.7 mM stevioside and various concentrations (0.01, 0.05 and 2.0 mM) of steviol on cell hypoxanthine content extracted from rabbit renal proximal tubule suspensions after a 20-minute treatment.	111
21. The AMP content in the incubation medium of renal proximal tubule suspensions treated with 0.7 mM stevioside and various concentrations (0.01, 0.05 and 2.0 mM) of steviol for 20 minutes.	112
22. The hypoxanthine content in the incubation medium of renal proximal tubule suspensions treated with 0.7 mM stevioside and various concentrations (0.01, 0.05 and 2.0 mM) of steviol for 20 minutes.	113
23. The time course of PAH uptake by rabbit renal proximal tubule suspensions.	115

**LIST OF FIGURES (CONT.)**

	<b>Page</b>
24. The Lineweaver-Burk plot of PAH uptake by rabbit renal proximal tubule suspensions with increasing concentrations of PAH in the medium.	115
25. The Lineweaver-Burk plot of PAH uptake by rabbit renal proximal tubule suspensions with increasing concentrations of PAH in the medium in the absence (solid diamonds) and presence (solid squares) of stevioside (0.7 mM).	117
26. The Lineweaver-Burk plot of PAH uptake by rabbit renal proximal tubule suspensions with increasing concentrations of PAH in the medium in the absence (solid diamonds) and presence (solid squares) of steviol (0.01 mM).	118
27. A schematic picture illustrating the possible mechanisms by which stevioside and steviol depress the transepithelial transport of p-aminohippurate (PAH) in rabbit renal proximal tubules.	140
28. Illustrations of a holding pipette (a); a perfusion pipette (b); and a collecting pipette (c).	193
29. An illustration of the system for perfusing the tubular segment using the <i>in vitro</i> microperfusion technique .	196

## LIST OF ABBREVIATIONS

%	percentage
[X]	concentration of substance X
<sup>131</sup> I	iodine-131
<sup>14</sup> C	carbon-14
<sup>3</sup> H	tritium
ADP	adenosine diphosphate
AMP	adenosine monophosphate
Å	Angstrom
ATP	adenosine triphosphate
ATPase	adenosine triphosphatase
BW	body weight
Ca <sup>++</sup>	calcium ion
CaCl <sub>2</sub>	calcium chloride
cm	centimeter
DMSO	dimethyl sulfoxide
fmol	femtomole
g	gram
GFR	glomerular filtration rate
HEPES	4-(2-Hydroxyethyl)-1-piperazine-ethanesulfonic acid
HPLC	high performance liquid chromatography

**LIST OF ABBREVIATIONS (CONT.)**

hr	hour
HX	Hypoxanthine
I.D.	inner diameter
$J_{\max}$	Michaelis-Menten maximum transport rate
$J_{\text{PAH}}$	transepithelial transport of PAH
$K^+$	potassium ion
$K_2\text{CO}_3$	potassium carbonate
kg	kilogram
$K_i$	inhibition constant
$K_m$	Michaelis-Menten constant
KOH	potassium hydroxide
L	liter
M	molar
mg	milligram
mg/ml	milligram per milliliter
min	minute
ml	milliliter
mM	millimolar
MRP	multidrug resistance protein
MW	molecular weight
$\text{Na}^+$	sodium ion

**LIST OF ABBREVIATIONS (CONT.)**

Na <sup>+</sup> -K <sup>+</sup> ATPase	Sodium and potassium-dependent adenosine triphosphatase
NaOH	sodium hydroxide
NH <sub>4</sub> H <sub>2</sub> PO <sub>4</sub>	ammonium dihydrogenphosphate
nmol	nanomole
O.D.	outer diameter
OAT	organic anion transporter
oatp	organic anion transporter polypeptide
°C	degree Celsius
OD	optical density
PAH	para-aminohippurate
P <sub>i</sub>	inorganic phosphate
pmol	picomole
POPOP	1,4-bis[2,5-phenyloxazole] benzene
PPO	2,5-diphenyloxazole
RBF	renal blood flow
RPF	renal plasma flow
RP-HPLC	reversed phase-high performance liquid chromatography
rpm	revolution per minute
SE	standard error
sec	second

**LIST OF ABBREVIATIONS (CONT.)**

SITS	4-acetamido-4'-isothiocyano-stilbene-2,2' disulfonic acid
SVL	steviol
SVS	stevioside
TLC	thin layer chromatography
v/v	volume by volume
vs	versus
w/v	weight by volume
w/w	weight by weight
x g	relative centrifugal force
$\alpha$	alpha
$\alpha$ -KG	alpha-ketoglutarate
$\beta$	beta
$\mu$ g	microgram
$\mu$ l	microliter
$\mu$ m	micrometer
$\mu$ M	micromolar
$\mu$ mol	micromole

## CHAPTER I

### INTRODUCITON

Stevioside is the major sweet component isolated from leaves of the plant *Stevia rebaudiana*. It is approximately 3-8% (w/w) of the dried leaf. Due to its sweetness (about 300 times sweeter than sucrose (1, 2)) and its non-caloric value, it has become popular as a sugar substitute in a variety of foods and beverages in Japan, Brazil, South Korea and Paraguay (3, 4). In addition to its use as a sweetener, several researchers have shown stevioside to have therapeutic value as a contraceptive (5), and to have cardiovascular (6-11) and metabolic effects (12), as well as an effect on glucose absorption (13-16). An influence on renal function has also been suggested for it.

Giving stevioside intravenously or orally to rats was found to have effects on systemic as well as renal systems (7-10, 17-19). The changes in renal function, renal blood flow (RBF), natriuresis and diuresis, observed after stevioside treatment may be due to either its direct effect on renal function or as a consequence of systemic changes. Thongouppakarn (20) also found that the injection of stevioside directly into the left renal artery of rat also caused diuresis and natriuresis without any significant changes in glomerular filtration rate (GFR) and renal plasma flow (RPF). These changes in renal function were mainly due to a decrease in proximal tubular fluid and sodium reabsorption as measured by lithium clearance and fractional urinary sodium excretion. Subsequently, the possible mechanism of stevioside that affected renal

proximal tubular function was examined by Limpanichakul (21) in the renal proximal tubule suspensions of rabbit. Stevioside was found to depress  $\text{Na}^+\text{-K}^+$  ATPase activity and [ $^{14}\text{C}$ ]-p-aminohippurate ( $^{14}\text{C}$ -PAH) accumulation in renal proximal tubule suspension. In toxicological studies, a dose of 1.5 g/kg BW of stevioside given subcutaneously and 4.1 g/kg BW of stevioside given via intragastric tube were found to cause nephrotoxicity in the rat and the hamster, respectively (22-24), as indicated by an increase in plasma biochemical parameters such as blood urea nitrogen (BUN) and plasma creatinine levels. Histopathological changes were found mainly in the proximal tubules, suggesting that a major target site of stevioside action might be the renal proximal tubule.

Steviol is the aglycone part of stevioside and many natural glycosides. It is also the major metabolite of stevioside by bacterial enzymatic degradation *in vitro* (25, 26). The intravenous injection of  $^{131}\text{I}$ -stevioside into rat increased the plasma level of radioactive  $^{131}\text{I}$ , and steviol was the major metabolite found in bile (27) detected by HPLC analysis. The intravenous infusion of steviol into rats has also affected kidney function, as it induced diuresis and natriuresis, while no significant change in GFR and RPF was observed (28). It is possible that the alteration in renal function observed after the intravenous infusion of stevioside may be due to the degradation of stevioside to steviol, resulting in renal functional changes. However, little is known about the effects of stevioside and steviol on proximal tubular function.

The renal proximal tubules serve an important function in the elimination of xenobiotics via the organic anion and cation secretory systems, and is known to be capable of eliminating a wide range of compounds (29). Due to their functional

importance, interfering with or inhibiting these secretory transport systems would lead to an accumulation of potentially toxic compounds in the body. It has been known that stevioside and steviol inhibit the accumulation of the prototypical organic anion, p-aminohippurate (PAH), in rat renal cortical slices (23). Thus, I hypothesized that stevioside and its metabolite, steviol, would affect the transepithelial transport of PAH in isolated S<sub>2</sub> segments of the rabbit renal proximal tubule as well. The present study was carried out to test this hypothesis using an *in vitro* microperfusion technique. This *in vitro* procedure has advantages for examining the direct effect of both substances (stevioside and steviol) on renal secretory function in well-defined conditions where any systemic effect was eliminated.

The objectives of this study were as follows:

1. To study whether stevioside and its metabolite, steviol, have a direct effect on proximal tubular function, using  $J_{PAH}$  as an indicator.
2. To study the possible mechanisms by which stevioside and steviol affect proximal tubular function.

## **CHAPTER II**

### **LITERATURE REVIEW**

#### **I. THE KIDNEY AND THE EXCRETION OF XENOBIOTICS**

In the body, the major organs that participate in the metabolism and excretion of xenobiotics (including both toxic substances and drugs) are the liver and kidney. Normally, the xenobiotics that enter the body can distribute to many tissues or organs. Some xenobiotics easily cross the cell membrane and distribute throughout the body, but some of them have transportation limits, so they tend to accumulate in certain tissues depending on protein binding, availability of active transport systems or their solubility. The liver and kidney are capable of binding numerous substances, as well as transforming and removing toxic substances out of the body.

The kidney has important physiological functions in the maintenance of water and electrolyte balance, and in the secretion and excretion of waste products from metabolisms. It also plays a major role in the excretion of drugs, hormones and xenobiotics (30). Several chemical substances are eliminated from the body via the kidney more than by other routes (31). The blood flow to the kidney is very high, being about 20-25% of cardiac output. The filtration of the plasma by the renal glomeruli is 5% of cardiac output. Compounds, including xenobiotics, with a molecular weight less than 60,000 are filtered freely at the glomeruli (32). The filtered xenobiotics may remain in the tubular lumen and be excreted in the urine, or may be reabsorbed across the renal tubular cells back into the blood, whereas, some

xenobiotics that escape this filtration may be secreted by the renal tubules into the urine. Numerous foreign compounds that enter the body, including toxins, drugs and environmental xenobiotics, as well as several endogenous substances, are organic anions and cations (29, 33, 34). Many of them are harmful to the body. Thus, their elimination is essential for the maintenance of homeostasis. The major routes of organic anion and cation elimination in the kidney occurs in the proximal tubular cells via organic anion and cation transporter systems. Both systems can transport a very wide range of substrates, requiring only an appropriate charge on their hydrophobic backbone (35). Their multispecificities make them suitable for the elimination of a variety of endogenous metabolites and xenobiotics. Recently, several isoforms of both transporters have been identified and cloned.

There are at least 3 organic anion transporters in the basolateral membrane of the proximal tubule. The first transport system, which seems to be the major one for the secretion of organic anions is the PAH/ $\alpha$ -ketoglutarate transport system (36, 37). The second one is the sulfate/oxalate transport system (38). The third one is the contraluminal  $\text{Na}^+$ -dicarboxylate cotransport system (35). However, in a study using the stopped-flow capillary perfusion method, Ullrich and colleagues reported that all three systems showed partial substrate overlapping. In the proximal luminal membrane, there are many transport systems such as the anion/anion transport system for PAH, urate,  $\text{Cl}^-$ ,  $\text{OH}^-$  and  $\text{HCO}_3^-$  (39), the  $\text{Na}^+$ -dicarboxylate cotransport system (40, 41), and the  $\text{Na}^+$ -sulfate cotransport system (38). Moreover, there are organic anion transporter polypeptides (oatp) that are located at the luminal side of the  $\text{S}_3$  segment of the proximal tubules (42), and the ATP-dependent organic anion

transporter which pumps organic anions, especially amphiphilic anions, out of the cell across the luminal membrane (43, 44). For the organic cation transport system, there are several organic cation transporters, such as OCT1 and OCT2 on the basolateral side of the tubule (45, 46), which are reported to be potential-dependent, the H<sup>+</sup>/organic cation transport system on the luminal membrane which is not potential-sensitive (35), and the ATP-driven multidrug transport system (mdr1) located on the luminal membrane (47, 48).

As mentioned above, exogenous substances that are taken into the body are mostly secreted by the kidneys via either organic anion or cation transport systems. However, it was found that various substances, including drugs, environmental compounds and endogenous organic anions, are the substrates of the PAH transporter. This makes the PAH transporter become a multispecific transporter for the tubular secretion of a variety of endogenous metabolites and xenobiotics. The PAH transport system is regarded as a prototype for renal tubular secretion. Thus, it is important to study the effects of stevioside and steviol on the PAH transport system.

## **II. THE RENAL PROXIMAL TUBULE AND THE P-AMINOHIPPURATE TRANSPORT SYSTEM**

The transport mechanisms of organic anions are involved principally in the elimination of foreign substances and endogenous metabolites from the body. In the past, the clearance and excretion of the prototypical organic anion, p-aminohippurate (PAH), has been used to estimate renal plasma flow. Cross and Taggart (49) showed that the amount of PAH accumulation in rabbit renal cortical slices was closely related

to the tubular secretion rate of PAH in the intact animal. Later, Tune et al. (50) directly measured the secretion of [ $^3\text{H}$ ]-PAH in isolated perfused segments of rabbit proximal tubule and found that the rate of PAH secretion was approximately three times greater in the straight portion (or pars recta) than in the convoluted segment. The division of the mammalian proximal tubule into two regions, the pars convoluta and the pars recta, was defined by certain gross and external macroscopic features. In contrast, the morphological observations using fluorescence and the electron microscope have revealed the presence of at least three morphologically distinct segments ( $S_1$ ,  $S_2$  and  $S_3$ ) in mammalian proximal tubules, defined according to cell types (51-53).

p-Aminohippurate (PAH) is a prototypical organic anion substance that plays an important role in the experimental study of renal tubular function. It is secreted by the proximal renal tubules of most vertebrates (both mammal and nonmammal). Transport of PAH was also studied in each segment of isolated perfused rabbit renal proximal tubule (53) and it was reported that the net secretory rate remained constant over time and was not altered by varying the perfusion rate over a range of 4-15 nl/min (53). The  $S_3$  segment of rabbit proximal tubule possessed the lowest net secretory rate of PAH. It was reported that the maximal rate of PAH secretion ( $V_{\max}$ ) was greater in  $S_2$  than in  $S_1$  or  $S_3$  segments, and the apparent affinity for PAH transport ( $K_m$ ) was not different among these three segments. This implied that the heterogeneity in the secretory rate may be due to a variable density of PAH transporter ( $S_2 > S_3 \simeq S_1$ ), whereas the same type of PAH transporter was found in all three segments (54, 55). However, the site of net PAH secretion along the proximal tubule

varies among species. In mammals, the primary proximal site appears to involve the pars recta in all species studied except pig, in which the pars convoluta was most important (50, 53, 56, 57). It was reported that all portions of the mammalian proximal tubule can secrete organic anions, but the highest rate occurs in the S<sub>2</sub> segment. In avians, the net PAH secretion occurs in all portions of the proximal tubule (58). In reptilians, the major tubule sites for PAH secretion appeared to be in the distal portion of proximal tubule of snake (59) and in the early and intermediate portions of the proximal tubule of frog (60).

The net process of PAH secretion has been found to saturate with the increased concentrations of substrates (PAH) in the bathing medium (basolateral side of the proximal tubule). The maximum rate of net PAH secretion in rabbit proximal tubule appeared to be about 10-20 times greater than that of frog and snake renal tubules, but the affinity of the secretory transport system for PAH in frog and snake is about 10 times greater than that of rabbit tubules (54, 59-62). Although kinetic studies of PAH transport in each segment of mammalian proximal renal tubules showed a difference in  $V_{max}$ , but no difference in  $K_m$  was observed (54). However, differences in the effects of inhibitors on PAH transport in S<sub>2</sub> and S<sub>3</sub> segments of rabbit tubules were observed (63). This suggested that there may be some different isoforms of the transporters in different tubule segments. It is interesting that the values of  $K_m$  and  $V_{max}$  for PAH were not different for both the transepithelial transport of PAH and PAH transport across the basolateral membrane into proximal tubule cells of the S<sub>2</sub> segment of rabbit proximal tubule (54, 62). These data suggested that the

transport step into the proximal tubule cells at the basolateral side is rate-limiting for transepithelial transport.

Studies of the transepithelial secretion of organic anions in isolated proximal renal tubules from several species (50, 58, 60, 64) have shown the transport of organic anions against a concentration gradient (the concentration of organic anion inside the cells was greater than that in the bathing medium). In addition, the electrical potential inside the cell was negative when compared with that of the bath and lumen, thus the transport of the organic anion into the cell at basolateral membrane was apparently against an electrochemical gradient as well, whereas its exit into the tubular lumen proceeds down an electrochemical gradient.

The apparent permeability of the luminal and basolateral membranes of the proximal tubule to PAH were also investigated (50, 60, 64). It was found that the apparent permeability of the luminal membrane was higher than that of the basolateral membrane. These data supported the preferable movement of organic anions from cell to lumen, rather than backflux to the basolateral side, as only a very small backflux was observed in most species. Thus, net secretion of organic anions was not influenced by backflux. Moreover, the secretory transport rate of PAH did not depend on the fluid flow rate along the proximal tubule lumen (61).

The process of PAH transepithelial transport involves the transport of PAH into the cell against an electrochemical gradient at the basolateral membrane and the transport of PAH across the luminal membrane from the cell into the lumen, although its exit mechanism at the luminal membrane is still unclear. Many studies have been performed on intact kidneys, kidney slices, isolated renal tubules and renal membrane

vesicles of both mammals and nonmammals to elucidate the details of the transepithelial transport processes of PAH (55, 65-67).

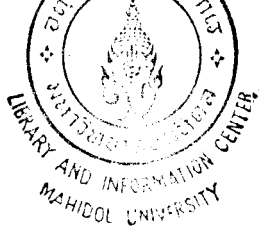
## 1. The PAH transport process at basolateral membrane

### 1.1 Mechanism

An earlier study showed that PAH transport required energy (49), but no evidence for a direct coupling of PAH transport to ATP hydrolysis was obtained (68-71). *In vitro* studies with kidney slices and renal tubules of rabbit, snake and chicken have found that the transport of PAH was inhibited by the removal of Na<sup>+</sup> or K<sup>+</sup> from the basolateral medium or by inhibition of Na<sup>+</sup>-K<sup>+</sup> ATPase with ouabain (49, 68, 72-75, 82, 281). This indicated that Na<sup>+</sup>, K<sup>+</sup> and the activity of Na<sup>+</sup>-K<sup>+</sup> ATPase are involved in PAH transport. Subsequent studies by Podevin et al. (76) and Sheikh and Moller (77) showed that it was not the extracellular Na<sup>+</sup> concentration alone, but the inwardly-directed Na<sup>+</sup> gradient as well, that were important in the PAH transport process. However, no direct coupling of basolateral organic anion transport to the Na<sup>+</sup> gradient was observed (66, 78-81). Dantzer and Bentley (65) found that the basolateral PAH uptake into isolated snake renal proximal tubule was inhibited by SITS, a disulfonic stilbene inhibitor of anion-exchange. The combination of the outwardly-directed PAH gradient and the inwardly-directed Na<sup>+</sup> gradient stimulated PAH uptake in the basolateral membrane vesicles of rat and rabbit (80, 83). The results implied that PAH transport across the basolateral membrane might involve an exchange with some anionic metabolites that were present in the cells, or that it might enter the cells by another pathway (78, 84-87). In 1987, Shimada et al. (66) and Pritchard (88) found that the entry step of PAH at the basolateral membrane involved

a countertransport for dicarboxylate, and the dicarboxylate could re-enter the cells again via cotransport with  $\text{Na}^+$ . It was also demonstrated that the process of PAH transport was a tertiary active transport using rat basolateral membrane vesicles (89). Therefore, a model of the transport process was proposed, that the transport of PAH (or other organic anions that share this system) into the cell exchanged with dicarboxylate ( $\alpha$ -ketoglutarate,  $\alpha$ -KG), moving down its electrochemical gradient. The outwardly-directed gradient of  $\alpha$ -KG was maintained by metabolism and uptake across the basolateral membrane via the  $\text{Na}^+$ -dicarboxylate cotransport system (90). The metabolic energy that was used to maintain the inwardly-directed  $\text{Na}^+$  gradient used for the entry of  $\alpha$ -KG involved  $\text{Na}^+$ - $\text{K}^+$  ATPase activity (33, 91, 92). The study of Schmidt and Burckhardt (93) in bovine renal basolateral membrane vesicles reported that the stoichiometry for PAH/ $\alpha$ -KG exchange was 1:1. They suggested that  $\alpha$ -KG might be exchanged in a monovalent form (or one divalent  $\alpha$ -KG plus one  $\text{H}^+$ ) or there may be some anion or cation cotransported during PAH/ $\alpha$ -KG exchange. From the studies in isolated perfused tubule in chicken, snake and rabbit (58, 63, 90, 94), it was found that preloading proximal tubules with  $\alpha$ -KG from the basolateral side stimulated PAH uptake into the cell, as well as transepithelial transport of PAH. However, the basolateral  $\alpha$ -KG preloading showed biphasic effects, wherein a low concentration stimulated, whereas a high concentration inhibited, PAH uptake, which was suggested to compete with PAH at the transporter. Similar to PAH transport, fluorescein (a fluorescent anion) transport was increased when  $\alpha$ -KG was added to the basolateral and/or the the luminal sides of rabbit proximal tubule (95, 96). The stimulation of PAH transepithelial transport after  $\alpha$ -KG preloading at the basolateral

side was eliminated when  $\text{Na}^+$ -dicarboxylate cotransporter was blocked by the removal of basolateral  $\text{Na}^+$  or the addition of  $\text{LiCl}$ , a specific inhibitor of  $\text{Na}^+$ -dicarboxylate cotransporter (58, 90, 94). These results showed that  $\alpha$ -KG preloading from the basolateral side stimulated PAH secretion. In studies in the renal proximal tubule of snake and rabbit,  $\alpha$ -KG in the bathing medium trans-stimulated PAH efflux across the basolateral membrane (90, 94), and studies using rat renal cortical slices indicated that PAH uptake was coupled directly with an outwardly-directed gradient for  $\alpha$ -KG (97). These findings supported the existence of PAH/ $\alpha$ -KG exchange at the basolateral membrane similar to that observed in OK kidney epithelial cells (98). In addition, the  $\alpha$ -KG taken up from the luminal fluid via the luminal  $\text{Na}^+$ -dicarboxylate cotransporter also increased the organic anion transport step into the cell at the basolateral membrane (95, 99). Moreover, it was found that the transepithelial transport of PAH in rabbit tubules bathed with a HEPES-buffered medium could be stimulated by extracellular  $\alpha$ -KG, whereas no stimulation occurred in tubules bathed with a bicarbonate-buffered medium (61, 63, 99). However, this was not found to occur in snake renal tubule (61). It is interesting that the buffer solutions used as perfusing and bathing solutions affected the control level of PAH transport in rabbit renal proximal tubule. A tubule perfused and bathed with a bicarbonate-buffered medium showed a PAH secretory rate 5-6 times greater than one bathed and perfused with a HEPES-buffered medium. It is possible that an outwardly-directed  $\alpha$ -KG gradient was established mainly by metabolic production within the cells (61). The metabolic state of the renal tubule cells in these two conditions may be different. The tubular cells in a bicarbonate-buffered medium may be in an optimal metabolic state,



but those in a non-bicarbonate-buffered medium may not be in the optimal metabolic state to produce a high amount of intracellular  $\alpha$ -KG. It was suggested that under optimal metabolic conditions, the intracellular pool of  $\alpha$ -KG was sufficiently large, so that no additive effect of the extracellular  $\alpha$ -KG preloading on basolateral  $\alpha$ -KG/PAH countertransport was observed. Dickman and Mandel (100) reported that incubation of rabbit renal tubule in the absence of bicarbonate reduced the cellular level of ATP and increased lactate production. They assumed that the cellular levels of tricarboxylic acid (TCA) cycle intermediates, such as  $\alpha$ -KG, malate and succinate were also reduced in this condition. This implied an important role for bicarbonate in maintaining normal renal tubular metabolism. The uptake of  $\alpha$ -KG via the basolateral  $\text{Na}^+$ -dicarboxylate cotransporter may help to maintain the outwardly-directed  $\alpha$ -KG gradient for the exchange of PAH or other organic anions transported by the classical organic anion transport system. The mechanisms of PAH transport across basolateral membrane are shown in Figure 1.

Factors that influence PAH secretion were recently reported. Reyes et al. (101) found an influence of sex difference on rat renal secretion of PAH. In an *in vivo* study, PAH was eliminated in male rats faster than in female rats, this difference being influenced by testosterone which increased the elimination rate of PAH (101). *In vitro* PAH uptake by renal cortical slices from intact male rats was higher than that of orchidectomized rats (101). A kinetic study showed that numbers of PAH transporters were reduced in orchidectomized rats (101). The results of this study suggested that testosterone could increase the number of PAH carriers in the kidney. In addition, activation of protein kinase A and C affected the PAH transport

into isolated S<sub>2</sub> segments of rabbit renal proximal tubule. Activation of the protein kinase C pathway enhanced PAH transport across the basolateral membrane of rabbit renal proximal tubule at the basolateral membrane (102, 103), whereas protein kinase A activation produced the opposite effects (102). This was suggested that protein kinase A and C influence the PAH uptake by the basolateral PAH transporter (102), whereas there was no effect on the function of the basolateral Na-dicarboxylate cotransporter (104, 105). However, controversial results were obtained in OK kidney epithelial cells and the renal proximal tubule of killifish, where the activation of protein kinase C inhibited PAH uptake across the basolateral membrane (106, 107).

Recently, a new pathway of organic anion transport across the basolateral membrane was discovered, using confocal microscopy to study the transport of fluorescein-methotrexate (FL-MTX) and sulforhodamine 101, which have molecular masses larger than fluorescein and PAH (molecular masses are 923 and 606 Da, for FL-MTX and sulforhodamine, respectively), in killifish proximal tubule (34, 108). It was reported that the large organic anions (FL-MTX) uptake into the cells and secretion into the tubule lumen was ouabain-insensitive, Na-independent and KCN, which inhibits cellular metabolism, did not affect cellular uptake. In addition, it was found that PAH and probenecid were weak inhibitors, for FL-MTX transport. This suggested that large organic anions entered the cell across the basolateral membrane via a different pathway from PAH, the classical organic anion transporter. Sulforhodamine 101 showed its transport pathways via both systems, with overlapping between the PAH and FL-MTX transport systems (34, 108).

## 1.2 Substrate specificity for PAH transporter at the basolateral membrane

It was reported that the renal organic anion transport system or PAH transport system at the basolateral membrane of renal proximal tubules accepted a large variety of organic compounds. As stated above,  $\text{Na}^+$  drives dicarboxylate into the cell which in turn exchanges for PAH. Thus, PAH transport is not directly, but indirectly dependent on the  $\text{Na}^+$  gradient. From the studies of Ullrich et al. (35), it was found that PAH transport was inhibited by fatty acids with a chain length greater than four carbons. In addition, hydrophobic aromatic monocarboxylates could inhibit PAH transport with different affinities, for example, the apparent  $K_i^{\text{PAH}}$  of benzoate: 1.5 mM, 1-naphthoate: 0.17 mM, 2-naphthoate: 0.14 mM, and diphenyl carboxylate 0.15 mM. This inhibition is not restricted to aromatic structure alone, but some aliphatics also interact with this transporter. These data are compatible with the carboxylic group and the hydrophobic moiety of substrates. Glutarate, PAH, and probenecid showed affinity values for PAH transporter with  $K_i$  values of 0.05, 0.08 and 0.05 mM, respectively. That means that these three substrates have a high specificity for the PAH transport system. Ionic charges also affect the specificity of a substrate for PAH transporter, as it was revealed that substrates with a hydrophobic core and 1 or 2 negative charges (no matter whether fully or partially negative charges) could bind with this transporter (109). It was postulated that, on the basis of their charges, 2 categories of substrates for the PAH transport system can be distinguished (84, 85, 109). The first one is compounds with at least one negatively charged ionic group ( $\text{COO}^-$ ,  $\text{SO}_3^-$ ,  $\text{O}^-$ ), and the second one is compounds with two

partially negative charges ( $\text{OH} < \text{NO}_2 < \text{CHO}$ ). The affinity rises with the decreasing pKa or increasing hydrophobicity (91).

From the studies of Ullrich and his coworkers concerning the specificity of the basolateral transporter for various compounds (35, 81, 84, 109-113), it can be concluded that substrate specificity of the basolateral PAH transporter could be governed by the following rules:

(i) The substrate must have hydrophobicity, whereby the hydrophobic domain has a length of 4 Å up to 10 Å, optimally 8-10 Å long.

(ii) The strength of the ionic charge is a determinant for interaction with the basolateral PAH transporter.

(iii) PAH transporter also accepts hydrophobic substrates which cannot be ionized, such as benzene aldehydes, steroid hormone and aniline derivative analgesics.

(iv) Electron-attracting side groups (Cl, Br,  $\text{NO}_2$ ) augment the interaction with the PAH transporter. It was reported that electron-attracting power, their number and location within the molecules of substrate, all play a role in this interaction (109, 112).

It can be postulated that affinity for the PAH transporter is influenced by hydrophobicity, charge, charge placement or distribution, and charge strength. The transporter could accept monovalent hydrophobic organic ions with a negative or partially negative charge, and could also interact with divalent compounds, including some switterions with two negative or partially negative charges. The compounds that showed effective binding to this transporter have a distance between charges about 6-7

A<sup>o</sup>, and their affinity is enhanced with increasing hydrophobicity of the compounds. Based on this model, potent inhibitors of the PAH system such as probenecid would be more tightly bound to the transporter than PAH. Thus, they are a very effective competitive inhibitor for PAH transport system.

## **2. Intracellular events of PAH transport**

After organic anions enter the proximal tubule cell across the basolateral membrane, they traverse the cell to the luminal membrane before secreting to the tubule lumen. Although very little has been studied concerning this step when compared with the basolateral and luminal steps, it was revealed that organic anions were not uniformly distributed within the renal tubular cells (114-116). It was evident that various anions such as phenol red, PAH and probenecid were subjected to extensive intracellular binding (29, 114-117). Studies using video-imaging and confocal microscopy (118, 119) found that fluorescein accumulated in intracellular punctate compartments during the transepithelial transport process. When the basolateral transport of fluorescein was inhibited, the vesicular uptake or sequestration was either eliminated or reduced. In addition, the microinjection of competitors for fluorescein such as PAH or probenecid into the cells could inhibit the sequestration. The compartmentation was eliminated when metabolism was inhibited (118). This suggested that intracellular organic anions might be sequestered within vesicular structures during the transport process. As we know that an organic anion secretory system handles a wide variety of xenobiotic and toxic compounds, the vesicular form should be useful. There were 2 possibilities suggested for the physiological roles of binding and sequestration of organic anions. Firstly, it decreases the free cytoplasmic

concentration of organic anions in the cells, which prevents toxicity. Secondly, it plays a role in transcellular organic anion movement within the cell. Fluorescein-loaded vesicles were shown to move from the basolateral to the luminal membranes, and this movement was blocked by nocodazole, which is a microtubule-disrupting drug (120). Nocodazole could reduce fluorescein secretion in the intact renal tubule of teleost (120). This suggests that vesicular uptake and movement within the cell may play a direct role in the transcellular movement of secreted organic anions. Dantzler and Wright (61) reported their observations on the S<sub>2</sub> segment of rabbit proximal tubule using confocal microscopy, that in a tris-buffered bathing medium identical to that used by Miller et al. (118), fluorescein accumulated in punctate compartments within the cells, whereas very little fluorescein appeared in the tubular lumen in the absence of bicarbonate. In contrast, when the bathing medium was changed to a bicarbonate-buffered solution (whether or not Tris remained in the solution), the appearance of fluorescein in the tubular lumen and its accumulation in punctate compartments in the cytoplasm was substantially reduced or eliminated. As mentioned earlier, a tubule in a bicarbonate-buffered medium produced the optimal metabolic energy (100). Therefore, it was suggested that, at least in mammals, the metabolic state of the tubules might be important for determining the rate of organic anion transport within the tubular cells. Under normal physiological conditions, in which the proximal tubule is in an optimal metabolic state, punctate compartmentation might play no role in the transport of organic anions through the cytoplasm (61).

### 3. The PAH transport process at the luminal membrane

The mechanism of organic anion transport at this side of the cell is still unclear. Studies of PAH transport with isolated perfused snake proximal tubules reported that the movement of PAH from the cells into the lumen during the net secretory process was down an electrochemical gradient and could be the result of simple passive diffusion (59). Subsequent studies with isolated proximal tubule of rabbit (50) and snake (59, 64) revealed that the apparent permeability of the luminal membrane to PAH was greater than that of the basolateral membrane. These results supported the preferable passive transport of PAH across the luminal membrane. In contrast, the transport process was also suggested to be carrier-mediated, and driven by an electrochemical gradient, because the lipid layer of the membrane is a barrier to the diffusive movement of charged solutes (61). This was supported by subsequent studies, both in isolated perfused snake tubules (65, 121, 122), in brush border membrane vesicles from flounder (79), and in snake kidneys (123). The studies in brush border membrane vesicles and isolated perfused snake renal tubules showed that PAH transport from the cells to the lumen was inhibited by SITS (4-acetamido-4'-isothiocyano-2,2'-disulfonic stilbene), unlabeled PAH, phenol red and probenecid (65, 79, 121, 123). These results suggested that PAH might move from the cytoplasm into the lumen via a carrier in the luminal membrane. In intact tubules, the mediated transport step for the luminal exit of PAH was not influenced by the presence or absence of  $\text{Na}^+$  or  $\text{K}^+$  in the lumen (64, 124), whereas initial studies with brush border membrane vesicles from snake kidney showed that PAH transport across the membrane was stimulated by a sodium gradient that was present in the same direction

as PAH transport (123). However, under normal physiological conditions in intact tubules, the secretion of PAH occurred in the opposite direction to the  $\text{Na}^+$  gradient across the luminal membrane of the tubule, thus, the sodium gradient is unlikely to directly stimulate PAH secretion under normal physiological conditions. In addition, the movement of PAH from the cells to the tubular lumen in intact snake and rabbit tubules did not require the presence of chloride ion in the lumen, but it did require the presence of an equivalent quantity of some anions which are highly permeable to luminal membrane, and this process may involve anion exchange (122, 125, 126). However, the mechanism for PAH movement from the cells to the lumen is still unclear. It is not known exactly whether it involves anion exchange, carrier-mediated diffusion, or both. It is interesting to see that when PAH transport from cell to lumen was inhibited, the uptake of PAH from the basolateral side into the cells was also reduced, suggesting that there might be some feedback coupling between transport processes at the luminal and basolateral membranes (65, 121, 122, 126-128).

In mammals, the mechanism of PAH transport at the luminal membrane varies among species. Studies with renal brush border membrane vesicles showed an organic anion exchanger at the luminal membrane which was shared by PAH, lactate and urate, as well as several inorganic anions ( $\text{Cl}^-$ ,  $\text{Br}^-$ ,  $\text{HCO}_3^-$ ,  $\text{OH}^-$ ). Anion exchange was also found in an *in vivo* study of rat kidney (39). This transporter had previously been found only in urate reabsorbers (dog, rat), but not in urate secretors (pig, rabbit) (29, 129-135). In brush border membrane vesicles from the kidneys of rabbits and pigs (urate secretors), evidence for potential-driven carrier-mediated transport was reported (134, 136). Ullrich and Rumrich (39) investigated the transport

systems for luminal PAH secretion using *in vivo* microperfusion techniques in rat renal proximal tubules. They reported that cell depolarization caused by  $K^+$  or by large changes in luminal  $OH^-$  and  $Cl^-$  concentrations did not have a significant effect on PAH transport. Moreover, PAH,  $\alpha$ -ketoglutarate, cGMP,  $PGE_2$ , cortisol, DIDS, pyrazinoate, lactate and urate did not induce a trans-effect on PAH transport across the luminal membrane. In contrast, phenol red, fluorescein,  $HCO_3^-$  and uricosuric substances in the luminal fluid caused trans-inhibition of PAH transport at the luminal membrane in an *in vivo* study of rat renal proximal tubule (39). They concluded that the transport of PAH across the luminal membrane *in situ* might not be contributed to by a potential-sensitive system, but rather that the major mode of luminal PAH transport may be an anion exchange system.

Miller and coworkers (137) studied the mechanisms concerning the driving force of fluorescent anion transport from renal proximal tubule cells to lumens in intact killifish using fluorescence microscopy. Their results showed that organic anion transport from cell to tubular lumen was a carrier-mediated and uphill process, because the concentration of fluorescence in the tubular lumen was higher than that in the cells. This transport process was not sensitive to the electrical potential difference across the luminal membrane. They also found that KCN, which inhibits energy metabolism, reduced organic anion secretion into the lumen during which no changes in cellular concentration were observed (34, 137). In 1999, Masereeuw and coworkers (138) studied the secretory processes of the organic anions, lucifer yellow and another fluorescent organic anion, in intact killifish proximal tubule using confocal microscopy. They demonstrated that organic anions entered the cells via the

classical basolateral transporter, sodium-dependent system, but about half of them transported into the lumen by a sodium-independent system which was suggested to be multidrug resistance-associated protein (138). This finding was further supported by Leier et al. (139) who found that PAH was a good substrate for an ATP-dependent export pump (apical multidrug resistance protein, MRP2). MRP2 is characterized as a unidirectional transport protein and contributes to the secretion of PAH and other amphiphilic anions (e.g., ochratoxin A) into the proximal tubular lumen (139). Another transporter, NPT1, localized in the apical membrane of renal proximal tubules, is characterized as human type I sodium-dependent inorganic phosphate ( $P_i$ ) transporter which taken up phosphate from the luminal fluid into the blood. However, this transporter was reported to mediate the secretion of PAH from renal proximal tubule cells and was sensitive to chloride ions (140). In addition, Bakos et al. (141) also reported that both MRP1 and MRP2 participated in the active secretion of organic anions such as diuretics and antibiotics.

The transepithelial transport process of PAH across the proximal tubule can be summarized as shown in Figure 1:

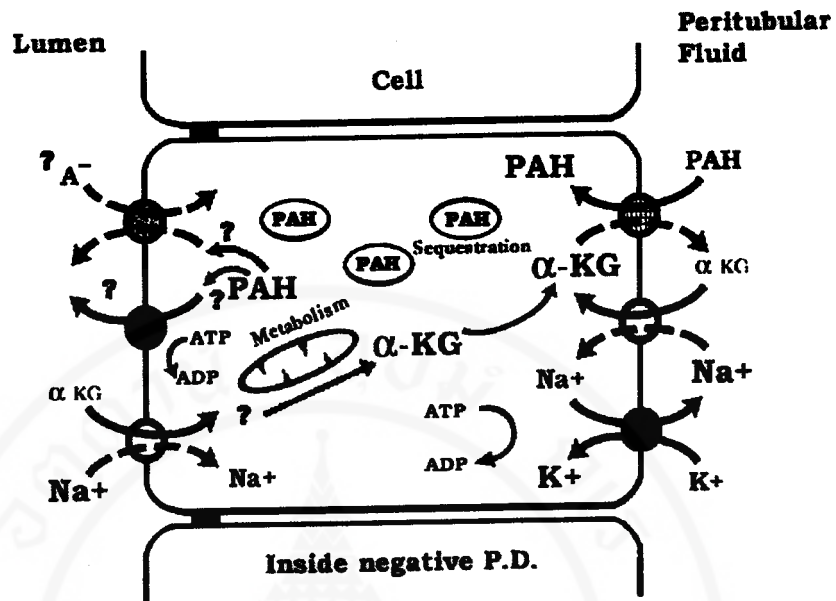


**Figure 1.** The model for organic anion (PAH) secretion by proximal renal tubules. Broken arrows with open circles indicate movement down an electrochemical gradient. Solid arrows with open circles indicate movement against an electrochemical gradient by some forms of secondary active transport. Solid arrows with solid circles indicate primary active transport.

### III. SODIUM AND POTASSIUM-DEPENDENT ADENOSINE TRIPHOSPHATASE (Na<sup>+</sup>-K<sup>+</sup> ATPase)

The Na<sup>+</sup>-K<sup>+</sup> ATPase is one of the most vital integral membrane proteins present in animal cells. This enzyme has an important role in maintaining the osmotic balance of the cell, the ionic gradient across the plasma membrane, the resting membrane potential of most cells, and the excitable property of muscle and nerve cells. The metabolic energy produced by the cell is required to establish a high intracellular potassium concentration and a low intracellular sodium concentration. The pumping of sodium out of the cell and potassium into the cell is, in both cases, against the electrochemical gradients for these ions. These processes are controlled by

the functional role of sodium pump which is fueled by the activity of the enzyme “Na<sup>+</sup>-K<sup>+</sup> ATPase”.

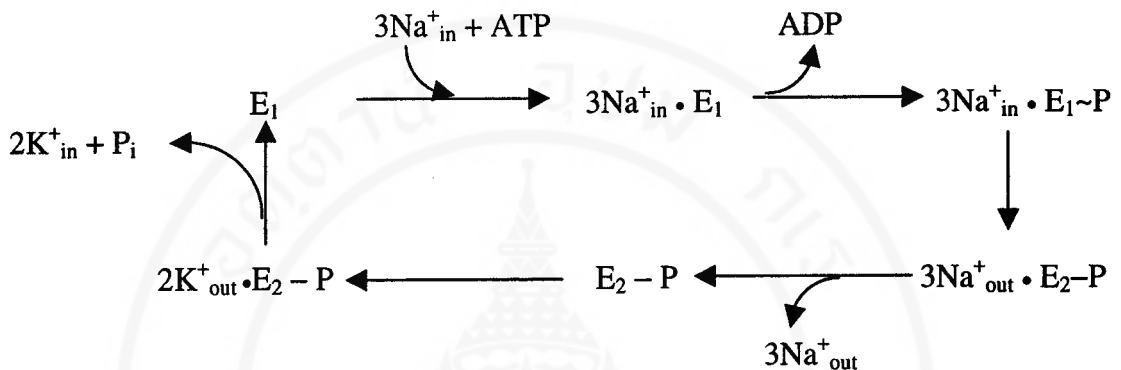
This enzyme is a member of the p-type ATPase, which involves the formation of a transient covalently phosphorylated intermediate during the reaction cycle (142). It has been purified from various kinds of tissue, including kidney cells. The structure of this enzyme is composed of two subunits, an alpha ( $\alpha$ ) or catalytic subunit, and a beta ( $\beta$ ) or glycoprotein subunit (143-146). The  $\alpha$ -subunit has a MW of approximately 104,000 daltons and forms 60-72% of total protein (144, 147). It was reported that the  $\alpha$ -subunit of the sheep kidney consists of a protein with a MW of 112,177 daltons (1,016 amino acid residues) (148). The  $\beta$ -subunit is a sialoglycoprotein with a MW of approximately 40,000 daltons plus 17,000 daltons for carbohydrate moiety (144, 147, 149). It was found that the  $\beta$ -subunit of the sheep kidney consists of 302 amino acid residues with a core protein that has a MW of 34,939 daltons (150). Both  $\alpha$  and  $\beta$ -subunits have many isoforms (151, 152). The  $\alpha_1\beta_1$  isoform is considered to be the housekeeping form of this enzyme, whereas the other isoforms may mediate tissue-specific roles. The  $\alpha_1$  isoform has been found in most tissues and cell types (152). In the kidney,  $\alpha_1$  is the major isoform (153), whereas an  $\alpha_2$  isoform has been found mainly in skeletal muscle, brain and in smaller amounts in the heart. The  $\alpha_3$  isoform has been found mainly in the brain and heart. The  $\alpha_4$  isoform has been found only in the rat and human testes. The  $\beta$ -subunit has been described as having 3 isoforms (150, 151). The  $\beta_1$  isoform is the major form that is expressed in all tissues,  $\beta_2$  has been found mainly in the brain, and  $\beta_3$  has been observed only during the early developmental stage of *Xenopus laevis*.

The  $\alpha$ -subunit of this enzyme contains the phosphorylation site and the binding sites for  $\text{Na}^+$ ,  $\text{K}^+$ ,  $\text{Mg}^{2+}$ , ATP and ouabain. The binding site for ATP locates in the cytoplasmic side, whereas that of ouabain locates on the extracellular side (149, 154). It could be said that the  $\alpha$ -subunit contains binding sites for ligands that regulate pump function. In contrast, the physiological functions of the  $\beta$ -subunit is unknown. However, it was found that the expression of  $\text{Na}^+$ - $\text{K}^+$  ATPase activity in yeast required both  $\alpha$ - and  $\beta$ -subunits to be cotransfected (155). This occurrence suggested that  $\beta$ -subunit was required for proper insertion of the  $\alpha\beta$  complex form into the cell membrane (156, 157). The  $\beta$ -subunit has also been postulated to be involved in stabilizing the enzyme's structure and to modulate the affinity of the enzyme to a cation (158). Thus, it may be involved in conformational changes associated with enzyme function (159). The molar ratio of  $\alpha$  to  $\beta$ -subunits was reported to be 1:1 stoichiometry (143, 145), or 2 $\beta$ -subunits per 2 $\alpha$ -subunits (160). In contrast, some investigations have suggested its stoichiometry to be 2 $\beta$ -subunits per one  $\alpha$ -subunit (144) and 1 $\beta$ -subunit per two  $\alpha$ -subunits (146).

The transport mechanism of the pump is the efflux (transport out of the cell) of  $\text{Na}^+$  coupled with the influx (transport into the cell) of  $\text{K}^+$ , using ATP. Under normal physiological conditions, the efflux of  $\text{Na}^+$  and influx of  $\text{K}^+$  occurs at a coupling ratio of 3  $\text{Na}^+$  : 2 $\text{K}^+$  : 1ATP (161, 162). However, a recent study has demonstrated that this ratio is not fixed, but can vary, depending on the concentrations of ions both inside and outside the cell (163).

Many reports about the enzyme  $\text{Na}^+$  - $\text{K}^+$  ATPase, prepared from fragmented membrane in the presence of  $\text{Na}^+$ ,  $\text{Mg}^{2+}$ , and ATP- $\gamma^{32}\text{P}$ , found that the  $\gamma\text{P}$  was

covalently transferred to the enzyme when  $K^+$  was added to the enzyme that has been phosphorylated in the presence of  $Na^+$ ,  $Mg^{2+}$  and ATP. The phosphate group was then rapidly cleaved and the enzyme was allowed to cycle, continuing to hydrolyze ATP, as shown in the following diagram (164):



There are 2 enzyme conformations, “E<sub>1</sub>” which has high affinity to intracellular Na<sup>+</sup> and “E<sub>2</sub>”, which has high affinity to extracellular K<sup>+</sup>. The cycling of the enzyme between these 2 forms results in the transport of ions across the membrane. In the E<sub>1</sub> form, the enzyme has a high affinity for intracellular Na<sup>+</sup> and Mg-ATP. After binding, the phosphate group of ATP is transferred to form a high-energy phosphoenzyme (E<sub>1</sub>~P). The high energy in the phosphate bond is used to drive the conformational change of the enzyme, resulting in the exposure of Na<sup>+</sup> to the extracellular side and change over to the low-energy phosphoenzyme, E<sub>2</sub>-P. The E<sub>2</sub>-P conformation has a low affinity for Na<sup>+</sup>, so Na<sup>+</sup> is released from the enzyme. In contrast, this conformation has a high affinity for extracellular K<sup>+</sup>. After the binding of K<sup>+</sup> to the extracellular surface of the enzyme, the phosphatase is activated to cleave a phosphate group, and then K<sup>+</sup> is translocated and released to the intracellular side. The enzyme is then returned to the E<sub>1</sub> conformation again and is once more capable of binding with ATP and Na<sup>+</sup> in the cycle (142, 165, 166). Na<sup>+</sup>-K<sup>+</sup> ATPase activity may

be differentially regulated by hormones (151, 167). The normal expression of this enzyme can be altered by pathological conditions to reestablish homeostasis that has been altered by the disease. In addition, the activity of this enzyme can be inhibited by ouabain (154, 168-170), a digitalis glycoside, which has its binding site at the extracellular surface of the cell, and by vanadate, whose binding site is located at the cytoplasmic surface and is most likely the site from which phosphate is released during enzyme activity (171, 172).

In the kidney, the localization of  $\text{Na}^+\text{-K}^+$  ATPase is mainly on the basolateral surface of the nephron segments (173-178, 183), but the density or its activity is different in each tubule segment. The highest activity of this enzyme occurs in the outer medulla, followed by the kidney cortex and the lowest part is in the inner medulla (179). It also differs among several species of animal. The activity of this enzyme in rat (179-181) and dog (179) is much higher than that in mouse (180, 181), guinea pig (179), monkey (179), rabbit (179, 181) and cat (179). Using microdissected nephron segments of rabbit (182), the  $\text{Na}^+\text{-K}^+$  ATPase activity in distal nephron segments is about 2-5 times higher than that in the proximal tubule. The distribution of enzyme activity is highest in the medullary thick ascending limb of Henle's loop, and the proximal convoluted tubule of juxtamedullary nephron has this enzyme activity twice that of the superficial nephron (182). However, Doucet et al. and Katz et al. in 1979 reported that the  $\text{Na}^+\text{-K}^+$  ATPase activity differed on the basis of tubule length of mammalian nephron. In rabbit (180, 181), the enzyme activity per tubule length in the proximal convoluted segment is 4-5 times higher than that of the pars recta, but not different from that of the medullary thick ascending limb. These

results were supported by the density of enzyme as measured by [ $^3\text{H}$ ] ouabain binding along the rabbit nephron (183). In rat and mouse, it has been shown that the pattern of enzyme activity distribution along the nephron segments was identical in both species (181). The highest activity per tubule length was in the distal convoluted tubule and thick ascending limb (both in medullary and cortical parts), followed by the proximal convoluted tubule, whereas enzyme activity in the pars recta and collecting tubule was lower (175, 181, 183, 184), with the lowest activity being in the thin limb of Henle's loop (175, 181, 184). The  $\text{Na}^+\text{-K}^+$  ATPase activity is heterogenous in the renal proximal tubule, as determined in the microdissected tubule of rabbit. The highest activity was observed in the  $\text{S}_1$  segment (the convoluted part of proximal tubule) of rabbit, which was 2.5 times greater than that in the  $\text{S}_2$  segment, and the lowest appeared in the  $\text{S}_3$  segment (distal straight part of the proximal tubule), which was approximately 2 times lower than that in the  $\text{S}_2$  segment (184). Schmidt and Horster (182) also found that enzyme activity was lower in neonatal than in mature rabbit kidney. However, a difference in ouabain-insensitive ATPase activity exists between the stages of kidney development. It's interesting that enzyme activity in neonatal was similar or higher than that in adult rabbit kidney.

The factors that influence the development of  $\text{Na}^+\text{-K}^+$  ATPase activity were studied (184-191). Two factors were mentioned as being involved in the postnatal development of the  $\text{Na}^+\text{-K}^+$  ATPase activity, the concentration of sodium inside the cell and hormones (glucocorticoid and mineralocorticoids). Aperia et al. (185, 186, 266) found that the immature proximal tubule cells of rats were sensitive to betamethasone and aldosterone for the induction of  $\text{Na}^+\text{-K}^+$  ATPase activity. Later

on, Aperia and Larsson (186) reported that long-term administration of adrenal corticoid hormone to young rats affected the increments of  $\text{Na}^+\text{-K}^+$  ATPase activity, fluid reabsorption and the basolateral membrane area in the proximal tubule. The increase in net fluid and solute transports was related to the increase in the basolateral membrane area, as well as to the amount of  $\text{Na}^+\text{-K}^+$  ATPase during postnatal development (182, 187, 192-195). Glucocorticoid treatment of 1 week-old rabbits caused a 40% increase in  $\text{Na}^+\text{-K}^+$  ATPase activity of rabbit proximal tubules during the second week of life, but glucocorticoid treatment during the second week of life had no effect on  $\text{Na}^+\text{-K}^+$  ATPase activity in the third week (191). This work was supported by Celsi et al. (188), who found that  $\text{Na}^+\text{-K}^+$  ATPase mRNA is regulated by betamethasone in the infant rat kidney, but not in the adult rat kidney, although some reports have suggested that an increase in intracellular  $\text{Na}^+$  concentration may induce enzyme activity (191), as found in the study of Larsson et al. (189). Klein and Lo (196), in contrast, showed that, indeed, corticosterone increased the  $\alpha_1$  and  $\beta_1$  mRNA levels of  $\text{Na}^+\text{-K}^+$  ATPase in adult rats, resulting in an increase in enzyme activity prior to any enhanced sodium delivery.

In addition, the correlation between  $\text{Na}^+\text{-K}^+$  ATPase activity and the transport of ions and fluid was found not only in the proximal tubule, but also in the thick ascending limb of immature rats (190). The developmental increase in this enzyme activity in the thick ascending limb of Henle's loop in immature rats was found to be correlated with an increase in serum corticosterone level, and this increment was abolished by adrenalectomy (190). The other hormone that could affect  $\text{Na}^+\text{-K}^+$  ATPase activity is thyroid hormone ( $\text{T}_3$ ).  $\text{T}_3$  increased the density of enzyme that then

caused an increase in  $\text{Na}^+\text{-K}^+$  ATPase activity (197, 198). In contrast,  $\text{Na}^+\text{-K}^+$  ATPase activity was reported to be inhibited by dimethyl sulfoxide (DMSO), which is used as a solvent for many substances. It was reported that 10% DMSO inhibited  $\text{Na}^+\text{-K}^+$  ATPase activity by about 30% in bovine kidney cortex and medulla (199). The site of DMSO-inhibited enzyme activity was suggested to be different from that of ouabain. This was due to the additive effect on  $\text{Na}^+\text{-K}^+$  ATPase inhibition that occurred during the addition of ouabain and DMSO simultaneously into the medium. This result was supported by McConnell et al. (200), who found an inhibition of  $\text{Na}^+\text{-K}^+$  ATPase activity of about 26% in human erythrocyte plasma membrane treated with 10% DMSO.

The  $\text{Na}^+\text{-K}^+$  ATPase not only plays an important role for the proximal tubular reabsorption of solutes such as  $\text{Na}^+$ , glucose and amino acids, but also participates in proximal tubular secretory function. There are several organic anions and cations that are secreted by the proximal tubule using ATP driven by  $\text{Na}^+\text{-K}^+$  ATPase. p-Aminohippurate (PAH) is a prototypical organic anion which is secreted by the proximal tubule. There are many studies that have shown the involvement of  $\text{Na}^+\text{-K}^+$  ATPase activity and the secretory transport of PAH. For example, active PAH uptake in kidney slices was depressed by ouabain, an inhibitor of  $\text{Na}^+\text{-K}^+$  ATPase activity (74). In addition, it has been found that intracellular  $\text{Na}^+$  and  $\text{K}^+$  concentrations were changed during ouabain treatment of rabbit renal cortical slices and showed a correlation with the change in active PAH uptake (75). This finding was later supported by the study of Maxild et al. (201), which found a relationship between renal accumulation of PAH,  $\text{Na}^+\text{-K}^+$  ATPase activity and the transmembrane  $\text{Na}^+$

gradient in cortical kidney slices of rabbits. An involvement of  $\text{Na}^+\text{-K}^+$  ATPase in the active transport of PAH was also revealed by an electrophysiological experiment in isolated newt kidney (82). By studying the relationship of  $\text{Na}^+\text{-K}^+$  ATPase activity and the renal organic anion transport system, using vanadate as an inhibitor (71), it was found that vanadate significantly reduced PAH accumulation into rabbit kidney cortical slices. The result obtained from this experiment suggested that the PAH transport process is linked to the function of  $\text{Na}^+\text{-K}^+$  ATPase. Therefore, it could be concluded that  $\text{Na}^+\text{-K}^+$  ATPase activity plays an important role in the PAH transport system in the kidney, as was stated in the section on the PAH transport mechanism (part II).

#### **IV. STEVIA PLANT, STEVIOSIDE AND STEVIOL**

##### **1. Background and History**

Sweet glycosides and their derivatives from the stevia plant are used as sweetening agents and their pharmacological, physiological and toxicological effects have been studied. This plant is a small shrub which was originally grown in Northern Paraguay and in parts of Brazil (202). It has been known as stevia or honey leaf, Caa-che, Azuca-caa, Kaa-he-e and Ca-a-yupe (202, 203). It was first botanically described by Moises Santiago Bertoni, a Paraguayan botanist, and initially named *Eupatorium rebaudianum* in 1899 (204), subsequently reclassified as *Stevia rebaudiana* Bertoni, belonging to the genus stevia in the family Compositae in 1905 (205). The sweetness from the leaves of this plant drew the attention of several scientists. The presence of various sweet compounds in stevia were reported by Rasenack in 1908 and Dieterich in 1909 (202). Later on, an extract from the leaves of

this plant was purified by two French chemists, Bridel and Lavieille, in 1931 and the product yielded a white crystalline compound named “stevioside”. It proved to be 250-300 times as sweet as sucrose (2, 202, 204).

Due to the sweetening property of stevia’s leaf, this plant has now been cultivated in many countries and seems to be a good potential economic plant for exportation. It was reported that, in 1971, Sumida brought the seeds of stevia from Brazil to cultivate in Japan, and successfully produced a sweetener, extracted from the leaves of *Stevia rebaudiana* (2). Since then, stevia has been introduced as a crop in many countries including Korea, Mexico, the United States and Indonesia, as well as recently in Canada (206). Stevioside, the major sweetening agent present in the leaves of this plant, was considered a sugar substitute and commercial sweetener, both in the form of stevioside and stevia extracts (207, 208). The use of these products has increased due to the health concerns related to sucrose usage, such as dental caries, obesity and diabetes. The stevia extracts and stevioside have been widely used in several countries, such as Japan, China, Korea, Israel, Brazil and Paraguay (2, 208). This sweetener is used in pickled vegetables, dried seafoods, soy sauce, beverages, candies and gums, yogurt and ice cream, as well as in toothpastes and mouthwashes. Besides stevioside, other sweet-tasting glycosides have also found in stevia extract, such as Rebaudioside A-E, Dulcoside A and Steviolbioside. The approximate sweetness of these glycosides compared to sucrose is shown in Table 1.

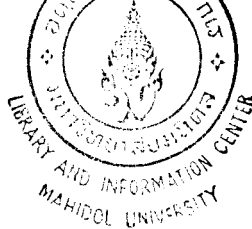


**Table 1.** The relative sweetness of diterpene glycosides in *Stevia rebaudiana* compared to sucrose (2).

Diterpene glycosides	Sweetening potency (sucrose = 1)
Stevioside	250-300
Rebaudioside A	350-450
Rebaudioside B	300-350
Rebaudioside C (Dulcoside B)	50-120
Rebaudioside D	200-300
Dulcoside A	50-120
Steviolbioside	100-125

The normal proportions (w/v) of 4 major glycosides isolated from the stevia plant are: stevioside 5-10%, rebaudioside A 2-4%, rebaudioside C 1-2% and dulcoside A 0.5-1%. The yield of sweetening compounds present in leaf tissue can vary according to the method of propagation (209), day-length (210) and also to agronomic practices as well as processing and storage procedures (208). It was reported that the cultivation of stevia under long days has been shown to cause up to a 50% increase in stevioside concentration, relative to plants grown under short days (210).

Bridel and Lavieille found that stevioside is a neutral substance, composed of one steviol aglycone, a diterpenic carboxylic alcohol, and three molecules of glucose. One glucose molecule forms an ester bond with the carboxylic group of steviol and the other two glucose residues form a glycosidic linkage with the hydroxyl group of steviol (204). The sweet property was found to depend on its ester bond in the

molecule, and was not due to carbohydrate moiety (211). The chemical structures of stevioside and steviol are shown in Figure 2.

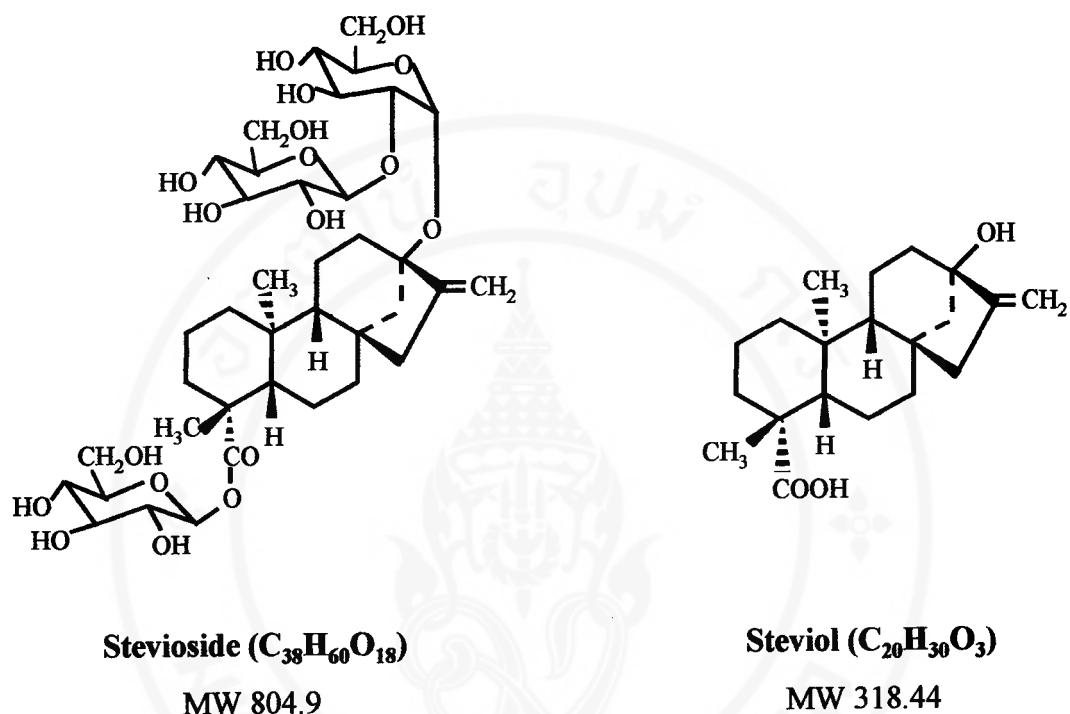


**Figure 2.** The chemical structures of stevioside and steviol

Stevioside was hydrolyzed by an enzyme from the digestive juices of the vineyard snail to yield aglycone, “*steviol*”, and the acid hydrolysis of stevioside yielded a product called “*isosteviol*”, an isomer of stevioside (202, 204, 212). Isosteviol was proved to be stable, as it could be distilled under atmospheric pressure without decomposition. Isosteviol was also obtained when steviol was heated in dilute sulfuric acid (206, 212). The alkaline hydrolysis of stevioside was used to prepare “*steviolbioside*” (212). A diagram of substances from stevioside hydrolysis is shown in Figure 3.

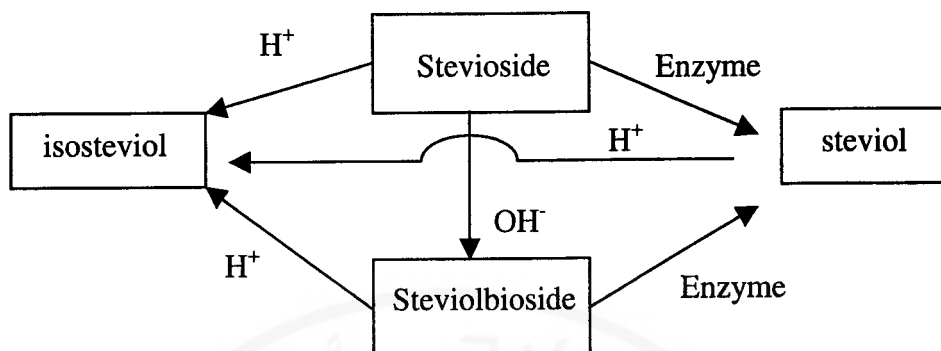


**Figure 3.** Diagram of substances from stevioside hydrolysis by  $H^+$  or  $OH^-$  or enzyme.

## 2. General Properties of Stevioside

Stevioside is a glycoside extracted from *Stevia rebaudiana* leaves. It consists of a  $\beta$ -glycosyl and a  $\beta$ -sophorosyl group bound to the  $C_{19}$  and  $C_{13}$  positions of a diterpenic carboxylic alcohol (212). It is a light, white and odorless powder with a slightly hygroscopic property. Its molecular weight is 804.9 with the chemical formula of  $C_{38}H_{60}O_{18}$ . Stevioside dissolves less in water than in dimethyl sulfoxide (DMSO), its very high purity causing its difficulty to solubilize. It is slightly soluble in ethyl and methyl alcohol, but almost insoluble in propylene glycol, ethyl acetate and chloroform. DMSO is the best solvent for this substance (213, 214). Stevioside is stable at high temperatures up to  $95^\circ C$ , and over a wide range of pH (pH 3 – pH 9). Under very strong alkali condition (pH > 10), the esteric bond at  $C_{19}$  of stevioside is hydrolyzed and decomposed into steviolbioside (215), which is about 2-3 times lower in sweetness than stevioside. The sweetness is also lowered if it is exposed to high temperatures (>  $95^\circ C$ ) for a long period of time (6-8 hours). During prolonged exposure to acidic solution, it is decomposed into glucose and isosteviol, resulting in

reduced sweetness (212, 216). Moreover, pure stevioside has little hygroscopicity. This is an advantage that makes stevioside popular in the pharmaceutical industry. It has no problems of bulky form for incorporation into drug tablets. It is also non-calorific, non-fermentable and does not darken upon cooking (2). Additionally, it is a growth suppressant of several oral bacteria (217). Tomita et al. (218) also found that a fermented aqueous extract from *S. rebaudiana* showed strong bactericidal activity towards a wide range of food-borne pathogenic bacteria.

### 3. General Properties of Steviol

Steviol is found as the aglycone part of various natural glycosides. It was found to be a major metabolite of stevioside from degradation by bacterial flora in the intestine *in vitro* (25). This substance has been examined both pharmacologically and for its toxicological effects by many researchers.

It has a tetracyclic diterpene structure with a molecular weight of 318.44 and the empirical formula of  $C_{20}H_{30}O_3$ . It is a light, odorless, colorless and tasteless powder. It was reported that steviol could be synthesized by treatment of stevioside with sodium periodate ( $NaIO_4$ ) and sodium hydroxide ( $NaOH$ ) (219), or by incubating stevioside with commercial pectinase (220), hesperidinase or hepatic pancreatic juice obtained from the vineyard snail (204). Hydrolysis of stevioside with 0.4% hydrochloric acid ( $HCl$ ) in aqueous methanol solution for 5 hours yields about 49% of steviol (221). Wingard et al. (25) reported that stevioside was completely converted into steviol after a 2-day incubation period in an anaerobic condition with rat intestinal microflora *in vitro*.

#### **4. Stevioside and Steviol: Absorption, Distribution, Metabolism and Excretion**

Stevia extract has been used in many countries and it has been reported to have therapeutic values such as contraceptive and hypoglycemic properties. The pharmacokinetics of some compounds in this extract, especially the major component of sweetening glycosides, stevioside, has been the subject of much scientific interest.

As mentioned earlier, stevioside is a high molecular weight glycoside (MW = 804.9), like oligosaccharide, which is difficult to be absorbed or transported into the epithelial cells. This knowledge brought awareness of the possibility that stevioside might be decomposed to steviol and glucose before absorption in the gastrointestinal tract. In 1980, Wingard et al. (25) reported that whole cell intestinal microflora prepared from rat cecal content was able to completely transform stevioside to steviol under *in vitro* anaerobic conditions within a 2-day incubation at 37°C. Under the same conditions, rebaudioside A required 6 days for complete degradation to steviol. In contrast, under aerobic conditions with cell-free extracts of rat cecal content, steviol was generated from stevioside and rebaudioside only in yields of 50% and 2%, respectively, after 7 days. These results indicated that stevioside and rebaudioside would be degraded to steviol by microflora in the lower bowel. They further determined the intestinal absorption of steviol in the lower bowel of rats. The results showed that steviol-17-[<sup>14</sup>C] was completely absorbed from the lower bowel of rat after oral and intracecal administration. After oral administration, radioactivity was excreted mainly in the feces (96% of administered dose), while only 1.5% of the administered dose was excreted in urine. However, radioactivity was detected totally

in biliary excretions in the bile duct. In contrast, radioactivity was largely detected in rat urine with the bile duct ligated after oral or intracecal administration. These results suggested that stevioside may be degraded into steviol in the large bowel of humans because of the similar quantity and quality of microflora in the human bowel and rat cecum, and after degradation, steviol would be absorbed and excreted in bile and urine (25). However, there was no report concerning the biotransformation or metabolism of stevioside in the body at that time. Five years later, Nakayama and colleagues (222) studied the distribution and metabolism of stevioside and/or its metabolites after single oral administration of  $^3\text{H}$ -stevioside into male Wistar rats at a dose of 125 mg/kg of body weight. They reported that the radioactivity in blood was highest at 8 hours after  $^3\text{H}$ -stevioside administration and the biological half-life of stevioside was exhibited to be 24 hours. The radioactivity was maximally detected in the gastrointestinal content, while a little of it was detected in the tissues of the stomach and intestine. At one hour after administration, radioactivity was highest in the content of the small intestine. From thin-layer chromatograms of gastro-intestinal content, stevioside was the major component detected in stomach, small intestinal and cecal content at that time. In the small intestinal content, stevioside and its metabolites were detected as 33 and 67% of total radioactivity, respectively, whereas very low radioactivity was detected in large-intestinal content. At 4 hours, the radioactivity was markedly increased in cecal content, while that in the small intestine and stomach were decreased. Thin-layer radiochromatograms of cecal content at 4 hours showed the highest radioactivity of stevioside, followed by steviolbioside and steviol. Twenty four hours after stevioside administration, stevioside was not detected

in cecal content, whereas a higher amount of steviol and unidentified metabolites appeared. At 72 hours, the percentage of radioactivity excreted into feces, urine, expired air and bile was 63.8, 2.2, 23.9 and 40.9% of administered dose, respectively. In bile and feces, steviol was found to be the major metabolite of stevioside after oral administration, but no information concerning metabolites in urine was reported. The investigators pointed out that stevioside was changed to steviolbioside and steviol in the cecal content at 4 hours and a large quantity of steviol appeared at that time. The same metabolites were also detected in bile, therefore, they suggested that the metabolites in cecal content at 24 hours originated from biliary excretion. The results mentioned above also supported the idea that stevioside is not absorbed by the upper part of the small intestine, but the metabolites formed by intestinal microflora and mainly in the cecum were absorbed by the lower part of the intestine. An increase in blood radioactivity was delayed, beginning at 4 hours after administration, which was related to the absorption of steviol and its metabolites from the intestinal tract. Most of the steviol that was changed to the conjugated form in the liver and excreted into the intestinal tract through the bile and the enterohepatic circulation was suggested to be involved in the reabsorption of steviol (222).

Later on, Cardoso and coworkers (27) also studied the pharmacokinetics of stevioside and its metabolites in male Wistar rats, but they used  $^{131}\text{I}$ -stevioside intravenous injection instead of the oral administration of  $^3\text{H}$ -stevioside, as reported by Nakayama et al. (222). The plasma radioactivity rapidly decreased within 30 minutes after intravenous injection, which demonstrated rapid distribution in the body. The highest radioactivity was observed in the liver and small intestine at 10 and 120

minutes after administration, respectively. At 4 hours after intravenous injection of  $^{131}\text{I}$ -stevioside, the level of radioactivity was highest in the large intestine, while radioactivity in the small intestine was decreased. They reported that radioactivity approximately 52% of the original dose was eliminated into bile within 120 minutes after injection. At that time, the radioactivity in the small intestine was also 52% and most of it occurred in intestinal content, while a small quantity appeared in intestinal tissue. The investigators did not report whether the radioactively-labeled compound detected in each organ or content was stevioside or its metabolites. By reversed phase high performance liquid chromatography (RP-HPLC) analysis, it was found that  $^{131}\text{I}$ -stevioside could be degraded *in vivo* into steviol and unidentified metabolites. Steviol was detected as the major metabolite in bile, and stevioside also appeared as 37.3% of the radioactivity present in bile. However, no steviol was detected in urine, only stevioside and unknown metabolites with the same retention time as that observed in bile were present in urine. From the results mentioned above,  $^{131}\text{I}$ -stevioside that was given intravenously into rats was probably metabolized in the liver to  $^{131}\text{I}$ -steviol, excreted in bile, entered the intestine and some parts were absorbed in the bowel of rats. This raised the question of whether stevioside could pass the cell membrane of liver and be converted to other byproducts, or not. Due to the discrepancy between results obtained from oral administration of  $^3\text{H}$ -stevioside into rats (222) and *in vitro* perfusion of stevioside to isolated perfused rat liver (223), it was found that, after oral administration, some stevioside was excreted unchanged in feces and urine, but most of it was believed to be degraded by intestinal microflora to steviol, steviolbioside, glucose and some unknown metabolites, and then they were absorbed in the cecum of

rat. Steviol was conjugated in the liver and excreted into the bile. The metabolism of stevioside was also studied using isolated perfused rat liver (223) to see whether stevioside could be metabolized in the liver. Stevioside at concentrations of 0.2 and 0.5 mM were recirculated for 2 hours. The perfusate was periodically collected for determination of the stevioside concentration in the perfusate at various time points using TLC. The result showed that the concentration of stevioside in the perfusate was not changed. This implied that stevioside could not be metabolized in isolated perfused rat liver. This result was in conflict with the data concerning the metabolism of stevioside reported by Cardoso and coworkers (27). Ishii-Iwamoto and Bracht (223) suggested possible explanations for the contradictory results mentioned above. Firstly, stevioside that was labelled with  $^{131}\text{I}$  at a double-bond in steviol moiety may cause a conformational change to a new structure that easily passes the hepatic membrane by transport systems and enzymatic systems. Secondly, the difference of experimental models between *in vivo* and *in vitro* experiments. Stevioside might interact with some factors in the blood that manage the passage of it to the liver, whereas no such factor was present in the perfusate medium.

In 1997, Hutapea et al. (26) examined the *in vitro* digestion of stevioside in various digestive enzymes such as  $\alpha$ -amylase, pepsin, pancreatin and intestinal brush border membrane enzymes, as well as the intestinal microflora of mice, rats, hamsters and humans. Using HPLC to detect stevioside and its metabolites after digestion, none of these enzymes digested stevioside except the intestinal microflora. More than 90% of stevioside was found to convert to steviol within 2 days of incubation by the microflora of rat and hamster cecal content. The incubation of stevioside with

microflora from humans and mice produced not only steviol, but also steviol-16, 17 $\alpha$ -epoxide at the end of a 2-day incubation period by human microflora, and 4 days by mouse microflora. Therefore, steviol was the major metabolite produced by intestinal microflora from various animal species *in vitro*. Further investigation of the metabolism of stevioside in the body was performed to detect various metabolites in plasma, feces and urine from hamsters treated with stevioside at an oral dose of 1 g/kg BW (224). Stevioside and its metabolites, steviol-16, 17 $\alpha$ -epoxide, 15 $\alpha$ -hydroxysteviol and steviolbioside, were found in plasma, feces and urine. Isosteviol, a metabolite of stevioside produced by acid hydrolysis, was detected in urine and feces. Steviol, the major metabolite of stevioside by intestinal microflora, only appeared in feces, not being detected in plasma or urine. From the distribution of stevioside and its metabolites in tissues, steviol was found only in brain. The metabolites appearing in the kidney and liver were similar, and were composed of stevioside, steviol-16, 17 $\alpha$ -epoxide, 15 $\alpha$ -hydroxysteviol and steviolbioside (225). The largest metabolite detected in kidney tissue was 15 $\alpha$ -hydroxysteviol, whereas in urine, the quantity of isosteviol was found to be slightly greater than 15 $\alpha$ -hydroxysteviol. From these results, stevioside appeared to be excreted from the body, both in the parent and degraded form, therefore it is probable that stevioside might be absorbed in the digestive tract, both in the form of stevioside and its metabolites. How stevioside is transported by any tissue in the body is still questionable and requires further investigation.

## **5. The Biochemical, Physiological and Pharmacological Effects of Stevioside and Steviol**

The extract of the stevia plant and its major active constituents exhibit a number of biochemical, physiological and pharmacological properties. It has been reported as being used in such commercial products as herbal tea, and to be used for flavor enhancement as well as a therapeutic agent. It was reported that stevia extract and stevioside have been used in a number of countries such as Japan, China, Malaysia and South Korea. The extract is approved to be used as a food ingredient in Brazil, Japan and South Korea (226). Investigations concerning the safety of stevia extract and stevioside have been performed in many aspects, including their physiological and pharmacological effects.

### **5.1 Toxicological, mutagenic, teratogenic and carcinogenic effects**

To test the toxicity of substances using laboratory animals, it is usual to increase the dose of the substance until a lethal dose is reached.  $LD_{50}$ , which is the dose of substance where 50% of the test animals die, is reported to reveal the toxicity of a substance. The  $LD_{50}$  value was variable according to the purity of stevioside, the animal species used and the route of administration (213).  $LD_{50}$  values in both mice and rats were in the range of 8.2-42 g/kg BW after oral administration, whereas that in hamsters and guinea pigs were in the range of 4.1-6.1 and lower than 4.1 g/kg BW, respectively. When stevioside and stevia products were given intravenously, intraperitoneally and subcutaneously, the  $LD_{50}$  values were decreased. This indicated that animals are more susceptible to stevia extract and stevioside when given

intravenously, subcutaneously and intraperitoneally than by oral administration (213). In 1997, Toskulkao et al. (227) reported that stevioside at a dose of 15 g/kg BW was not lethal to mice, rats and hamsters after oral administration. Steviol, a product of the enzymatic hydrolysis of stevioside, was, however, found to be lethal to the animals. The LD<sub>50</sub> value of steviol in hamsters was in the range of 5.2-6.1 g/kg BW, which was lower than that of rats and mice (15 g/kg BW).

Toxicity found after stevioside (90% pure) treatment was reported by Panichkul et al. (24). When rats and hamsters were treated with 4.1 g/kg BW of stevioside (90% pure) intragastrically, at 6 hours after treatment a depression of urinary excretion and an elevation of blood urea nitrogen, creatinine and uric acid were observed. This showed that stevioside affected renal function. Histopathological changes were observed in the kidneys, such as necrosis of epithelial cells and dilatation of convoluted tubules. Toskulkao et al. (22) confirmed this effect of stevioside by subcutaneous injection into rats at a dose of 1.5 g/kg BW. They found nephrotoxicity, the same as that observed by Panichkul (24), and that the proximal tubule seems to be the target site of stevioside action. In contrast, a high purity of stevioside (96% pure) at doses as high as 15 g/kg BW given intragastrically to rats, mice, and hamsters did not harm renal function, and no histopathological changes were observed (227). Similar results were obtained in anesthetized dogs given 26 mg/kg BW of stevioside intravenously (228). This showed that a high purity of stevioside seemed to be safe. In contrast, steviol (93% pure) was shown to be more toxic than stevioside. Steviol at a dose of 15 g/kg BW given intragastrically into rats and mice resulted in weakening of the limbs and the animal became drowsy at 1 hour

after treatment, but no histopathological changes were observed. In hamsters, treatment of steviol at doses of 5.2-6.1 g/kg BW orally caused them to become drowsy and lose strength in their limbs. Most of the hamsters died within 48 hours after treatment. Histopathological changes were also observed in the kidney, it being swollen, pale and showing a marked vacuolar degeneration in the cytoplasm of the proximal tubular cells. It was suggested that steviol caused acute renal failure resulting in the death of animals, because BUN and creatinine were also increased (227). This result was supported by the studies of Jitrawang (229) and Chairoungdua (230). Additionally, *in vitro* incubation of rat renal cortical slices with steviol 1.56-100  $\mu$ M for 30 min inhibited PAH accumulation significantly (23). This result also indicated the nephrotoxicity of steviol, because PAH accumulation is widely used for screening unknown chemicals for the evaluation of nephrotoxicity.

One month of stevioside (2.5 g/kg BW/day) administration via stomach tube into male and female rats did not induce any change in blood serum components and no histopathological changes were observed in the liver (231). High doses of 2.98 g/kg BW/day of stevia given to male rats and 3.02 g/kg BW/day given to female rats for 3 months did not induce any change in blood serum components (232). Long-term stevioside administration was performed in male and female rats and hamsters (213, 233). The rats fed with stevia extracts (92.5% stevioside) at a level of 1 g% in diet (corresponding to 550 mg/kg BW) for 2 years showed no significant change in growth, organ weights, hematological or kidney histological appearance (233). The same results were obtained from hamsters treated with stevioside (1 g/kg BW) for 6 months (213), and stevioside was reported to not be

carcinogenic in rats and hamsters. In 1992, a similar study was performed by Xili and coworkers (234). The rats were fed with a diet containing stevioside (85% pure) in the amounts of 0.2, 0.6 and 1.2% (w/w) for 2 years. No stevioside treatment-related changes were observed at the end of 6, 12 and 24 months. Moreover, no differences of food utilization, growth, lifespan, hematological and urinary biochemistry, as well as neoplasm incidence between the rats in the control and stevioside-treated groups were observed.

From the results obtained by Xili et al. (234), an acceptable daily intake of stevioside was calculated and reported to be 7.938 mg/kg BW/day. A likely maximum intake of stevioside by humans was about 2 mg/kg BW/day, which was far below the dose of stevioside suggested to be safe to use without toxic effects. Recently, the toxicity of stevioside was also studied (235). Rats were fed with a powdered diet containing stevioside in the amounts of 2.5 and 5% (w/w) for 2 years (104 weeks). The rats who received stevioside weighed less than those in the control group, this result perhaps being explained by stevioside having no caloric value. A reduction in growth rate was also observed in hamsters treated with stevioside at a dose of 2.5 g/kg BW/day orally for 12 weeks (13). Histopathological examination of the organs and tissues of rats showed no difference between stevioside-treated and control animals, and there was no significantly altered development of neoplastic and non-neoplastic lesions in any organ or tissue. However, one interesting difference was that the female rats who took stevioside had a decreased incidence of breast tumors, while the male rats displayed a lesser incidence of kidney damage. Thus, it was concluded that stevioside was not carcinogenic in rats (235).

Concerning the contraceptive property of stevioside as reported by Planas and Kuc (5), female rats who received a 5% stevia extract showed a fertility rate that was significantly reduced by approximately 65%. In male rats, a concentrated crude extract of *Stevia rebaudiana* leaves was given orally to the rats, starting at prepubertal age (25-30 days old) and continuing for 60 days. The results showed that their body weight gain and the final weight of testis and prostate did not significantly differ from the control group. Only seminal vesicle weight fell by about 60% in stevia extract-treated rats. It was concluded that the decreased fertility was not exerted on male rats treated with stevia extract. In 1991, a study was performed by researchers in Thailand to study the consequences of daily ingestion of stevioside in hamsters and its effects on two subsequent generations (236). One-month-old hamsters of both sexes were treated with 0.5, 1.0 and 2.5 g/kg BW/day of oral stevioside daily. At the age of 2 months, the animals were mated. The next 2 generations of hamsters were treated with the same procedure. The study showed no significant difference in the average growth of each generation of hamsters in the stevioside-treated groups. The fertility of the hamsters, their gametogenesis and reproductive tract function were normal in both sexes, and mating was efficient and successful. The duration of pregnancy and the number of implanted fetuses were also unaffected by stevioside (211, 236). A study by Mori and coworkers also found that a diet containing 3% (w/w) stevioside given to male rats for 60 days before and during mating, and to female rats for 14 days before mating and 7 days during gestation did not show any adverse effects on fertility or on fetal development (237). Stevioside at doses of 0.25, 0.5 and 1 g/kg BW/day given orally to pregnant rats once a day on day

6 through day 15 of gestation did not cause the fetal malformation, and no toxic signs in the pregnant rats or fetuses were observed (238). Given gastrically, stevioside at 0.5, 1.0 and 2.0 g/kg BW/day for 5 consecutive days for 8 weeks into male hamsters did not affect fertility, sperm motility or morphology (230). There was also no effect on the total number of all implants and live implants or on general reproductive parameters in dams and pups (229).

It has been known that stevioside is converted to steviol by intestinal microflora (25), so stevioside taken orally may change to steviol, and steviol may cause any effect in the tested animals. Previous studies by Pezzuto et al. (239) and Matsui et al. (240) reported a highly mutagenic effect of steviol after metabolic activation on the *Salmonella typhimurium* strain TM 677, as well as chromosomal aberration in the Chinese hamster lung fibroblast cell line. This showed the mutagenicity of steviol in bacteria, but it seemed likely that steviol itself was not mutagenic, but required further transformation in the body to elicit a mutagenic substance. No investigations were performed in animals *in vivo* until 1998, when Wasuntarawat and colleagues studied the toxicity of steviol in hamsters. Steviol at doses of 0.25, 0.5, 0.75 and 1.0 g/kg BW/day were given orally to pregnant hamsters on days 6-10 of gestation. Toxicity to both dams and fetuses was observed in hamsters treated with 0.75 and 1.0 g/kg BW/day, maternal body weight gain was decreased and maternal mortality rate was high, as well as the number of live fetus and mean fetal weight also being significantly decreased in both steviol-treated groups (241). The dose of steviol used in this experiment was equivalent to stevioside 625 mg/kg BW/day, which is approximately 80 times higher than the dose suggested for

human consumption (7.938 mg/kg BW/day). Thus, if human daily intake is considered, toxic effects of steviol from stevioside degradation should not occur.

## 5.2 Pharmacological and biochemical effects

The pharmacological effect of stevioside was studied by Kurahashi and coworkers (242), and showed that oral administration of stevioside at a dose of 0.5 g/kg BW/day did not affect sleeping time in mice (242). In addition, stevioside did not cause physiological changes in vital signs, blood pressure, body temperature or EKG after oral administration in rabbits, even at a dose as high as 15 g/kg BW (242). Therefore, stevioside seems to have no harmful effect when taken orally. However, the intravenous injection of stevioside at a dose of 0.4 g/kg BW caused bradycardia, hypotension and hyperventilation (242). A subsequent study by Melis et al. in 1986 (243) had also demonstrated that intravenous infusion of stevioside (16 mg/kg BW/hr) caused hypotension, diuresis, natriuresis and kaliuresis in rats. They suggested further that the mechanism by which stevioside produced these effects was through either a calcium or prostaglandin pathways, since these effects were analogous to those of verapamil (a calcium antagonist), and indomethacin (a prostaglandin inhibitor) could abolish these actions of stevioside (7, 8). These findings showed the effects of stevioside when injected directly into the blood circulation. Steviol, the major metabolite of stevioside, was also reported to cause diuresis and natriuresis without any significant change in blood pressure after doses of 1.0 and 3.0 mg/kg BW/hr were given by intravenous injection to rats (28).

The contraceptive property of *Stevia rebaudiana* extract and stevioside has been studied by several researchers, but no final conclusion has been

reached. Planas and Kuc (5) reported that the leaves and stem of the stevia plant which are supposed to contain stevioside were used successfully as an oral contraceptive drug in native people in Paraguay. They also reported that there was a reduction in the conception rate of female rats drinking a 5% (w/v) aqueous extract of *S. rebaudiana*, an effect that was apparently not reversible following drug withdrawal (5). Similar results were reported later by Portella-Nunes and Pereira (244) in female mice. However, Mori et al. (237) found contradictory results, that various doses of a high purity of stevioside (95-98%) given orally to rats did not have a contraceptive property. On the other hand, a previous report described anti-androgenic activity due to dihydroisosteviol, a diterpenoid acid derived from *S. rebaudiana* (245). Administration of dihydroisosteviol to the chick's comb at a dose of 3.0 mg/comb inhibited the action of testosterone. Purified stevioside was shown *in vitro* to displace 5 $\alpha$ -dihydrotestosterone specifically bound to prostate androgen receptors (246). Later studies carried out in male rats showed that chronic administration of Stevia extract did not alter the number of binding sites for androgens (247). However, it produced a decrease in final weight of testis, seminal vesicles and cauda epididymis. The fructose content of accessory sex glands and epididymal sperm concentration were also decreased (248).

In addition, a hypoglycemic effect was reported due to total extracts of *Stevia rebaudiana* and purified stevioside (12, 249), but contradictory or results were reported by Suanarunsawat & Chaiyabutr (16) and Lee et al. (250).

The biochemical effect of stevioside and its derivatives on carbohydrate metabolism and oxidative phosphorylation was reported. Susuki et al.

(249) found that 0.5 g% stevioside or 10 g% of powdered *Stevia rebaudiana* leaves in either a high-carbohydrate or high-fat diet significantly decreased blood glucose level and liver glycogen storage during a four-week period of study, while a lower concentration, 0.1 g% stevioside, showed a reduction in liver glycogen storage but not blood glucose level (249). In 1985, Bracht et al. (251) studied the effect of stevioside and other steviol derivatives extracted from *Stevia rebaudiana* leaves on rat liver mitochondrial functions *in vitro*. Stevioside and its derivatives, steviolbioside, isosteviol and steviol, had an inhibitory effect on oxidative phosphorylation and the activity of several mitochondrial enzymes such as ATPase, NADH-oxidase, succinate oxidase, succinate dehydrogenase and L-glutamate dehydrogenase. The potency of this inhibitory activity of stevioside was lower than that of steviolbioside, steviol and isosteviol (251, 252). In contrast, Yamamoto and coworker (253) demonstrated that stevioside was different from other steviol derivatives with respect to the oxidative phosphorylation inhibitory effect in intact cells. They observed that steviol and isosteviol could inhibit oxygen consumption, energy metabolism and gluconeogenesis in both isolated mitochondria and intact rat renal tubules, but stevioside and steviolbioside did not show an inhibitory effect in intact isolated rat renal tubular cells (253). From these observations, stevioside, which has a disaccharide molecule in the structure, may not directly inhibit energy metabolism in intact cells because it cannot enter the cells. This idea was later supported by Ishii et al. (15). They reported that stevioside inhibited D-glucose transport across the cell membrane of intact rat liver, but did not affect D-glucose metabolism (15). Steviol was also reported to inhibit mitochondrial adenine nucleotide translocation (254). Taken together, it can be

concluded that stevioside and its metabolites could inhibit oxidative phosphorylation in mitochondria, based on *in vitro* studies. However, stevioside seems to exhibit less of an inhibitory effect than its metabolites. Recently, a contradictory result was obtained from *in vivo* study of the influence of stevioside and steviol on glycogen levels in fasted rats (255). When 24-hour fasted rats were given a single dose of stevioside (200  $\mu\text{mol}$ ) or steviol (200  $\mu\text{mol}$ ) orally, both stevioside and steviol increased initial glycogen deposit in the liver. The level of increased liver glycogen was higher in rats treated with stevioside plus fructose or steviol plus fructose than in rats treated with stevioside or steviol alone. Due to the small tendency toward higher glycogen levels when stevioside or steviol were given alone, it could not be concluded with certainty whether these compounds influence glycogen synthesis in the absence of exogenous substrates. Therefore, steviol and stevioside were administered to the rats via the drinking water at concentrations of 1.0 and 2.0 mM during fasting periods of 24 and 48 hours. The hepatic glycogen level was increased at 48 hours with 1.0 mM stevioside treatment, and at 24 hours with 2.0 mM stevioside treatment. Steviol had no effect on hepatic glycogen levels when given in drinking water (255). This result showed that stevioside ingested during 24- and 48-hour fasting influenced glycogen levels, and there were complex time effects superimposed on the dose effects. However, the amount of stevioside ingested during 24- and 48-hour fasting were between 30 and 80  $\mu\text{mol}$ , which was below the single dose of 200  $\mu\text{mol}$  given orally, as mentioned above. The results implied that stevioside had a stimulatory action on glycogen deposition in rat liver under *in vivo* gluconeogenic conditions, this being contradictory to results obtained with stevioside treatment under *in vitro*

conditions. Thus, it is very difficult to define the mechanism underlying the effects found in these experiments.

### 5.3 The effect on glucose absorption

A high dose of stevioside at 2.5 g/kg BW/day given intragastrically to hamsters for 12 weeks caused inhibition of glucose absorption, whereas lower doses of 0.5 and 1 g/kg BW/day had no significant effect (13). They also found that reduction in the activity of intestinal  $\text{Na}^+\text{-K}^+$  ATPase and the absorptive surface area were responsible for the inhibition of glucose absorption. Subsequently, Toskulkao and coworkers (14, 256) studied the effect of stevioside (96% pure) and steviol (90% pure) on intestinal glucose absorption in hamster jejunum *in vitro* using jejunal ring tissue and everted jejunum sac. It was found that the presence of stevioside at concentrations of 1 and 5 mM in the media had no inhibitory effect on glucose absorption. In contrast, steviol at a concentration of 1 mM and higher inhibited glucose absorption, in a manner related to its concentration and incubation time. However, steviol at concentrations of 0.1 to 2 mM did not inhibit glucose absorption into brush border membrane vesicles of hamster jejunum (256). After exposure of the hamster jejunum to 1 and 2 mM steviol for 60 minutes, the villus absorptive cells were degenerated, swollen and ruptured (14). A decrease in intestinal mucosal ATP content and activities of mitochondrial NADH cytochrome c reductase and cytochrome oxidase were also observed after steviol treatment, but no inhibitory effect on intestinal  $\text{Na}^+\text{-K}^+$  ATPase activity was observed (256). These results suggested that the inhibitory effect of steviol on intestinal glucose absorption was due to the alteration in morphology of intestinal absorptive cells and the reduction in mucosal

ATP content. The reduction in mucosal ATP content was accompanied by a decrease in the activities of mitochondrial enzymes. It is probable that the decreased glucose absorption involved the inhibitory effect of steviol on intestinal mitochondria at the level of phosphorylation.

#### **5.4 The hormonal effects of stevioside and steviol**

In 1980, Usami and coworkers (257) studied the effect of stevioside on arginine-induced insulin and glucagon secretion in isolated perfused rat pancreas. Stevioside at a concentration of 0.015 mM produced a slight increase in insulin and a slight decrease in glucagon induced by arginine, but these changes were not significant (257). It seemed likely that stevioside had only slightly influenced arginine-induced insulin and glucagon secretions in the perfused rat pancreas. However, they concluded that stevioside has no direct action on pancreatic A and B cells. An *in vivo* study by Curi et al. (12) in Brazil showed that aqueous extracts of 5 g of stevia leaves significantly decreased plasma glucose levels in normal adult humans who received the extract at 6-hour intervals for 3 days. Some hormonal changes might be involved in the decreased plasma glucose level after stevioside treatment (12). Subsequent studies showed the effect of stevioside on glucose metabolism. Experiments were performed in male rats treated with stevioside given orally at doses of 2 g/kg BW twice (2 consecutive 45-minute periods) or 0.1, 0.15 and 0.2 g/kg BW/hr given intravenously for 1 hour (258). The results showed that plasma glucose levels significantly increased with the intravenous infusion of stevioside but did not show any effect with orally-administered stevioside. The plasma insulin level did not change during stevioside infusion. This result implied that the increase in

plasma glucose level during the intravenous infusion of stevioside was not due to the reduction of plasma insulin level. It was probably the effect of stevioside interfering with the transport process of glucose across the cell membrane. Furthermore, norepinephrine, prostaglandin and nitric oxide were found to participate in the increase of plasma glucose levels and the inhibition of glucose-stimulated insulin release after stevioside was given intravenously (258). In contrast, *in vitro* studies performed by Belgian and Danish researchers showed an increase in insulin release from pancreatic islets isolated from female rats and mice (259, 260). Malaisse and coworkers (259) incubated the rat pancreatic islets with 0.1 to 1.0 mM stevioside in the presence of 7.0 mM (or 126 mg/dl) D-glucose, they found that a progressive increase in insulin release and a significant elevation of insulin output occurred only when a high concentration (1.0 mM) of stevioside was used (259). Recently, Jeppensen and colleagues reported that stevioside and steviol at concentrations of 1 nM to 1 mM showed dose-dependent enhanced insulin secretion from incubated mouse islets in the presence of 16.7 mM (or 300 mg/dl) glucose (260). They also demonstrated potentiated insulin secretion from the islets of mice produced by 1 mM stevioside and 1  $\mu$ M steviol in the presence of glucose 8.3 mM (or 150 mg/dl) or above in the incubating medium. Stevioside and steviol did not show the insulinotropic effect on pancreatic  $\beta$ -cells when lower concentrations of glucose (3.3 mM or 60 mg/dl) were used in the medium. At present, the mechanisms responsible for stevioside and steviol effects are still unclear. Recently, it was reported that both stevioside and steviol did not influence the plasma membrane  $K^+$  adenosine triphosphate ( $K^+_{ATP}$ ) –sensitive channel activity and cyclic adenosine monophosphate

(cAMP) levels in islets (260). However, these results suggested that stevioside and steviol stimulated insulin secretion via a direct effect on pancreatic  $\beta$ -cells. Therefore, this might be important for the treatment of type 2 diabetes. Both stevioside and steviol seem to have an advantage in their lack of insulin stimulation at subnormal glucose levels, thus, they may reduce or eliminate the risk of hypoglycemia which can occur with other hypoglycemic drugs used for diabetic treatment.

### 5.5 Cardiopulmonary effects

In 1992, Kurahashi et al. reported that oral administration of stevioside at a dose of 15 g/kg BW did not affect blood pressure, respiration, body temperature or the electrocardiogram of rabbits, whereas the intravenous administration of a lower dose (0.4 g/kg BW) produced a reduction in heart rate and blood pressure (242). Later on, Melis et al. (243) also demonstrated that stevioside at a dose of 16 mg/kg BW/hr given intravenously to rats could reduce blood pressure and alter renal function. A hypotensive effect was observed in both normal and hypertensive rats treated by intravenous infusion of 16 mg/kg BW/hr stevioside (10). The possible mechanisms by which stevioside reduced mean arterial blood pressure were suggested to act through the calcium and prostaglandin pathways (7-9). Verapamil, a calcium antagonist, tended to increase the renal and systemic effects of stevioside, whereas  $\text{CaCl}_2$  infusion induced a reduction in the vasodilating responses to stevioside (7-9). Indomethacin, a prostaglandin inhibitor, was able to abolish stevioside's action on blood pressure (7). Additionally, the chronic oral administration of *Stevia rebaudiana* extract, corresponding to 2.67 g dry leaves/day, in rats resulted in a significantly decreased mean arterial blood pressure after a 30-day treatment in

both normal and hypertensive rats (19). Similar results were obtained from 40- and 60-day extract treatment with the same dose in normal rats (18). Furthermore, Chan and colleagues (11) studied the effect of stevioside on blood pressure in conscious spontaneously hypertensive rats (SHR) after intravenous injection at doses of 50, 100 and 200 mg/kg BW. The results displayed a reduction in both systolic and diastolic blood pressure in a dose-dependent manner for more than 60 minutes following the injection. Serum dopamine, norepinephrine and epinephrine levels were not changed significantly during 60 minutes after intravenous injection of stevioside 100 mg/kg BW into anesthetized SHR. Therefore, it was concluded that stevioside had antihypertensive activity through a mechanism unrelated to changes of sympathetic tone (11). From these findings, researchers speculate that stevioside and stevia extract may be applied to the treatment of hypertensive patients in future, since they can reduce blood pressure as mentioned above. Steviol, the metabolite of stevioside, was also investigated for its effect on blood pressure. The intravenous infusion of steviol at doses of 0.5, 1.0 and 3.0 mg/kg BW/hr did not significantly alter mean arterial blood pressure in rats (28).

### **5.6 Renal effects**

In 1986, Melis and coworkers (243) studied the effect of stevioside on renal function and mean arterial pressure. The intravenous infusion of stevioside at doses of 8 and 16 mg/kg BW produced a statistically significant decrease in mean arterial blood pressure in rats. A dose of 16 mg/kg BW produced a diuretic effect. In 1992, Melis confirmed the effect of stevioside on rat renal function using an *in vivo* clearance technique (9, 10, 17). The continuous intravenous infusion of stevioside at

various doses into rats produced several changes in renal functions. Infusion of stevioside at higher doses (8, 12 and 16 mg/kg BW/hr) could induce natriuresis, diuresis and increased renal plasma flow (RPF), but did not affect the glomerular filtration rate (GFR), whereas infusion of stevioside at lower doses (4 mg/kg BW/hr) did not affect any of the above-mentioned parameters. From these results, it was suggested that stevioside may cause vasodilation of both afferent and efferent arterioles similar to other vasodilator substances such as prostaglandins, bradykinin and acetylcholine. The mechanisms of stevioside that underlay the effects mentioned above were subsequently studied by the same research group in Brazil. The renal effects of stevioside were suggested to work through  $\text{Ca}^{++}$  and prostaglandin pathways (7, 8). The decrease in mean arterial pressure and increased renal plasma flow observed by a stevioside dose of 16 mg/kg BW were inhibited by the administration of indomethacin, an inhibitor of prostaglandin synthesis, at a dose of 2 mg/kg BW (7, 8). Indomethacin was able to abolish stevioside-induced diuretic, natriuretic and kaliuretic effects. Therefore, the action of stevioside on renal function, including an increase in renal plasma flow, diuresis and natriuresis, seems to be dependent on prostaglandin activity. Moreover, the effect of stevioside on the changes of renal function were reported to involve the inhibition of the  $\text{Ca}^{++}$  pathway (7-9). Verapamil, a specific inhibitor of calcium, tended to increase the renal effects of stevioside, while, in contrast, an infusion of  $\text{CaCl}_2$  in rats induced attenuation of renal function changes in response to stevioside (8). The urine flow rate and the fractional excretion of sodium and potassium that were increased by stevioside were abolished

after  $\text{CaCl}_2$  treatment (8). These data indicated that a mechanism evoked by  $\text{Ca}^{++}$  ions may be involved in the effects of stevioside on renal function.

In addition, an increased excretion of water and sodium was observed following stevioside infusion, in spite of no change being seen in GFR. This may have been produced by decreased water and sodium reabsorption in the proximal tubules due to an increase in hydrostatic pressure and a decrease in oncotic pressure in peritubular capillaries. These studies were supported later by studies with oral administration of a crude extract of *Stevia rebaudiana* in rats (18, 19). Melis (17) also found that stevioside clearance was higher than inulin clearance at all doses of stevioside used (4, 8, 12 and 16 mg/kg BW/hr) after intravenous infusion into rats at 30-minute intervals. These results indicated that stevioside was secreted by renal tubular epithelium. Moreover, glucose clearance was also increased after stevioside at doses of 8, 12 and 16 mg/kg BW/hr were given to rats, indicating a fall in glucose reabsorption by renal tubular cells. This also suggested that stevioside might inhibit monosaccharide transportation in rat renal tubules, as was seen in intact rat liver cells by the study of Ishii et al. (15). Therefore, it is possible that stevioside may induce an osmotic diuresis.

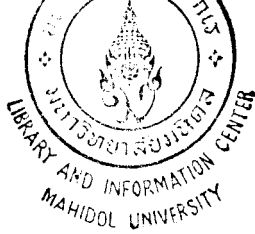
It has been shown that stevioside affected both cardiovascular and renal systems. Therefore, as regards the alteration in renal functions as mentioned above, it could not be concluded whether there were due to a primary effect of stevioside on renal functions or to a secondary effect from cardiovascular disturbance. Panichkul and colleagues (24) demonstrated that the intragastric treatment of hamsters with stevioside at a dose of 4.1 g/kg BW resulted in a

significant increase of BUN and creatinine and also markedly depressed urine volume. In addition, they found that stevioside induced the necrosis and dilatation of the proximal convoluted tubules (24). These findings suggested that stevioside caused nephrotoxicity. Further investigations were performed by Toskulkao and coworkers in 1994 (22, 23). They reported that subcutaneous injection of stevioside (1.5 g/kg BW) into rats caused an increase in brush border membrane enzymes such as alkaline phosphatase and  $\gamma$ -glutamyl transpeptidase in urine. Stevioside was also found to induce nephrotoxicity, as indicated by an increase in blood urea nitrogen and plasma creatinine levels of about 180% and 132%, respectively, at 9 hours after stevioside treatment (22). A decrease in PAH accumulation in rat renal cortical slices was also demonstrated with the same treatment of stevioside as mentioned above (23). The *in vitro* incubation of rat renal cortical slices with 6.25-100  $\mu$ M stevioside showed that it significantly reduced the accumulation of PAH into the slices after a 30-minute incubation (23), and histopathological changes of the proximal convoluted tubules were observed after stevioside at a dose of 1.5 g/kg BW was given subcutaneously to rats. It is possible that stevioside may directly affect the proximal convoluted tubular cells; in other words, the major site of stevioside action might be at the renal proximal tubules. Later on, Thongouppakarn (20) investigated the effect of stevioside on rat renal function by injecting stevioside directly into the left renal artery. He found that intrarenal arterial injection of stevioside at a dose of 0.8  $\mu$ g/min caused natriuresis and diuresis without any changes in the RPF and GFR, whereas a higher dose of stevioside (6.4  $\mu$ g/min) increased the RPF and caused diuresis without any change in the GFR. Its effects on proximal tubular water and sodium reabsorptions were determined using

lithium clearance. He reported that sodium and water reabsorption in proximal tubules was decreased, and concluded that the major cause of natriuresis and diuresis was the inhibition of water and sodium reabsorption in the proximal tubules (20). However, it could not be concluded with certainty that stevioside had a direct effect on proximal tubular function. The results observed above may be due to the dilation of afferent and efferent arterioles, resulting in increased peritubular capillary pressure, which then caused a reduction in the tubular reabsorption of sodium and water. This possibility of direct action as the possible mechanism of stevioside's effects was investigated in rabbit renal proximal tubule suspensions by Limpanichakul in 1995 (21). The effect of stevioside on the  $\text{Na}^+\text{-K}^+$  ATPase activity of rabbit renal proximal tubules was determined and  $^{14}\text{C}$ -PAH accumulation into the tubular cells was used as an indicator for renal proximal tubular function. The results showed that stevioside (0.1 and 1.0 mM) decreased  $\text{Na}^+\text{-K}^+$  ATPase activity and  $^{14}\text{C}$ -PAH accumulation in a dose-dependent manner. However, the decrease in  $\text{Na}^+\text{-K}^+$  ATPase activity was completely reversible after a low dose of stevioside (0.1 mM) was removed from the incubation medium, whereas the depression of PAH accumulation was only partially reversible. But a higher dose (1.0 mM) of stevioside caused the partial reversibility, both in PAH accumulation and  $\text{Na}^+\text{-K}^+$  ATPase activity (21). This finding led to the suggestion that the changes in proximal tubular function after stevioside treatment may partially involve  $\text{Na}^+\text{-K}^+$  ATPase activity. A contradictory result was obtained in a subsequent study by Podprasart (261). She demonstrated that stevioside (up to 2 mM) with the higher purity (98%) used in her experiment neither inhibited nor changed the activity of  $\text{Na}^+\text{-K}^+$  ATPase activity in isolated renal proximal tubular

suspensions. These conflicting results may be due to the difference in purity of stevioside used in Limpanichakul's and Podprasart's experiments. Recently, the mechanisms of stevioside's effects on rat renal function were investigated *in vivo* using a lithium clearance study to demonstrate the effect of stevioside on proximal tubular sodium and water reabsorption (258). This was similar to the experiment performed by Thongouppakarn in 1994 (20), except for the doses and route of stevioside administration. They infused stevioside intravenously at a dose of 0.2 g/kg BW/hr, whereas Thongouppakarn had used 0.8 and 6.4  $\mu\text{g}/\text{min}$  (approximately 0.192 and 1.54 mg/kg BW/hr) injected directly into the left renal artery. The results from both experiments showed a decrease in water and sodium reabsorption by the proximal tubules. After a 0.2 g/kg BW/hr intravenous infusion of stevioside for 30 minutes, a reduction of  $\text{Na}^+\text{-K}^+$  ATPase activity was observed in both renal cortex and the whole kidney, and the activity of mitochondrial ATP synthetase declined, indicating an inhibition of oxidative phosphorylation following stevioside treatment. The reductions in renal mitochondrial ATP synthetase and  $\text{Na}^+\text{-K}^+$  ATPase activities might be the causes of natriuresis and diuresis in stevioside-treated rats (258). However, these findings were in conflict with the results obtained by Yamamoto et al. in 1992 (253), wherein they reported that stevioside did not affect the gluconeogenesis and oxygen uptake in rat renal cortical tubules (253).

The effect of steviol, the aglycone part of stevioside and other natural glycosides, on renal function was initially investigated in rats by Melis in 1996 (28), using an *in vivo* clearance technique. Steviol at doses of 0.5, 1.0 and 3.0 mg/kg BW/hr given intravenously resulted in no significant changes in mean arterial blood



pressure, GFR or RPF. Only doses of 1.0 and 3.0 mg/kg BW/hr of steviol infusion induced a significant increase in urinary flow (V/GFR) and fractional sodium and potassium excretion ( $FENa^+$ ,  $FEK^+$ ), when compared to those of control levels. It was suggested that steviol may affect the water and salt transport in the renal tubules, but the mechanism of this action is still unknown. The *in vitro* study, the incubation of rat renal cortical tubules in a medium containing various concentrations of steviol (0-3 mM) for 60 minutes, produced an inhibition of gluconeogenesis and oxygen uptake into the renal tubules (253). The data obtained from this study suggested that steviol might exhibit an action related to mitochondrial function.

#### 6. Other Effects of Stevioside and Some Utilization

Besides the pharmacological and physiological effects mentioned above, studies on the antimicrobial activity of stevia extract have indicated that stevia has a potential role in the prevention of dental caries (262). In addition, a fermented aqueous extract from *Stevia rebaudiana* exhibited bactericidal activity toward a wide range of food-borne pathogenic bacteria, but this extract was no significant killer of normal microflora in the gastrointestinal tract such as Lactobacilli and Bilidobacteria (218). Previously, stevioside and rebaudioside A were tested for cariogenicity in rats (262). Stevioside or rebaudioside A or sucrose was added to a basal diet fed to rat pups for 5 weeks. The results showed a significant difference in caries scores between the rats fed with a diet that contained sucrose as a component and other groups fed with a diet containing natural glycosides, including a control group. No significant difference in the incidence of cariogenicity was observed in rats fed with a diet containing stevioside or rebaudioside A and the no-addition groups. Therefore, it was

suggested that stevioside and rebaudioside A are noncariogenic. Recently, Kinghorn and colleagues (263) reported a relationship between the dietary consumption of sucrose substitutes including stevioside and rebaudioside A and the incidence of dental caries. Stevioside and rebaudioside A were shown to be noncariogenic intense natural sweeteners (263). There were reports from the Hiroshima University School of Dentistry and Purdue University's dental research group concerning the noncariogenic property of stevia. It was found to retard plaque accumulation on the teeth and also to suppress the bacterial growth that causes cavities. Therefore, stevia added to toothpaste and mouthwash may be able to improve dental health (264).

Additionally, stevia was reported to have an excellent healing capability. A significant reduction in pain, as well as accelerated healing were observed when stevia was placed on a cut or scrape (264). The stevia extract could be used as a facial mask by smoothing the dark liquid over the entire face for 30-60 minutes. It was reported to help tighten the skin, smooth out wrinkles and heal skin blemishes and acne, and can also be used on seborrhea, dermatitis and eczema, as well. It could be added to shampoo to benefit hair and scalp (264).

With its sweetness and zero calorie content, the stevia plant, added to dog food was reported to increase its palatability in place of the usual sugar addition. This could be useful for older and obese dogs (265).

Based on the various findings mentioned above, stevia extract and stevioside seem to be herb products with potential applications in both therapeutic and commercial products. However, more information concerning its safety is still

required. *Stevia rebaudiana* could be an important economic plant and generate more income for our country in the future.



## CHAPTER III

### MATERIALS AND METHODS

#### ANIMALS

Male New Zealand white rabbits weighing 1.5-2.5 kg were obtained from the Faculty of Veterinary Science, Chulalongkorn University, and were cared for by the Animal Center, Faculty of Science, Mahidol University. The rabbits were housed in stainless-steel cages (1 rabbit/cage), fed with a standard rabbit diet *ad libitum* and had free access to water.

#### CHEMICAL SUBSTANCES

The chemicals using for buffered media were analytical grade obtained from many sources.

Ouabain and mineral oil were purchased from Fluka Chemie AG, Switzerland.

PAH, Fiske and Subbarow reducer, probenecid, dextran, ATP, bovine serum albumin, stevioside, Folin-ciocalteu's phenol reagent and collagenase type IV (from *Clostridium histolyticum*) were purchased from Sigma Chemical Co., MO, USA.

Percoll was purchased from Pharmacia Biotech AB, Uppsala, Sweden.

For radioisotope chemicals: Aminohippuric acid, p-[Glycyl-1-<sup>14</sup>C]- (specific activity 40.60 mCi/mmol) was purchased from DuPont NEN<sup>®</sup>, Boston, MA, USA. Triton X-100, toluene, and 1,4-bis-[2-5-phenyloxazole] (PPO) was purchased from Sigma Chemical Co., MO, USA.

High-purity steviol was kindly supplied by Dr. Chaivat Toskulkao, Department of Physiology, Faculty of Science, Mahidol University.

Other substances not mentioned above were of the highest grade available from many sources.

## **INSTRUMENTS**

- Double beam UV/VIS Spectrophotometer Jasco model 7850 (Japan Spectroscopic Co., Ltd.) was used to measure protein and inorganic phosphate by colorimetry.
- The Advanced™ Micro-osmometer Model 3MO (Advanced Instruments, Inc., Massachusetts, USA.) was used for measuring a solution's osmolality.
- Vertical puller (Narishige Scientific Instrument Laboratory, Tokyo, Japan) was used to pull glass tubes.
- Manipulators (Narishige, Japan) were used for controlling the movement and holding micropipettes during microperfusion experiments.
- Stereomicroscope (Wild model M3C, Heerbrugg Switzerland) with ocular lens 20x was used to magnify tubules during dissection and perfusion.
- Microforge (American Optical Corporation, New York, USA) with Heating current control (Stoelting Co., Chicago, USA) was used to make the shape of a pipette's tip.
- Fiber-Lite (Dolan-Janner Industries, Inc.) and Olympus fiber optic (Olympus Optical Co., Germany) were used as light sources during microscopy.
- HPLC system: Model 600 pump from Waters (Milford, MA, USA) and Model 996 photodiode array detector (Waters Assoc., Milford, MA, USA) with

Millennium<sup>32</sup> software were used for the separation and determination of ATP content from proximal tubule suspension.

- Liquid Scintillation Counter Model 1214 Rackbeta (LKB Wallac, Sweden) was used to measure the activity of radioactive substances.
- Shaking water bath (polytest<sup>®</sup> 20, Bioblock Scientific) was used to incubate the tubules during treatment periods.
- Homogenizer (Glas-Col, Terre Haute, USA) was used for homogenization of proximal tubule suspensions.
- Centrifuge (Dupont-Sorvall, RC-28S) was used to separate proximal tubules in percoll solution (40%).

## **EXPERIMENTAL PROCEDURES**

### **I. Animal preparation and tubule dissection**

The rabbits were sacrificed by an intravenous injection of pentobarbital sodium (60 mg/kg BW). The abdominal cavity was opened via midline incision. The left renal artery was infused with sucrose-HEPES-buffered medium (Appendix I) to remove blood from the left kidney, which was then rapidly removed and placed in a chilled medium. The kidney was then cut into thin slices on a chilled petri-dish covered with soaked filter paper. The kidney slices were kept in sucrose-HEPES-buffered at 4°C and bubbled with 100% O<sub>2</sub>. The dissection of proximal tubules from the thin slices was performed manually under a stereomicroscope in a chilled (on ice) bicarbonate-buffered medium (Appendix II) without the aid of enzymatic agents, modified the method of Burg et al. (267). Two curved fine forceps (5/14) were used to separate the kidney slice into small bundles and then the S<sub>2</sub> segment of the proximal tubule was dissected using 2 needles.

The dissected tubular segments were cleared from the attached tissues. The preparation was continuously gassed with a 5% CO<sub>2</sub> and 95% O<sub>2</sub> mixture for the entire duration of dissection and experiment. The isolated tubules were transferred to the bathing chamber, covered with water-saturated light mineral oil and gassed with 95% O<sub>2</sub> and 5% CO<sub>2</sub> for the perfusion experiments. In the experiments, only the S<sub>2</sub> segment of the proximal tubule was used because maximal PAH secretion is found in this segment of mammalian renal tubules (53, 54).

## II. Perfusion of isolated tubules

The technique for perfusing the isolated renal tubule used in the experiment was first described by Burg et al. (267) and modified by Dantzler (268). The dissected tubule chosen for perfusion was transferred to a special temperature-controlled, Lucite bathing chamber on the stereomicroscope stage. The lucite bathing chamber was connected to a circulating water bath (Julabo F10) to maintain the temperature of the bathing medium at 37°C. The bathing medium was a bicarbonate-buffered solution containing 3 g/100 ml dextran (MW 40,000±3,000) to approximate plasma protein concentration. The osmolality of this solution was 290 mOsm/kg.H<sub>2</sub>O. The buffered medium was continuously gassed with 95% O<sub>2</sub> and 5% CO<sub>2</sub> to maintain its pH at 7.4.

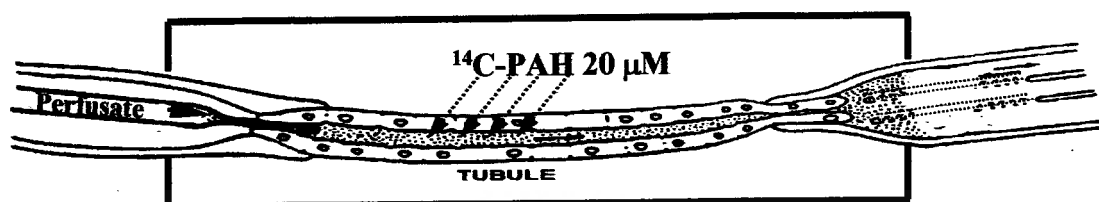


**Figure 4.** The perfusion of an isolated tubule. The left end of the tubule is held by the perfusing pipette and the right end is held by the collecting pipette.

Both ends of the tubule were held on the glass micropipette as shown in Figure 4 (for details, see appendix XI) and the tubule was perfused through a micropipette (perfusion pipette) lying inside the holding pipette with its tip centered at the tubular lumen. Another permanent concentric pipette (pressure pipette) was maintained inside the perfusion pipette to enable the perfusion fluid to be rapidly changed during the course of the experiments. The perfusion pressure was set and maintained through the regulating perfusion pressure system. The perfusion rate was in the range of 10-15 nl/min, as this range did not affect the secretion rate of PAH (53). The *in vitro* microperfusion set is shown in Figure 5. During perfusion, fluid samples that accumulated in the collecting pipette were removed at the end of each period (every 5 minutes) using a calibrated glass capillary tube (sampling pipette) connected with the polyethylene tube and a syringe (as described in appendix X). The length of the fluid column in the calibrated sampling pipette was measured to determine the volume of collected fluid. All of the experiments were carried out at 37°C.

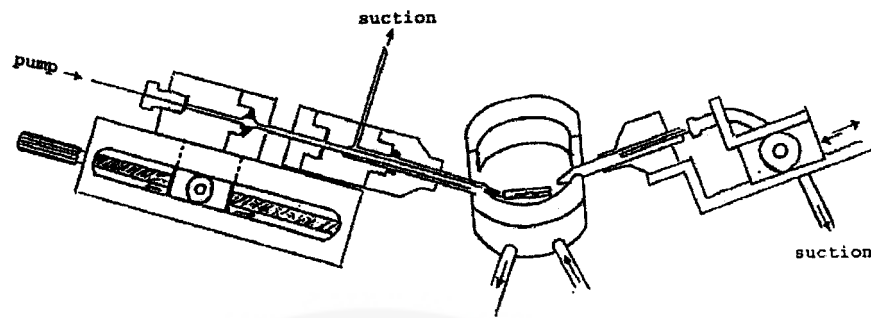


**Figure 5.** Apparatus for perfusing isolated tubule fragment (Burg *et al.* 1966)

### III. Transepithelial PAH flux

To measure transepithelial PAH flux ( $J_{\text{PAH}}$ ),  $^{14}\text{C}$ -PAH was added to the bathing medium at a concentration of  $20\ \mu\text{M}$ . This concentration does not saturate the transport of PAH (55, 62). No PAH was present in the initial perfusate or the tubular lumen. Net transepithelial secretory transport of PAH ( $J_{\text{PAH}}$ ) was determined from the amount of  $^{14}\text{C}$ -PAH appearing in the perfusate on the collecting side, and was expressed per unit time (duration between each collection), using the following relationship (90):  $J_{\text{PAH}} = (V_c C_c) / (X_b L)$ . In this equation,  $V_c$  is the fluid collection rate (in nl/min) measured directly by collecting the luminal fluid at the end of each period,  $C_c$  is the concentration of  $^{14}\text{C}$ -PAH in the collected luminal fluid (in dpm/nl),  $X_b$  is the specific activity of  $^{14}\text{C}$ -PAH in the bathing medium, and  $L$  is the length of the perfused tubule (in mm), measured by ocular micrometry.  $J_{\text{PAH}}$  was expressed as fmol/min/mm of tubule length.

### IV. Isolation of the proximal tubule suspension

Suspensions of rabbit renal proximal tubules were isolated from male New Zealand white rabbits, weighing between 1.5-2.5 kg, based on the method of Viney *et al.*

(269) and modified by Groves et al. (270). This method involved the digestion of the renal cortex by collagenase and subsequent differential centrifugation in 40% isoosmotic percoll in a bicarbonate-buffered medium (see Appendix V).

Rabbit were sacrificed by an intravenous injection of sodium pentobarbital at a dose of 60 mg/kg BW, following which both kidneys were perfused via the abdominal aorta with sucrose-HEPES-buffered medium (Appendix I) to remove blood. The kidneys were then gently removed and decapsulated. They were then placed in an ice-cold bicarbonate-HEPES-buffered medium. The renal cortex of both kidneys was dissected out with a scalpel blade in a petri-dish covered with an ice-cold bicarbonate-HEPES-buffered medium. After the medium was aspirated by suction, the renal cortical slices were minced (on ice) with two razor blades into small pieces and transferred to 25 ml of a digestion medium (Appendix IV) composed of a bicarbonate-HEPES-buffered medium supplemented with 150 units/ml collagenase, 2 mg/ml bovine serum albumin and 10 mM deferoxamine mesylate in a 125 ml Erlenmeyer flask. The minced cortex was incubated in a digestion medium that was continuously gassed with 95% O<sub>2</sub> and 5% CO<sub>2</sub> for 30 min at 37°C in a shaking water bath. At the end of the digestion period, 20 ml of an ice-cold bicarbonate-HEPES-buffered medium was added to stop the enzymatic reaction. The tubules were separated from undigested tissue by filtering through 250 µm tissue sieves and rinsed with 20 ml of an ice-cold bicarbonate-HEPES buffered solution. The tubule suspension was then placed in 2 polypropylene centrifuge tubes and rinsed three times with the same buffered medium by centrifugation at 4°C, 100 x g for 1 min to remove the digesting enzyme. Proximal tubules were isolated from other nephron segments and glomeruli by centrifugation in a Percoll gradient solution (40% (v/v)) at

37,520 x g (using sorvall ss-34 rotor at a speed 17,250 rpm) for 30 min at 4°C. The proximal tubules were removed from the percoll solution with a Pasteur pipette and were rinsed 3 times with an ice-cold bicarbonate-buffered solution by centrifugation at 100 x g, 4°C for 1 min. The final pellets, which were mainly composed of the proximal tubules (more than 95% pure), were resuspended in bicarbonate buffered solution (using the concentration of 0.03 g of pellet/1 ml of solution). The viability of proximal tubules was tested by using 1% trypan blue (a dead cell allows the entry of trypan blue into the cell). The proximal tubule suspensions were incubated with various solutions, as described in the Experimental Protocols section.

#### **V. Determination of ATP content by HPLC analysis**

The separation system consisted of a model 600 pump from Waters (Milford, MA), equipped with an injection valve connected to a 20- $\mu$ l sample loading loop. Peak monitoring was performed with a Model 996 (Waters) photodiode array detector which monitored the absorbance of the eluents at 254 nm using Millennium<sup>32</sup> software. Each sample was manually injected via a 100- $\mu$ l injection syringe (Exmire microsyringe, Ito Co., Fuji, Japan).

Separation was performed by reversed-phase HPLC on a 5- $\mu$ m Delta Pak C18 column (3.9 x 150 mm, Waters Assoc.) protected by a guard column using isocratic elution. The mobile phase consisted of 0.1 M  $\text{NH}_4\text{H}_2\text{PO}_4$ , adjusted to pH 5.5 with 3 N ammonium hydroxide (271). The mobile phase buffer solution was filtered through a 0.45  $\mu$ m aqueous filter (type HA, Millipore) before use. The buffer solution was freshly prepared prior to each group of sample runs. The samples and the standards were thawed at room temperature and were filtered through a 0.22  $\mu$ m syringe nylon filter before the

injection. The injection volume was 10  $\mu$ l, and the flow rate was set at 1.2 ml/min. The values of cell ATP, ADP, AMP, hypoxanthine and xanthine content were expressed as nmol ATP/mg of tubule protein.

Standard ATP was prepared by dissolving ATP (Sigma) in perchloric acid, and then neutralized with 1.55M  $K_2CO_3$ /2.14M KOH. Various concentrations of ATP, ADP, AMP, hypoxanthine and xanthine mixture (0.05, 0.025, 0.01, 0.005 and 0.002 mM) were used to construct standard curves. The coefficient of variation was 5.96% from 4 separate determinations and the detection limits for ATP, ADP, AMP, hypoxanthine and xanthine were 0.01, 0.015, 0.01, 0.01 and 0.02 nmol, respectively.

## **EXPERIMENTAL PROTOCOLS**

### **I. Perfusion study**

#### **1.1 Time control of $^{14}C$ -PAH transport in isolated perfused renal proximal tubules**

Initially, time control experiments were performed to be certain that the isolated perfused renal proximal tubules functioned normally throughout the experimental duration used in all experiments.

The tubule was perfused and bathed with the same control buffered media as was used for other experiments for 65 minutes.  $^{14}C$ -PAH 20  $\mu$ M was added to the bathing medium and fluid was collected from the collecting side at 5-minute intervals to determine the  $^{14}C$ -PAH transport into the tubular lumen.

## **1.2 Effect of stevioside on $^{14}\text{C}$ -PAH transport in isolated perfused renal proximal tubules**

This experiment was designed to study the effect of stevioside: 1) when present in the bathing solution, which is similar to the presence of stevioside in a peritubular capillary *in vivo*, 2) in the perfusate, which is similar to stevioside present in the filtrate after glomerular filtration, and 3) in both bath and perfusate at the same time, which is similar to the appearance of stevioside in the body, where it will enter the tubular lumen via glomerular filtration, following which some of it will escape to peritubular capillaries, on net transepithelial transport of PAH from the bath to the lumen of the S<sub>2</sub> segments of renal proximal tubules.

### **1.2.1 Concentration-response effect of stevioside on $J_{\text{PAH}}$**

It was not possible to construct a full dose-response curve for stevioside due to its limited solubility in the medium. We did not use solvents such as ethyl alcohol or dimethylsulfoxide (DMSO) to solubilize this agent because our purpose was to imitate the condition under which stevioside has been used, that is, as a sugar substitute in beverages. However, we did perform the experiment using various concentrations of stevioside (0.45, 0.50, 0.60 and 0.70 mM) to examine the concentration-response effect of stevioside.

The concentration of 0.45 mM stevioside was initially used in the experiment because this concentration is equivalent to the dose of 16 mg/kg BW/hr that Melis (9, 10, 17) used and showed significant effect on renal function in an *in vivo* clearance study. The other concentration used in this study was 0.7 mM, which is the maximum concentration of stevioside that could be dissolved in the buffered medium.

### 1.2.2 Effect of 0.45 and 0.7 mM stevioside in bathing medium on $J_{PAH}$

These concentrations of stevioside were chosen based on the data obtained from study part 1.2.1. First, the isolated S<sub>2</sub> segment of the proximal tubule was transferred to the Lucite bathing chamber using a pasteur pipette. The medium in the bath was changed to a dextran-bicarbonate-buffered medium, covered with water-saturated mineral oil. After the tubule was hooked to the holding and collecting pipettes, the bathing solution was changed to the one containing 20  $\mu\text{M}$   $^{14}\text{C}$ -PAH. The perfusate was a standard bicarbonate-buffered medium without  $^{14}\text{C}$ -PAH. Three control collections were performed before any treatment and were used as control samples. Each collection was performed at an interval of 5 minutes. At the end of these control collections, the bathing medium was changed to the medium containing stevioside (0.45 or 0.7 mM). After changing the medium, the tubule was allowed to equilibrate in the new solution for 5 minutes, then the fluid in the collecting pipette was discarded and another 4 collections were performed (one every 5 minutes) in these treatment periods. After that the bathing medium was changed back to the dextran-bicarbonate buffered medium which was used in the control periods. Another 4 collections were performed after 5 minute-equilibration period. All collected samples were examined for  $^{14}\text{C}$  activity by liquid scintillation counter (1214 Rack beta, LKB Wallac). The  $^{14}\text{C}$ -PAH flux was expressed as fmol/min/mm of tubule length.

### 1.2.3 Effect of 0.45 and 0.7 mM stevioside in perfusate on $J_{PAH}$

These experiments were designed to study the effect of stevioside when present in the perfusate (luminal fluid), which is similar to its presence

in filtrate (through glomerular filtration), on net transepithelial transport of PAH from the bathing medium to the lumen, using the same concentrations as those in part 1.2.2. The experiments were performed as per what was described in part 1.2.2, but stevioside (0.45 and 0.7 mM) was added to the perfusate instead of the bathing medium during the treatment period. In other words, the bathing medium containing  $^{14}\text{C}$ -PAH was not changed throughout the experiment, but the perfusate was changed to one containing stevioside during the treatment periods, and then changed back to the control solution during the recovery period.

#### 1.2.4 Effect of 0.45 and 0.7 mM stevioside in both perfusate and bathing medium on $J_{\text{PAH}}$

This experiment was designed to investigate whether stevioside (0.45 and 0.7 mM), when present in both luminal and basolateral sides of the proximal tubule at the same time could exhibit an additive effect. The experiments were performed as per what was described in parts 1.2.2. and 1.2.3, but stevioside was added simultaneously into both perfusate and the bathing medium during treatment periods, as shown in the diagram. The results obtained from this experiment were compared with those obtained from the experiments when stevioside was presented in either luminal side or basolateral side separately (part 1.2.2 and 1.2.3).

#### **1.3 Effect of steviol on $^{14}\text{C}$ -PAH transport in isolated perfused rabbit renal proximal tubules**

This experiment was designed to investigate whether steviol has any effect on proximal tubular PAH transport, and if it has, which side of the tubule was more responsive to the steviol's action.

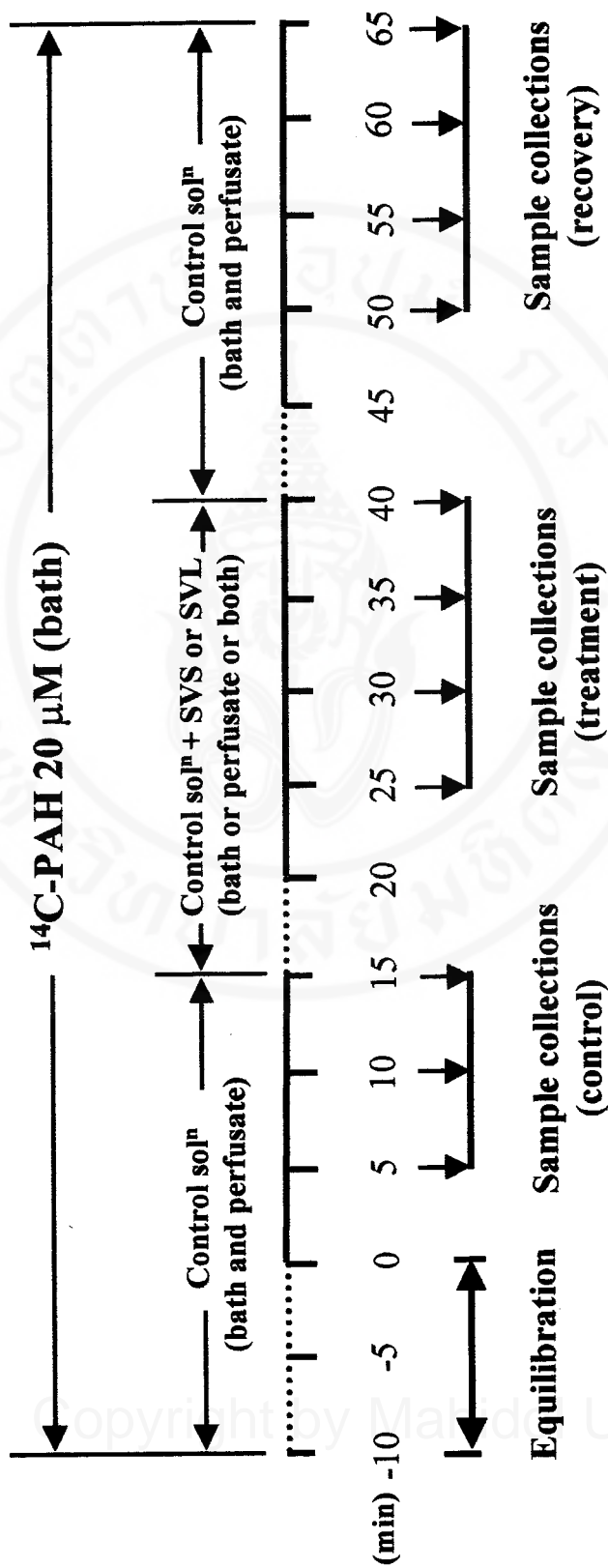


Figure 6. Timing diagram of changing perfusate and bathing medium, as well as time for sample collections

Due to the hydrophobicity of steviol, DMSO was added to the buffered medium to dissolve this compound. DMSO has been known to have some toxic effect on cellular function, therefore, we first tested its effect on PAH transport compared to the control value. Subsequently, we examined the concentration-response effect of steviol on  $J_{PAH}$  in order to select the concentration which showed 50% inhibition of control  $J_{PAH}$  to use for further study. We examined the effect of steviol on  $J_{PAH}$  when it was present in the bathing medium, in the perfusate or in both bath and perfusate at the same time, as in the experiment done with stevioside.

#### 1.3.1 Effect of DMSO in bathing medium on $J_{PAH}$

We tested the effect of 0.125% (v/v) DMSO on PAH transport in isolated rabbit renal proximal tubules to see whether DMSO at the maximum concentration (0.125%) used in the experiments had any effect on PAH transport throughout the experimental periods.

The experiments were performed using the same procedures as in the time control study, with a standard control solution in both the bathing medium and the perfusate, except that the bathing medium contained 0.125% (v/v) DMSO. Fluid samples on the collection side were collected every 5 minutes for 65 minutes (the duration that was used throughout the experiments).

#### 1.3.2 Concentration-response effect of steviol on PAH transport

This experiment was designed to examine the concentration-response effect on PAH transport and to select the concentration that produced the 50% inhibition of PAH transport from control value.

Briefly, after both ends of the tubule were held between micropipettes, the bathing medium was changed to a dextran-bicarbonate-buffered medium containing  $^{14}\text{C}$ -PAH (20  $\mu\text{M}$ ). Three control collections were performed, one every 5 minutes, and then the bathing medium was changed to a medium containing various concentrations of steviol (0.005, 0.010, 0.015, 0.025, 0.050, 0.100 and 0.250 mM, one tubule for one concentration). Five minutes' duration was allowed for an equilibration period, after which 6 collections were performed, one every 5 minutes. The collected fluid samples were counted for  $^{14}\text{C}$ -PAH activity. The values of  $^{14}\text{C}$ -PAH transport were expressed in % of control value. The concentration of steviol that exhibited 50% of PAH transport from control value (50% inhibition) was selected for the next experiment.

### 1.3.3 Effect of 0.01 mM steviol in the bathing medium on $J_{\text{PAH}}$

This experiment was designed to examine whether steviol at a concentration of 0.01 mM (which caused approximately 50% inhibition from control  $J_{\text{PAH}}$ , as determined in part 1.3.2) when it was added to, and then removed from, the bathing medium (basolateral side) had a reversible inhibitory effect on  $J_{\text{PAH}}$ .

The experiment was performed similar to the experiments with stevioside in the bathing medium. After 3 control collections, the bathing medium was changed to the one containing 0.01 mM steviol and 4 collections were performed. At the end of treatment period, the bathing medium was changed back to the one used in control period, and another 4 samples were collected during the recovery period. The amount of  $^{14}\text{C}$ -PAH in the samples were measured using a  $\beta$ -counter and calculated for PAH transport from the bath to the lumen of the proximal tubules.

#### 1.3.4 Effect of 0.01 mM steviol in perfusate on $J_{PAH}$

This experiment was aimed to study whether steviol when present at luminal side at a concentration of 0.01 mM had any inhibitory effect on the transepithelial transport of PAH. We also examined whether PAH transport could recover after steviol was removed from the perfusate or not.

The experiment was performed as mentioned above (part 1.3.3). 0.01 mM steviol was added to the perfusate during the treatment periods and was removed after 4 sample collections were performed. Another 4 sample collections were made during the recovery period. All samples were examined for  $^{14}\text{C}$ -PAH activity, and calculated for  $^{14}\text{C}$ -PAH transport from the bath to the lumen.

#### 1.3.5 Effect of 0.01 mM steviol in both bathing medium and perfusate on $J_{PAH}$

This experiment was designed to investigate whether the presence of steviol simultaneously in the perfusate and the bathing medium could produce an additive inhibitory effect on PAH transport.

The experiment was performed as previously mentioned in the other stevioside treatments, both the perfusate and the bathing medium were changed to media containing 0.01 mM steviol after 3 control samples were collected over the first 15 minutes. The recovery periods were also investigated in a manner similar to the other experiments mentioned above.

#### 1.3.6 Effect of 0.05 mM steviol in perfusate on PAH transport

This experiment was designed to study whether the higher concentration of steviol (0.05 mM, that had maximal inhibitory effect on PAH transport

when it was present at the basolateral side, as seen in part 1.3.2) when it was present in perfusate could inhibit PAH transport or not.

The experiment was performed as mentioned earlier in parts 1.2.3 and 1.3.4, except that 0.05 mM steviol was added to the perfusate during the treatment period.

## II. Stevioside and steviol effects on $\text{Na}^+\text{-K}^+$ ATPase activity

These experiments were designed to examine whether the inhibition of PAH transport by stevioside or steviol involved an alteration in  $\text{Na}^+\text{-K}^+$  ATPase activity or not.

In this experiment, we examined the  $\text{Na}^+\text{-K}^+$  ATPase activity of the proximal tubules using a proximal tubule suspension instead of isolated single segments of proximal tubules, to ensure that enough tissue for determination could be obtained. The renal proximal tubule suspensions were prepared as mentioned in experimental procedure IV. After the separation of the proximal tubule suspension, the proximal tubules were divided into 8 tubes. Each tube was incubated with different treatments as follows:

1. Control group: bicarbonate-buffered solution
2. 0.7 mM stevioside treatment in bicarbonate-buffered solution
3. 0.005% (v/v) DMSO treatment in bicarbonate-buffered solution  
(paired control for 0.01 mM SVL)
4. 0.025% (v/v) DMSO treatment in bicarbonate-buffered solution  
(paired control for 0.05 mM SVL)
5. 1.0% (v/v) DMSO treatment in bicarbonate-buffered solution (paired control for 2.0 mM SVL)

6. 0.01 mM steviol in 0.005% (v/v) DMSO treatment
7. 0.05 mM steviol in 0.025% (v/v) DMSO treatment
8. 2.0 mM steviol in 1.0% (v/v) DMSO treatment

Each sample contained approximately 0.03 g/ml of proximal tubule cells (w/v). The volume of each sample was 2 ml of tubule suspension. After the proximal tubule suspensions were equilibrated for 10 minutes and incubated at 37°C in a shaking water bath (1,200 rpm) for 20 minutes, the treatments were stopped by adding an ice-cold bicarbonate-buffered medium, and then centrifuged at 4°C, 1,000 rpm for 1 min. The supernatant was discarded and the pellets were resuspended with a bicarbonate-buffered medium. This washing procedure was repeated 3 times. Then, the pellet of each tube was resuspended in 1 ml of a hypotonic solution (1 mM imidazole, 1 mM MgCl<sub>2</sub> and 0.25 mM EDTA) and placed on ice. The tubule suspensions were homogenized with a Teflon-glass homogenizer at a speed of 3,000 rpm on ice, 20 strokes for 1 minute. The homogenate was kept on ice for further determination of Na<sup>+</sup>-K<sup>+</sup> ATPase activity and protein determination, as described in the method, Appendices VI and VII.

### **III. Stevioside and steviol effects on cell ATP content**

These experiments were designed to examine whether the inhibition of PAH transport by stevioside or steviol involved an alteration of cell ATP content in the proximal tubules or not.

The proximal tubule suspensions were divided and treated in same manner as in part II, except that the suspensions contained approximately 0.06 g/ml of proximal tubule cell (w/v). After the incubation period, 0.5 ml of suspension for each treatment was added to equal volumes of ice-cold 6% (v/v) perchloric acid to extract ATP from the

proximal tubular cells. This extraction was performed on ice for 20 minutes. The following processes were performed to measure the total ATP content of the proximal tubule cells and extracellular medium. To measure the ATP content of the extracellular medium, 0.5 ml aliquots of suspension were first layered onto 0.4 ml of 2:1 mixture of dibutyl/dioctyl phthalate (272) in a 1.5 ml microcentrifuge tube, and centrifuged for at least 10 seconds. The supernatant was then added to an equal volume of 6% (v/v) perchloric acid. For both types of samples, the total extract and extracellular extract, the supernatant was separated by centrifugation at 3,000 rpm, 4°C for 15 minutes, and neutralized with 2 N KOH/1.5 M K<sub>2</sub>CO<sub>3</sub>. The centrifugation was then performed again to remove the precipitation of potassium perchlorate. The final supernatant was kept at -70°C until used. The determination of ATP was performed by HPLC analysis using isocratic elution, 0.1 M NH<sub>4</sub>H<sub>2</sub>PO<sub>4</sub> was the mobile phase, as described by Hull-Ryde et al. (271). The method for sample preparation and analysis is shown in experimental procedure (part V). The intracellular ATP content was calculated from the difference between the ATP content of the total suspension and that of the extracellular medium. The values of the ATP content were expressed as nmol ATP/mg of tubule protein.

#### **IV. Kinetic study**

##### **4.1 Determination of the appropriate time for PAH uptake into the renal proximal tubule suspension.**

This experiment was designed to determine the appropriate time to use for kinetic analysis of PAH uptake, which is the time that showed the initial rate of PAH uptake into rabbit renal proximal tubule suspension.

This experiment was performed using renal proximal tubule suspensions preincubated in a bicarbonate-buffered medium at 37°C for 15 minutes. Then  $^{14}\text{C}$ -PAH was added to the suspension to obtain a final PAH concentration of 5  $\mu\text{M}$ . After various incubation periods of 15, 30, 45, 60, 120 and 300 seconds, the uptake was terminated by adding 5 ml of a cold sucrose-HEPES-buffered medium containing 1 mM probenecid, the suspensions were then rapidly filtered through a glass microfiber filter (GF/G, Whatman), suctioned with a vacuum pump, and rinsed with 5 ml of an ice-cold 1 mM probenecid solution. The filters were placed into a glass vial (20 ml) and 0.5 ml of 1 N NaOH was added to the vial to extract  $^{14}\text{C}$ -PAH from the renal tubules. The vials were kept out of the light for at least 3 hr or until no tissue particles were observed on the membrane filter. The extract was neutralized with 0.5 ml of 1 N HCl. A scintillation fluid was added to the vial, mixed and counted for radioactivity using a beta counter. PAH uptake was shown as the amount of PAH per milligram of tubule protein. The data were plotted between PAH uptake on the ordinate and time on the abscissa. The time that showed the most rapid rise of PAH uptake was chosen for the next experiments.

#### **4.2 Kinetic study of PAH uptake into renal proximal tubule suspensions**

A renal proximal tubule suspension (~ 0.05 g wet weight/ml of bicarbonate-buffered medium) was pre-warmed to 37°C for 15 min before the uptake study so that the tubule would be fully functional at the time of study. A bicarbonate-buffered medium containing  $^{14}\text{C}$ -PAH 10  $\mu\text{M}$  and various concentrations of cold PAH (0, 40, 200, 400, 2,000 and 4,000  $\mu\text{M}$ ) were added to the incubated tubule suspension with the same volume to obtain a final concentration of  $^{14}\text{C}$ -PAH at 5  $\mu\text{M}$ . After the addition

of  $^{14}\text{C}$ -PAH, the tubule suspension was incubated at  $37^{\circ}\text{C}$  for 30 sec (this period was chosen based on the data from part 4.1). The uptake time was terminated by the addition of 5 ml of a cold sucrose-HEPES buffered solution containing 1 mM probenecid, and then rapidly filtered through a microfiber filter with a vacuum suction. The membrane filter was rinsed again with a 5 ml solution containing 1 mM probenecid before transfer to the glass vial. The tubules on the membrane filter were dissolved in 0.5 ml of 1 N NaOH for at least 3 hours and neutralized with 0.5 ml of 1 N HCl. The extract was counted by a liquid scintillation counter. The radioactivity was calculated for the amount of PAH uptake and expressed as pmol of PAH uptake/mg of tubule protein. These data were plotted as a Lineweaver-Burk plot ( $1/[\text{PAH}]$  vs  $1/\text{PAH uptake}$ ) and estimated  $K_m$  (Michaelis-Menten constant), which is the PAH concentration at the half-maximal uptake of PAH, from the x-axis intercept. The maximal PAH transport ( $J_{\text{max}}$ ) by proximal tubules was also estimated from the y-axis intercept.

#### **4.3 Kinetic study of stevioside and steviol on inhibition of PAH uptake into renal proximal tubule suspensions**

This experiment was designed to find out the  $K_i$  of stevioside and steviol for PAH, the concentrations of stevioside and steviol that caused a half-inhibition of maximum PAH transport. The  $K_i$  can be used to evaluate the specificity of stevioside and steviol to the PAH transporter. In addition, the  $K_m$  and  $J_{\text{max}}$  in the presence of stevioside and steviol would be able to indicate whether stevioside and steviol interact with the PAH transporter or not.

The experiment was performed as in experiment 4.2, except that either 0.7 mM stevioside or 0.01 mM steviol was added to the incubating medium. After a 30-

second incubation, the uptake was terminated by adding 1 mM probenecid solution to the incubated sample. The radioactivity was counted by a  $\beta$ -counter and PAH uptake was calculated as pmol of PAH per mg of tubule protein. A Lineweaver-Burk plot was performed. The type of inhibition was estimated from the  $K_m$  and  $J_{max}$  obtained.

In competitive inhibition, if the inhibitor interacts directly with the transporter, only  $K_m$  is changed, but  $J_{max}$  is not altered. The  $K_i$  value was calculated by the following equation:

$$K_i = [I] / \left[ \frac{K_m \text{ (with inhibitor)}}{K_m \text{ (without inhibitor)}} - 1 \right]$$

In noncompetitive inhibition, if the inhibitor does not interact directly with the transporter,  $J_{max}$  is decreased, but no change in  $K_m$  is observed. The  $K_i$  value was calculated by this equation:

$$K_i = [I] / \left[ \frac{J_{max} \text{ (without inhibitor)}}{J_{max} \text{ (with inhibitor)}} - 1 \right]$$

where  $K_i$  is the concentration of inhibitor that caused a half-maximum PAH uptake;  $[I]$  is the concentration of inhibitor (in this experiment, either stevioside (0.7 mM) or steviol (0.01 mM);  $J_{max}$  is the maximum PAH uptake (from the Lineweaver-Burk plot, the y-intercept is  $1/J_{max}$ );  $J_{max}$  (with inhibitor) is the maximum PAH uptake in the presence of inhibitor;  $K_m$  is the PAH concentration that caused a half-maximum PAH uptake (from the Lineweaver-Burk plot, x-intercept is  $-1/K_m$ ).

Copyright by Mahidol University

## STATISTICAL ANALYSIS

Results are expressed as mean $\pm$ SE. The n value is the number of experiments (one tubule from a single animal was used for each experiment). In the perfusion

experiments, the mean value for the three control periods was compared with the values for each experimental period in the same group, and the comparisons of the value for each experimental period between different treatments at the same period were performed using a two-way analysis of variance with repeated measure design. The significance of difference between these values was determined with Fisher's protected least significant difference post hoc test. For the experiments on  $\text{Na}^+\text{-K}^+$  ATPase activity and ATP content, the difference between control and experimental means was determined by a one-way analysis of variance and a post hoc test with Student Newman-Keul's test. The comparison between control and experimental mean in the kinetic study was determined by a t-test for paired observations. The values were considered to be statistically significantly different when the P-value was less than 0.05.

## CHAPTER IV

### RESULTS

#### 1. TIME CONTROL STUDY OF TRANSEPITHELIAL TRANSPORT OF PAH BY ISOLATED S<sub>2</sub> SEGMENTS OF RABBIT RENAL PROXIMAL TUBULES

This experiment was performed using isolated S<sub>2</sub> segments of proximal tubules to study the transepithelial transport of PAH from the basolateral side to the luminal side of the tubule. This experiment was done to be certain that the isolated perfused renal proximal tubule functioned normally throughout the experimental duration used in all subsequent experiments. As shown in Figure 7, the rabbit renal proximal tubule (S<sub>2</sub> segment) was perfused and bathed with a control bicarbonate-buffered medium for 65 minutes. The transepithelial transport of PAH ( $J_{PAH}$ ) did not change significantly during this time period, as shown previously by Chatsudthipong and Dantzler (90, 94). This observation helps us to eliminate the effect of time on  $J_{PAH}$ . However, low values of  $J_{PAH}$  were observed for the first 10 minutes of the experiment. This time period may be required for the tubular activity to reach a steady state after being transferred into the perfusion chamber. Thus, in the subsequent experiments, the tubules were perfused for 10 minutes prior to sample collection.

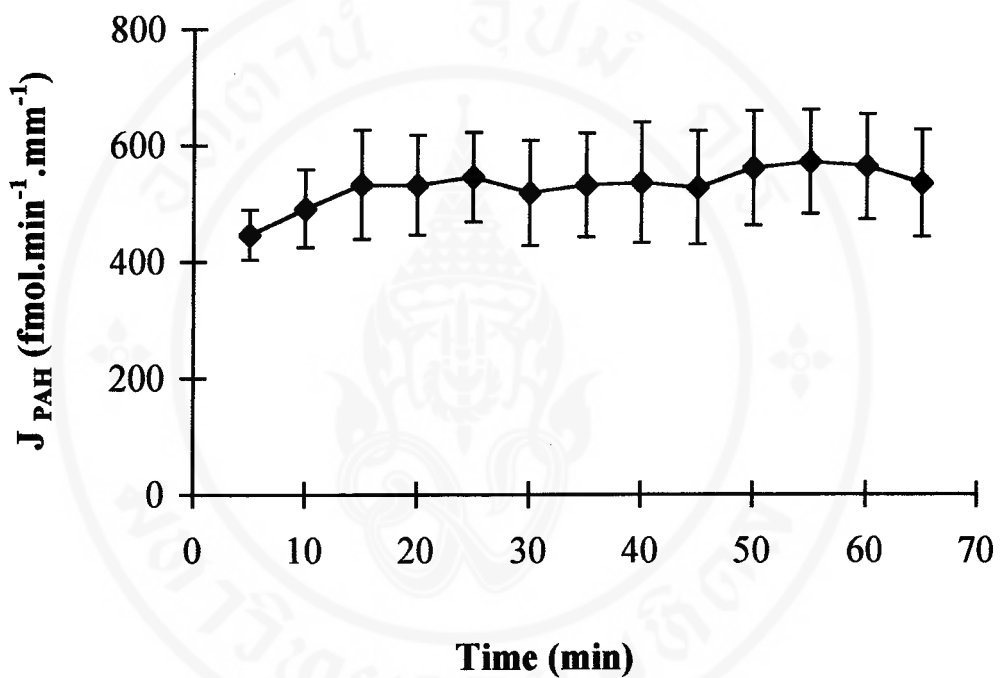


**Figure 7.** Control transepithelial secretory transport of p-aminohippurate (PAH),  $J_{PAH}$  in isolated proximal tubules perfused and bathed with a bicarbonate-buffered medium. Absolute values of  $J_{PAH}$  given in  $\text{fmol}\cdot\text{min}^{-1}\cdot\text{mm}^{-1}$  (mean  $\pm$  SE) were determined at 5-minute intervals over a period of 65 minutes,  $n = 5$ .

## 2. STEVIOSIDE EFFECT ON TRANSEPITHELIAL TRANSPORT OF PAH ( $J_{PAH}$ )

### 2.1 The effect of 0.45 mM stevioside on transepithelial transport of PAH

From previous *in vivo* rat studies by Melis (7-10, 17), was suggested that intravenous injection of stevioside had effects on renal function, but little is known about its effect on tubular function. A high concentration of 0.45 mM stevioside was chosen because this concentration is equivalent to the dose used in the previous studies by Melis (9-10, 17), which had been shown to alter several parameters of renal function. In these experiments, each tubule was initially perfused and bathed with a control bicarbonate-buffered medium for 15 minutes to obtain control values for  $J_{PAH}$ . After this period, the perfusate was changed to one containing 0.45 mM stevioside.  $J_{PAH}$  was only slightly decreased during the first period but not significantly from the control value (Figure 8a). Removal of stevioside from the perfusate had no effect on  $J_{PAH}$ . The addition of 0.45 mM stevioside to the bathing medium also had no significant effect on  $J_{PAH}$  (Figure 8b). Normally, exogenous compounds that need to be eliminated from the body are present in both luminal (from glomerular filtration) and peritubular sides of the tubule at the same time. Therefore, the effect of stevioside when simultaneously presented to both sides of the tubule to mimic the *in vivo* condition was studied. As shown in Figure 8c, stevioside at a concentration of 0.45 mM, added to both perfusate and bathing medium, did not alter  $J_{PAH}$  throughout the experimental period.

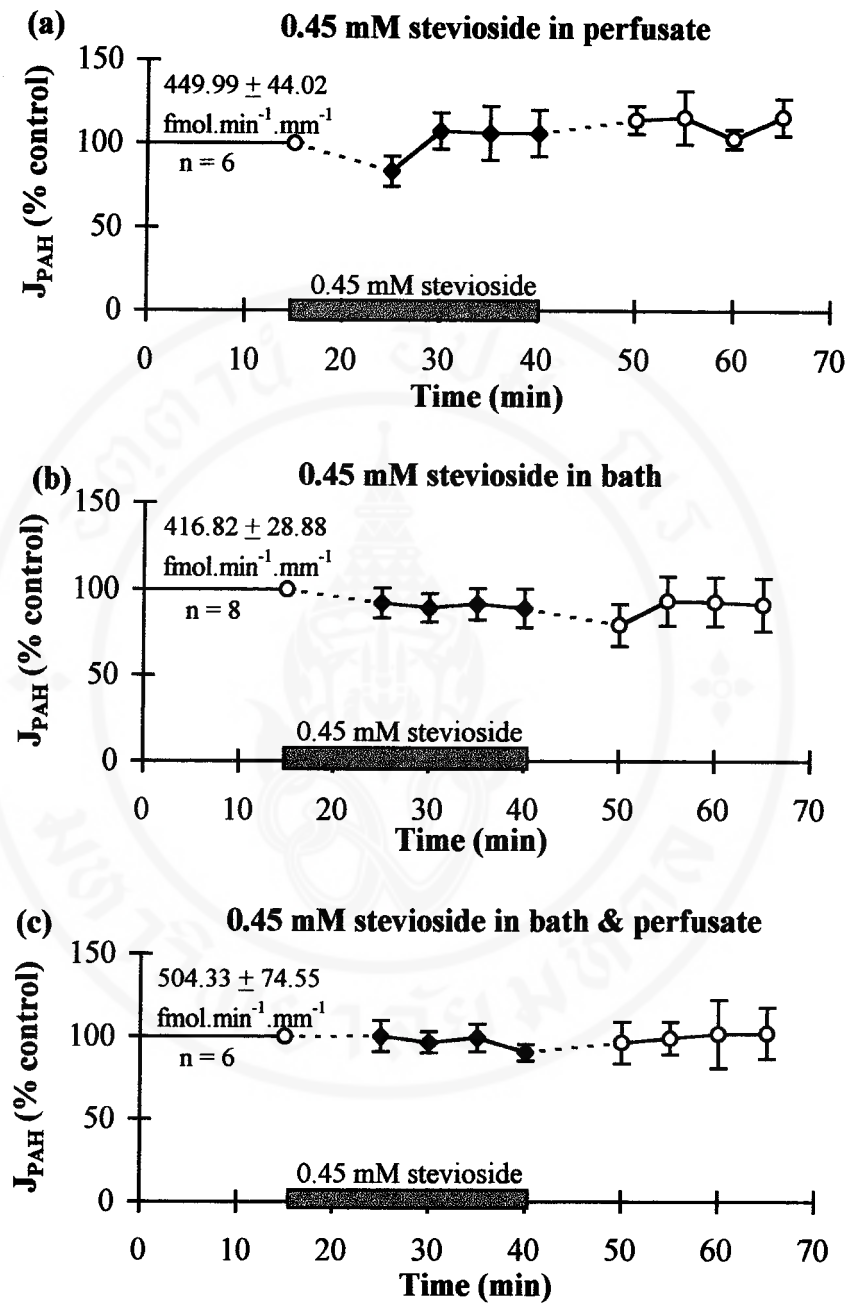
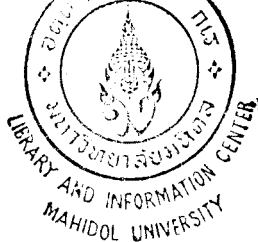


**Figure 8.** The effect of 0.45 mM stevioside (a) in perfusate, (b) in a bath, and (c) in both a bath and perfusate on  $J_{\text{PAH}}$  in tubules perfused and bathed with a bicarbonate-buffered medium. Values for  $J_{\text{PAH}}$  are shown as percent of the mean control value (control being 100%) for each tubule for the first 15 minutes. Absolute mean  $J_{\text{PAH}}$  ( $\text{fmol} \cdot \text{min}^{-1} \cdot \text{mm}^{-1}$ ) value  $\pm$  SE for all tubules in the first 15 minutes is indicated,  $n$  = number of tubules. The shaded bar indicates the time when 0.45 mM stevioside was present in the medium.



To be certain that the lack of 0.45 mM stevioside effect on  $J_{PAH}$  observed in this experiment was not due to the unresponsiveness of the tubule to stevioside treatment, probenecid (0.1 mM), a competitive inhibitor of PAH, was added to the bathing medium at the end of the experiment. These tubules were found to respond well to probenecid treatment (Figures 9 a, b and c).

## **2.2 Concentration-response: the effects of various concentrations of stevioside on $J_{PAH}$**

Due to the lack of 0.45 mM stevioside effect on  $J_{PAH}$  observed in the previous experiment, higher concentrations of stevioside (0.5, 0.6 and 0.7 mM) were also examined. Earlier studies (95, 272) had strongly suggested that the basolateral transport of PAH into the cells is the rate-limiting step for transepithelial transport. Thus, in this series of experiments, stevioside was only added to the bathing medium. The protocol for these experiments was the same as that for the experiment with 0.45 mM stevioside in the bath mentioned above, except that stevioside at a concentration of 0.5 or 0.6 or 0.7 mM was added to the bathing medium, instead of 0.45 mM. The concentration of stevioside used in these experiments was maximal at a concentration of 0.7 mM so that it could be completely dissolved in the buffer without the aid of any solvent. The effects of these concentrations of stevioside on  $J_{PAH}$  are shown in Figure 10. The presence of stevioside in the bath at concentrations of 0.45, 0.5 and 0.6 mM produced no significant change in  $J_{PAH}$  from the control value after either a 10- or 20-minute treatment. Only 0.7 mM stevioside, the maximum concentration that could be dissolved completely in the bathing medium, depressed  $J_{PAH}$  significantly by about 30% after a 10-minute treatment and remained depressed after 20 minutes of

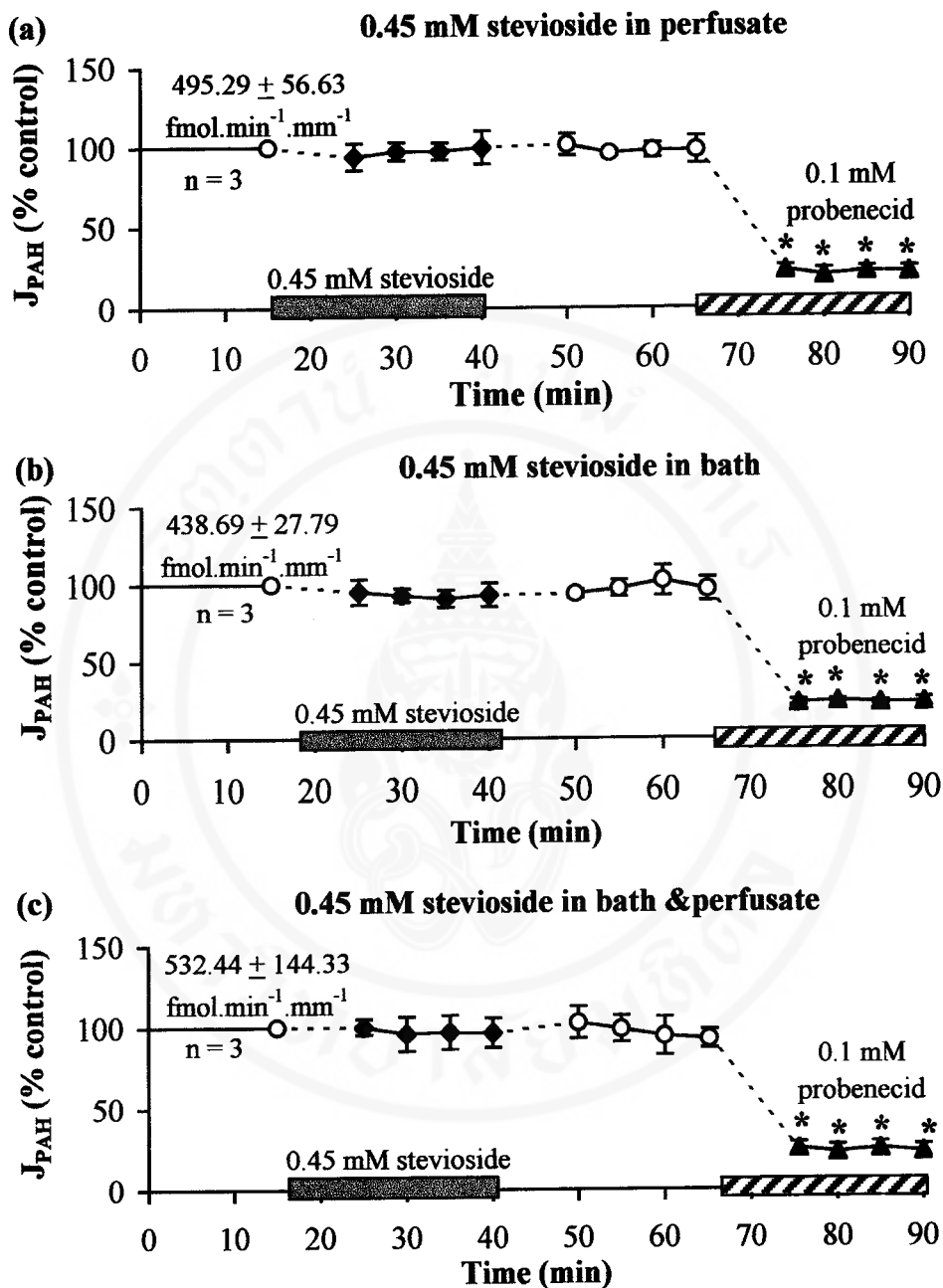


**Figure 9.** The effect of 0.1 mM probenecid addition to bathing medium at the end of the recovery period of 0.45 mM stevioside treatment in (a) perfusate, (b) bath, and (c) both bath and perfusate on  $J_{\text{PAH}}$ . Values for  $J_{\text{PAH}}$  are shown as percent of the mean control value (control being 100%) for each tubule for the first 15 minutes. See legend of Figure 8 for a complete description of symbols. The shaded bar indicates the time when stevioside (0.45 mM) was present in the medium. The striped bar indicates the time when probenecid (0.1 mM) was present in the bathing medium. \*Significant difference from control,  $p$ -value < 0.05.

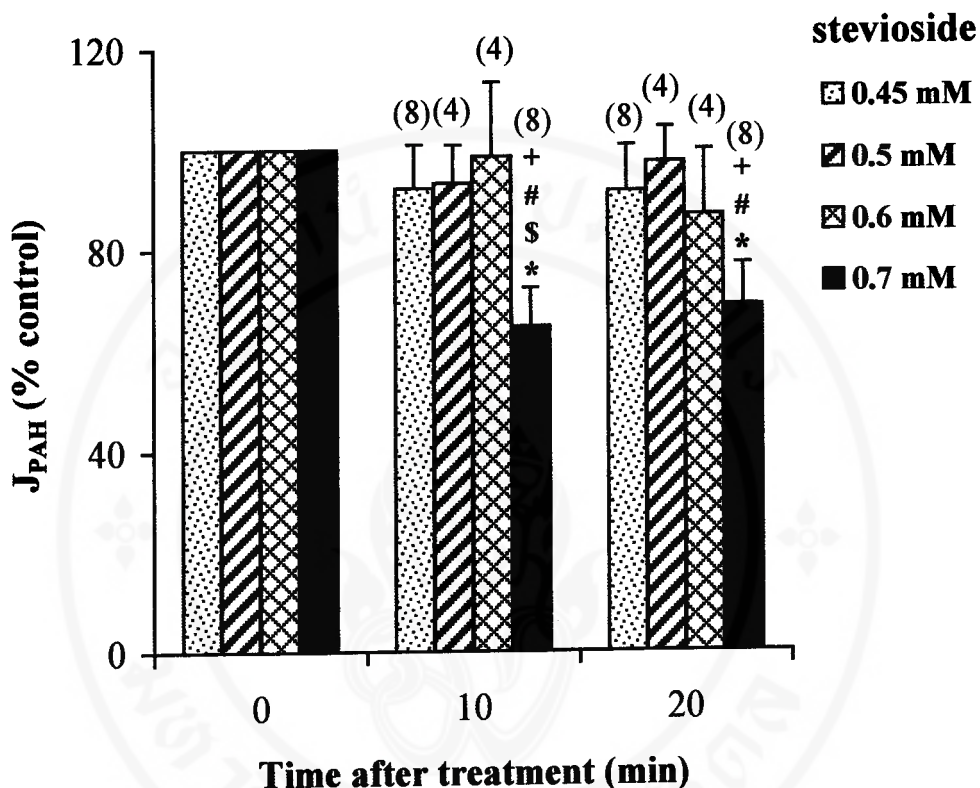


**Figure 10.** The effects of various concentrations (0.45, 0.5, 0.6 and 0.7 mM) of stevioside in a bath on  $J_{PAH}$  of isolated proximal tubules after incubation periods of 10 and 20 minutes. \*Significant difference from control value, +Significant difference from the value of 0.45 mM stevioside treatment, #Significant difference from the value of 0.5 mM stevioside treatment, \$Significant difference from the value of 0.6 stevioside treatment. The p-value of the significant difference is less than 0.05. Values are means  $\pm$  SE. Number of tubules is shown in parentheses on each bar.

treatment. The effect of 0.7 mM stevioside on  $J_{PAH}$  was statistically significantly different from the lower concentrations (0.45, 0.5 and 0.6 mM) at the same time points. Thus, stevioside at a concentration of 0.7 mM was chosen for the next experiment.

### **2.3 The effect of 0.7 mM stevioside on the transepithelial transport of PAH ( $J_{PAH}$ )**

The effect of stevioside at a concentration of 0.7 mM was further examined. As shown in Figure 11a, when the perfusate was changed from the control solution to one containing 0.7 mM stevioside,  $J_{PAH}$  did not significantly change from control values. In contrast,  $J_{PAH}$  was significantly depressed by about 30% when 0.7 mM stevioside was present in the bathing medium and remained depressed while stevioside was in the bath (Figure 11b). The depression of  $J_{PAH}$  under this condition was significantly different from that seen when stevioside was in the perfusate (Figure 11a). When stevioside was removed,  $J_{PAH}$  gradually increased and was not significantly different from control values by 20 minutes after removal of stevioside from the bath. Thus, the inhibition of  $J_{PAH}$  by 0.7 mM stevioside in the bath appeared to be reversible. When 0.7 mM stevioside was simultaneously added to both the perfusate and the bathing media, there was no added inhibitory effect compared with that observed with stevioside addition to the bath medium alone (Figure 11c). Similar to what was observed when stevioside was in the bath alone,  $J_{PAH}$  gradually recovered when stevioside was removed from perfusate and bath, and  $J_{PAH}$  was not significantly different from control values by 20 minutes after the removal of stevioside.

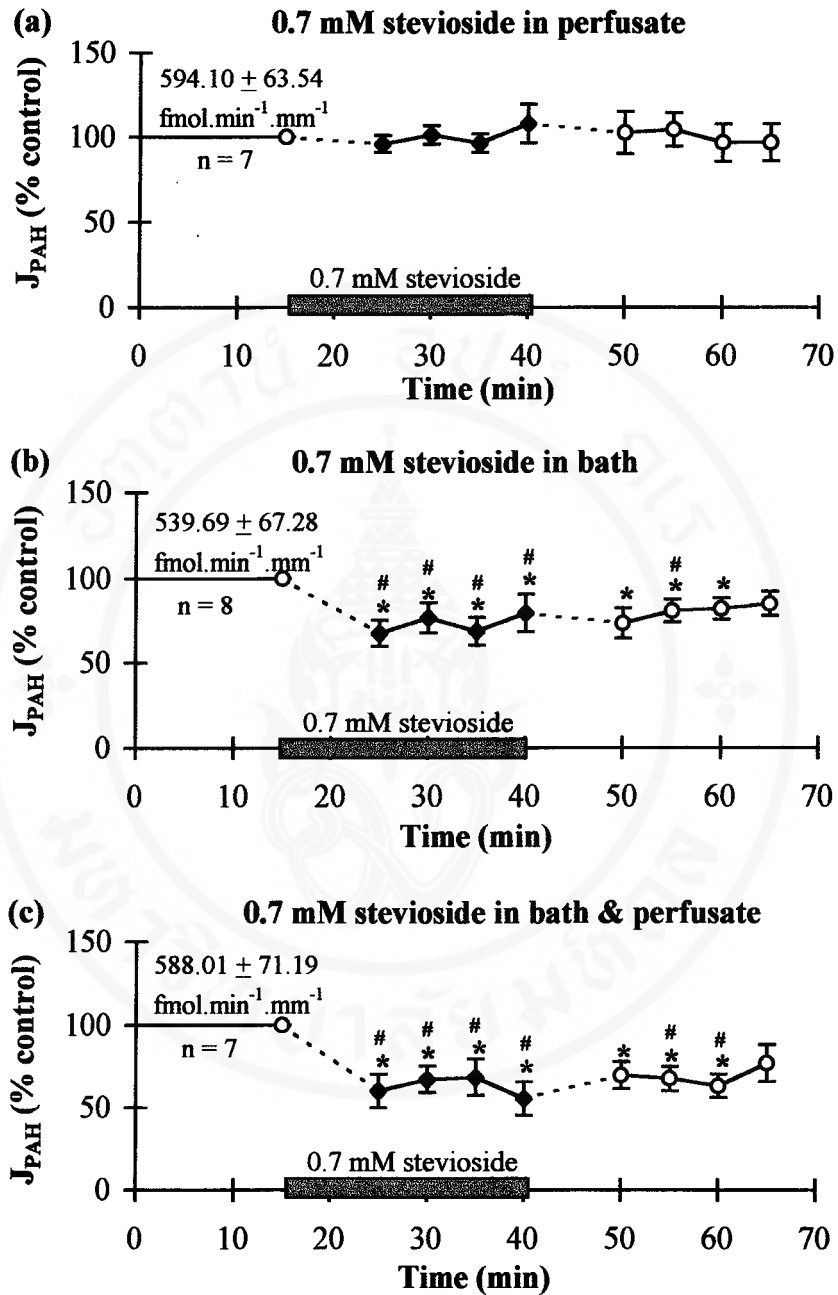


**Figure 11.** The effect of 0.7 mM stevioside (a) in perfusate, (b) in a bath, and (c) in both a bath and perfusate on  $J_{PAH}$  in the tubules perfused and bathed with a bicarbonate-buffered medium. See legend of figure 8 for a complete description of symbols. \*Significant difference from control, #Significant difference from the value at the same time period of stevioside treatment in perfusate,  $p$ -value < 0.05. The shaded bar indicates time when 0.7 mM stevioside was present in the medium.

### **3. STEVIOL EFFECT ON $J_{PAH}$**

#### **3.1 Time control of DMSO treatment in the bath on the transepithelial transport of PAH**

This experiment was performed to be certain that DMSO (that would be used as a solvent for subsequent experiments) did not disturb the normal function of the isolated perfused renal proximal tubules throughout the experimental duration. As shown in Figure 12, the rabbit renal proximal tubule was perfused with a control solution and DMSO 0.125% (v/v) was added to the bathing medium. The transepithelial transport of PAH ( $J_{PAH}$ ) did not change significantly during 65 minutes of experiment. This result helped us to eliminate any effects of DMSO (that would be used as a solvent to solubilize steviol in the next experiments) on  $J_{PAH}$ . This meant that any alteration in  $J_{PAH}$  observed after steviol treatment would be due to the effect of steviol itself.

#### **3.2 Concentration-response: effects of various concentrations of steviol on $J_{PAH}$**

For the same reason as mentioned earlier, the effects of steviol at various concentrations were examined only when steviol was present either in the bath or on the basolateral side, because the basolateral transport of PAH into the cell is the rate-limiting step for the transepithelial transport of PAH (95, 272). We perfused and bathed each tubule initially with a control bicarbonate-buffered medium containing DMSO at the same concentration as that used to dissolve steviol for 15 minutes. This procedure was performed to obtain control values for  $J_{PAH}$ . After this period,

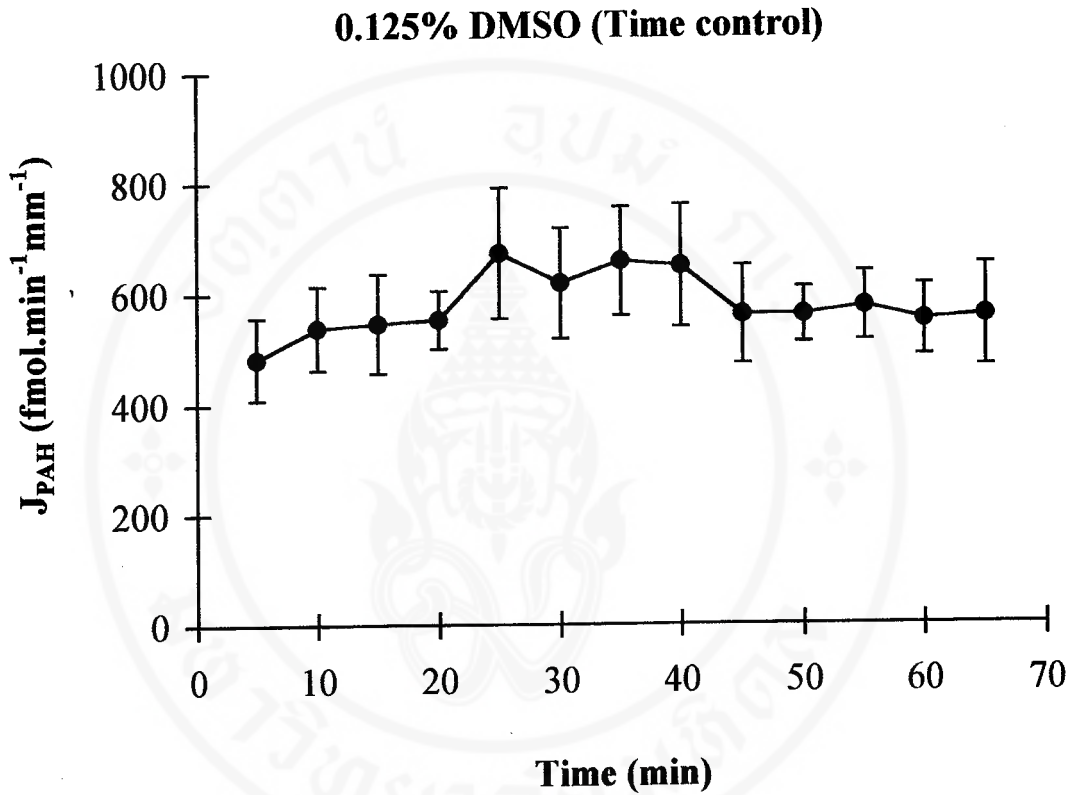


**Figure 12.** Control transepithelial secretory transport of p-aminohippurate (PAH),  $J_{PAH}$  in isolated proximal tubules perfused with a bicarbonate-buffered medium and bathed with a medium containing 0.125% (v/v) dimethylsulfoxide (DMSO). Absolute values of  $J_{PAH}$  given in fmol.min<sup>-1</sup>.mm<sup>-1</sup> (mean  $\pm$  SE) were determined at 5-minute intervals over a period of 65 minutes, n = 4.

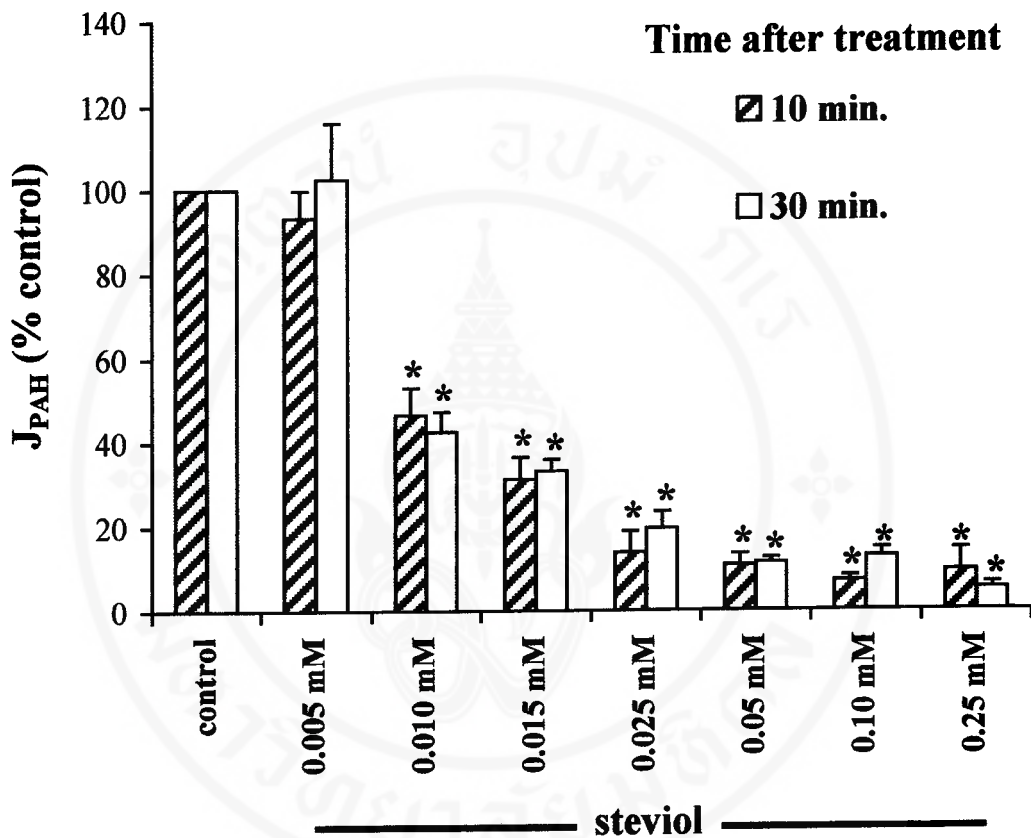


**Figure 13.** The effects of various concentrations (0.005, 0.010, 0.015, 0.025, 0.05, 0.10 and 0.25 mM) of steviol in a bath on  $J_{PAH}$  of isolated proximal tubules after incubation periods of 10 and 30 minutes. \*Significant difference from the control values,  $p$ -value < 0.05. Values are mean  $\pm$  SE of three separate experiments.

the bathing medium was changed to one containing steviol and  $J_{PAH}$  was determined at 10 and 30 minutes after steviol treatment. As shown in Figure 13, the presence of steviol in the bath at a concentration of 0.005 mM produced no significant change in  $J_{PAH}$  from the control values after either a 10- or 30-minute treatment. When the concentrations of steviol that bathed the tubule were increased from 0.01 to 0.25 mM,  $J_{PAH}$  was significantly depressed from control values. With a concentration of 0.01 mM steviol,  $J_{PAH}$  was inhibited by about 50% after a 10-minute treatment and remained depressed after steviol treatment for 30 minutes. The maximum inhibition of  $J_{PAH}$  by approximately 90% occurred when a concentration of steviol over 0.05 mM was present in the bathing medium.

To examine the steviol action when it was present at each side of the proximal tubule, a concentration of 0.01 mM steviol, which showed a half-inhibition of  $J_{PAH}$  from the control value was chosen for further experiments.

### 3.3 The effect of 0.01 mM steviol on $J_{PAH}$

In these experiments, the  $S_2$  segments of rabbit renal proximal tubules were perfused and bathed initially with a control bicarbonate-buffered medium containing 0.005% (v/v) of DMSO (the same concentration as that used to dissolve 0.01 mM steviol) for the first 15 minutes to obtain the control values of  $J_{PAH}$ . After this period, the perfusate was changed to one containing 0.01 mM steviol.  $J_{PAH}$  was slightly decreased, but not significantly different from control values (Figure 14a). In contrast, the addition of 0.01 mM steviol to the bathing medium caused  $J_{PAH}$  to be significantly depressed by about 50-60% compared with control values.

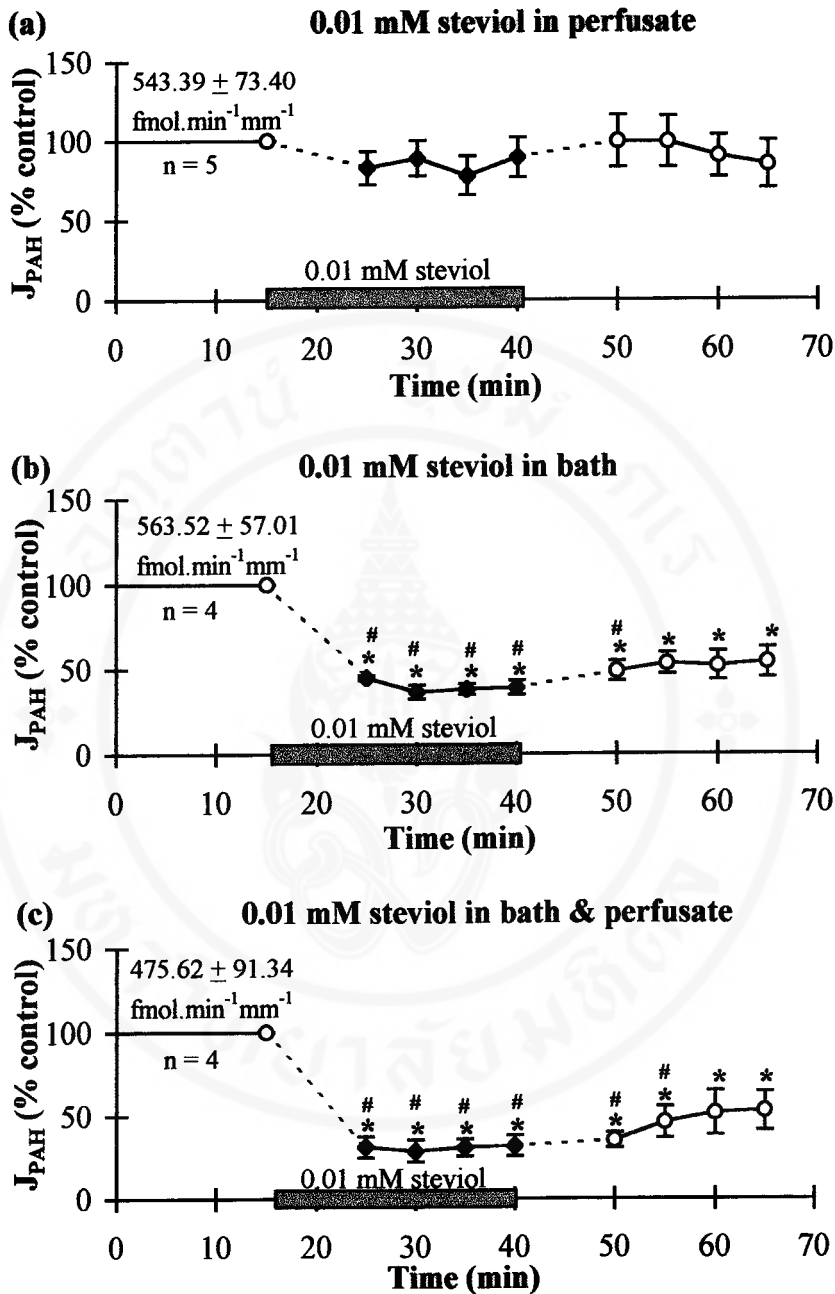


**Figure 14.** The effect of 0.01 mM steviol (a) in perfusate, (b) in a bath, and (c) in both a bath and perfusate on  $J_{PAH}$  in tubules perfused and bathed with a bicarbonate-buffered medium containing 0.005% (v/v) DMSO. Values of  $J_{PAH}$  are shown as percent of the mean control value (control being 100%) for each tubule in the first 15 minutes. Absolute mean  $J_{PAH}$  (fmol.min<sup>-1</sup>mm<sup>-1</sup>) value ± SE for all tubules in the first 15 minutes is indicated. N = number of tubules. The shaded bar indicates time when 0.01 mM steviol was present in the medium. \*Significant difference from the control, #Significant difference from the values at the same time period of 0.01 mM steviol treatment in perfusate, p-value < 0.05.

The depression of  $J_{PAH}$  remained significantly different from control values even after steviol had been removed from the bathing medium for 20 minutes (Figure 14b). The depression of  $J_{PAH}$  under these conditions was significantly different from that seen when steviol was in the perfusate (Figure 14a). When 0.01 mM steviol was simultaneously added to both the perfusate and the bathing medium (Figure 14c), there was a slight increase in the inhibitory effect on  $J_{PAH}$  when compared to that observed with steviol addition to the bathing medium alone, however, this the difference was not statistically significant. Similar to that observed when steviol was in the bath alone,  $J_{PAH}$  remained depressed when 0.01 mM steviol was removed from both the bathing medium and the perfusate (Figure 14c).

#### **3.4 The effect of luminal steviol at a concentration of 0.05 mM on $J_{PAH}$**

From the result mentioned above, the presence of 0.01 mM steviol in the lumen had no significant effect on  $J_{PAH}$ . We thus further examined the effect of a 0.05 mM steviol addition to perfusate on  $J_{PAH}$ . As shown in the concentration-response study (Figure 13), steviol at a concentration of 0.05 mM was the lowest concentration that showed the maximum inhibitory effect (90% inhibition) on  $J_{PAH}$  when it was in the bathing medium. The addition of 0.05 mM steviol to the luminal side significantly depressed  $J_{PAH}$  from that of the control values by about 70% (Figure 15). After the removal of steviol from the perfusate,  $J_{PAH}$  remained depressed for at least 20 minutes. This result showed that the inhibition of  $J_{PAH}$  by luminal steviol required a higher concentration of steviol than that present on the basolateral side.

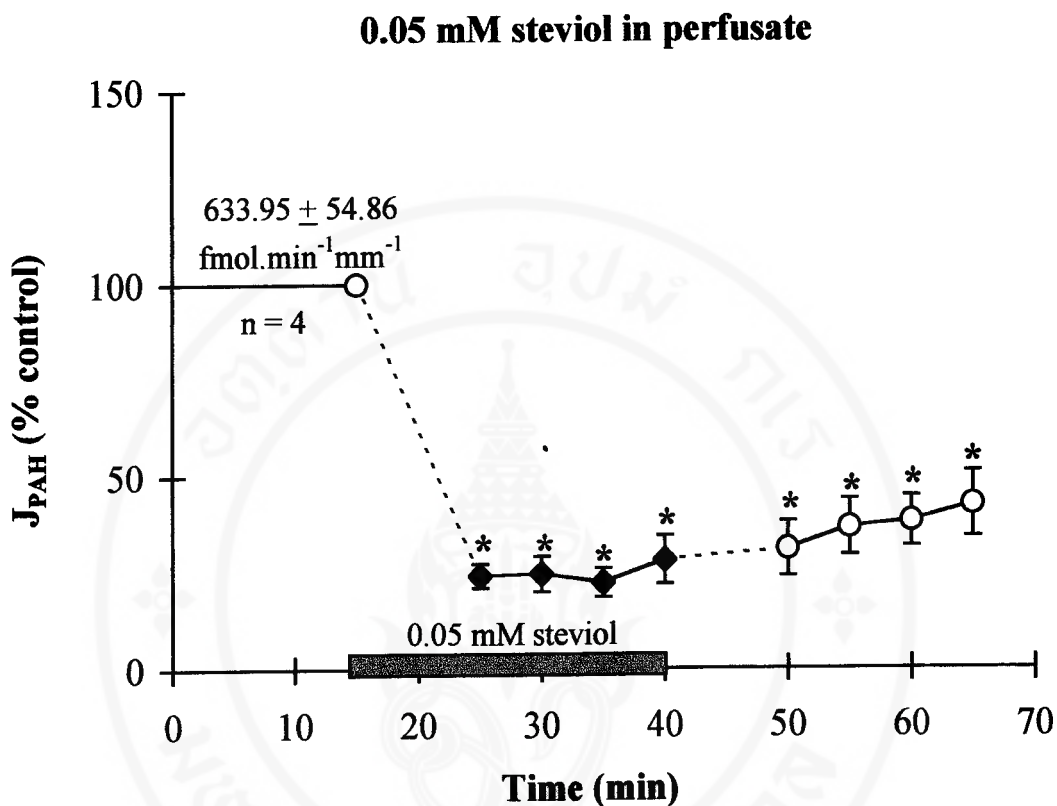


**Figure 15.** The effect of 0.05 mM steviol in the perfusate on  $J_{PAH}$  in tubules perfused and bathed with a bicarbonate-buffered medium containing 0.025% (v/v) DMSO. Values for  $J_{PAH}$  are shown as percent of mean control value (control being 100%) for each tubule in the first 15 minutes. Absolute mean  $J_{PAH}$  ( $\text{fmol}\cdot\text{min}^{-1}\cdot\text{mm}^{-1}$ ) value  $\pm$  SE for all tubules in the first 15 minutes is indicated. The shaded bar indicates the time when 0.05 mM steviol was present in the perfusate. \*Significant difference from control,  $p$ -value  $< 0.05$ .

#### **4. THE MECHANISM BY WHICH STEVIOSIDE AND STEVIOL INHIBIT $J_{PAH}$**

The mechanism of transepithelial PAH transport in the proximal tubule requires the energy from ATP hydrolysis and the activity of  $Na^+K^+$  ATPase, especially entry step of PAH transport across the basolateral membrane (29, 33). As previously mentioned, transepithelial transport of PAH was inhibited by stevioside (0.7 mM) and steviol (0.01 mM and higher). Thus, investigations of the effects of stevioside and steviol on  $Na^+K^+$  ATPase activity and ATP content were performed to explore the mechanism underlying the depression of  $J_{PAH}$ .

##### **4.1 The effects of stevioside and steviol on $Na^+K^+$ ATPase activity**

These experiments were performed using rabbit renal proximal tubule suspension so that enough tissue could be obtained for the determination of  $Na^+K^+$  ATPase activity. The proximal tubule suspension was incubated with a treatment solution (0.7 mM stevioside and various concentrations of steviol and DMSO) for 20 minutes, which was the same period as was used to study  $J_{PAH}$ , as mentioned earlier. A bicarbonate-buffered solution was used as the control solution and various concentrations of DMSO (0.005, 0.025 and 1.0% (v/v)) were used as the paired control to match the various concentrations of steviol (0.01, 0.05 and 2.0 mM) used, respectively. As shown in Figure 16,  $Na^+K^+$ -ATPase activity did not change significantly after a 20-minute incubation of all groups, either compared to the incubation with the control bicarbonate medium or to its paired control group for each treatment. In response to increasing the steviol concentration to 2 mM, a higher

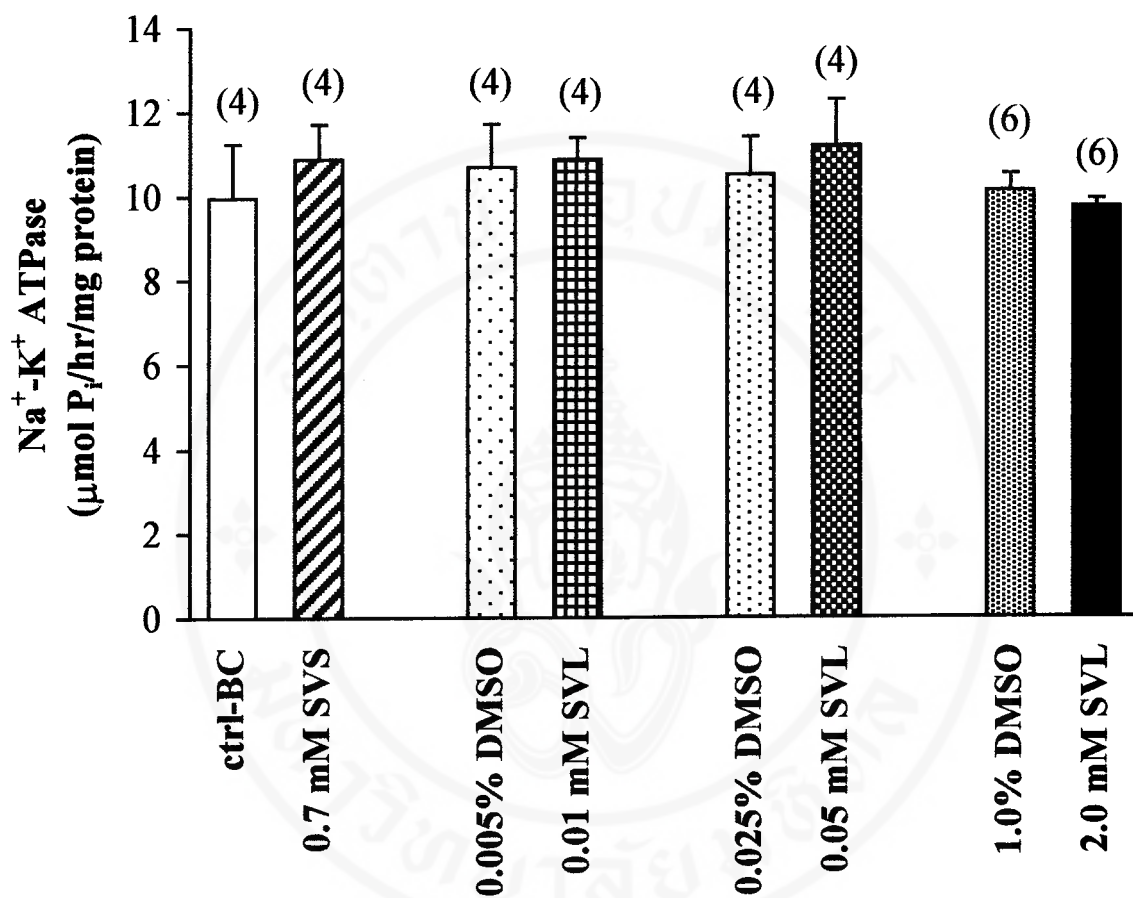


**Figure 16.** The effects of 0.7 mM stevioside and various concentrations (0.01, 0.05 and 2.0 mM) of steviol on Na<sup>+</sup>-K<sup>+</sup> ATPase activity in rabbit renal proximal tubule suspension after a 20-minute treatment. The values are shown as μmol P<sub>i</sub>/hour/mg of tubule protein, as means ± SE of duplicate measurements. Number of separate experiments is shown in parentheses on each bar.

concentration than that used for the  $J_{PAH}$  studies, the  $Na^+-K^+$ -ATPase activity was slightly decreased but not significantly changed from its control value. From these results, it is unlikely that the inhibitory effects of stevioside and steviol observed on  $J_{PAH}$  at the concentrations used in the previous experiments involved alteration of the proximal tubular  $Na^+-K^+$ -ATPase activity.

#### **4.2 The effects of stevioside and steviol on cell ATP content**

As previously mentioned, ATP is an important factor for the active transport of PAH across the basolateral membrane of the proximal tubule (33, 88). We used RP-HPLC to analyze the ATP content extracted from proximal tubules after treatment with stevioside or steviol. Using HPLC analysis, low amounts of ATP and its degradation products in samples could be quite accurately detected. We found that stevioside (0.7 mM) and steviol (0.01 and 0.05 mM) at the concentrations which were able to depress the  $J_{PAH}$  of renal proximal tubules, did not significantly change the ATP, ADP and AMP contents as well as hypoxanthine in the proximal tubules after a 20-minute treatment (Figures 17-19). In addition, no intracellular xanthine of renal proximal tubules was detected in any treatment group. The extracellular AMP and hypoxanthine contents, which are the indicators of nucleotide degradation processes, mainly appeared in the condition of cell ATP depletion, were also not significantly different from the control group in any treatment group. In contrast, steviol at the higher concentration, 2.0 mM, showed a significant reduction of proximal tubule cell ATP content (Figure 17). It was found that, during the time when cell ATP content was decreased with the 2.0 mM steviol treatment, the cell AMP content was dominantly high (Figure 19).

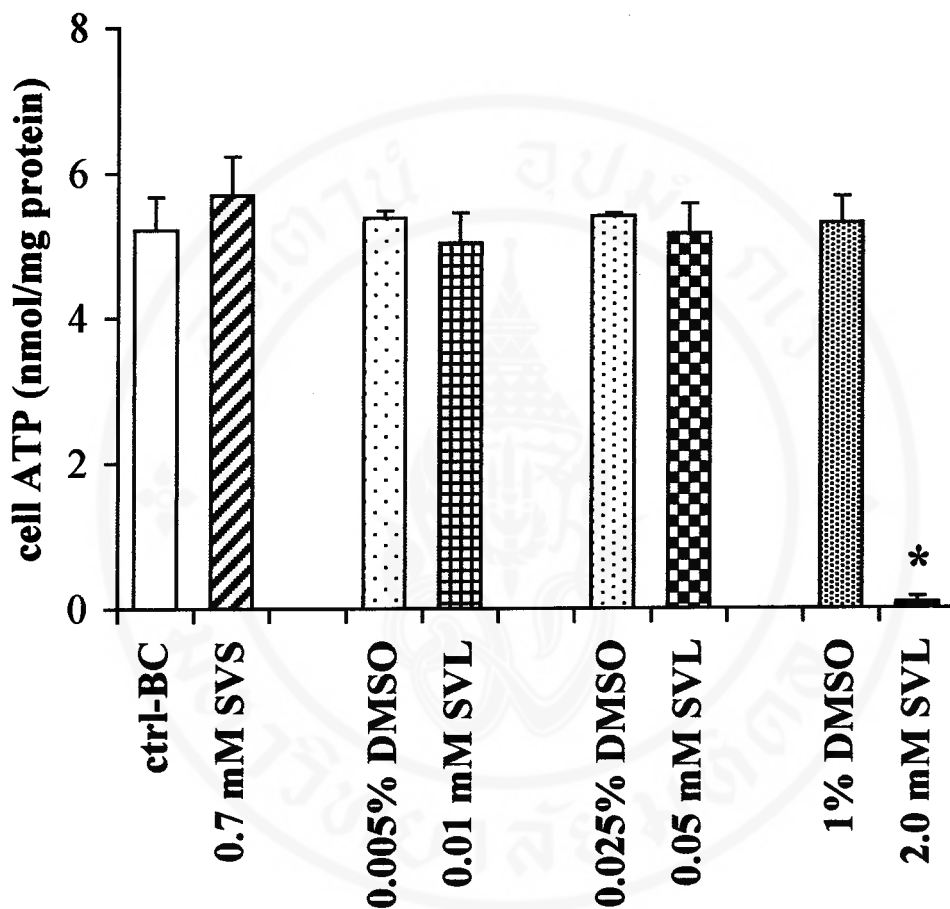


**Figure 17.** The effects of 0.7 mM stevioside and various concentrations (0.01, 0.05 and 2.0 mM) of steviol on cell ATP content extracted from rabbit renal proximal tubule suspensions after a 20-minute treatment. The values are shown as nmol of ATP/mg of tubule protein;  $n = 4$ . \*Significant difference from the other treatments,  $p$ -value  $< 0.05$ .

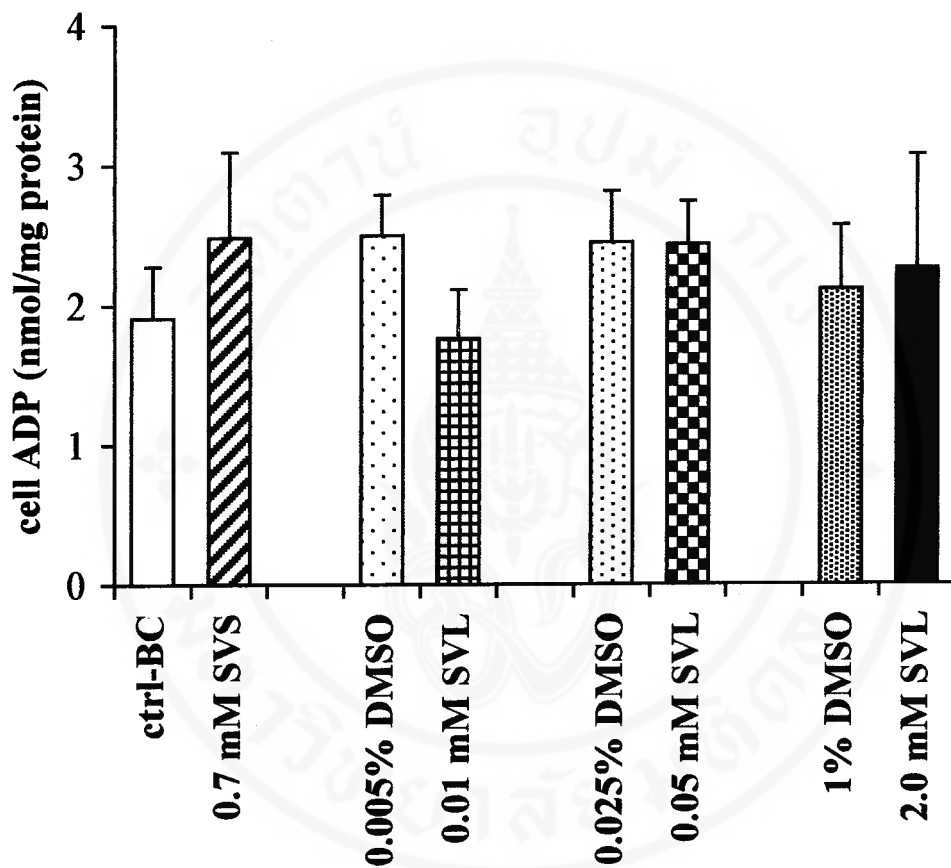


**Figure 18.** The effects of 0.7 mM stevioside and various concentrations (0.01, 0.05 and 2.0 mM) of steviol on cell ADP content extracted from rabbit renal proximal tubule suspensions after a 20-minute treatment. The values are shown as nmol of ADP/mg of tubule protein; n = 4.

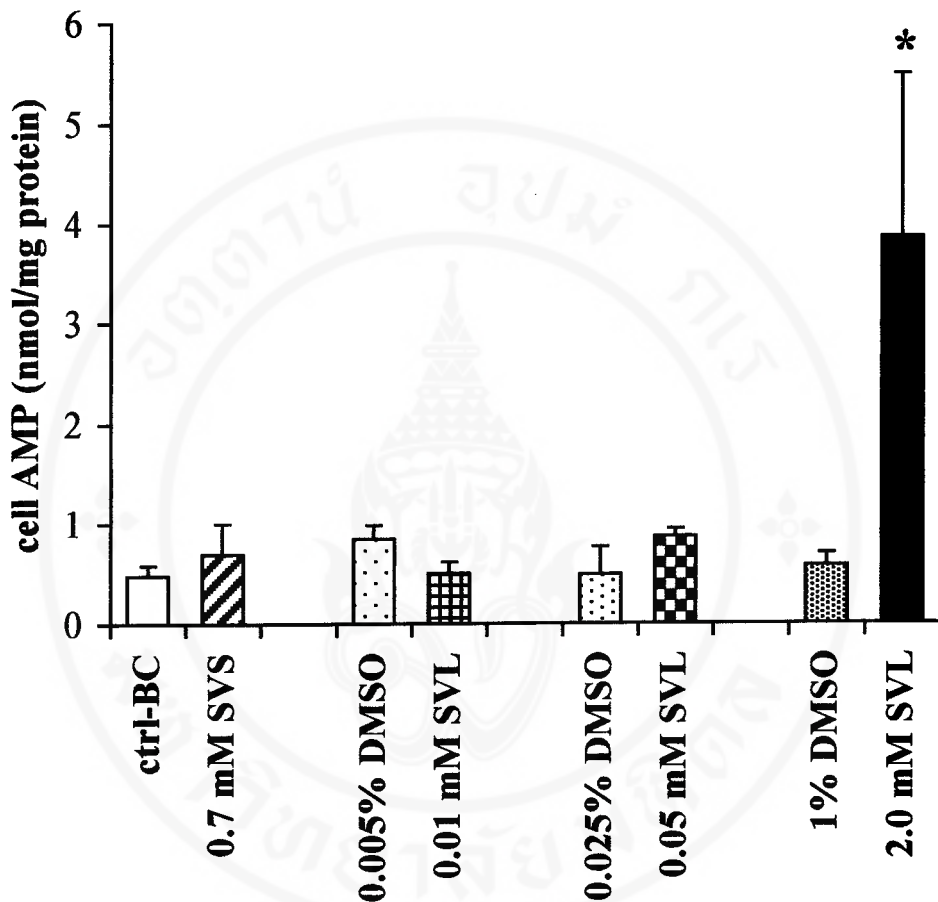


**Figure 19.** The effects of 0.7 mM stevioside and various concentrations (0.01, 0.05 and 2.0 mM) of steviol on cell AMP content extracted from rabbit renal proximal tubule suspensions after a 20-minute treatment. The values are shown as nmol of AMP/mg of tubule protein;  $n = 4$ . \*Significant difference from the other treatments,  $p$ -value  $< 0.05$ .

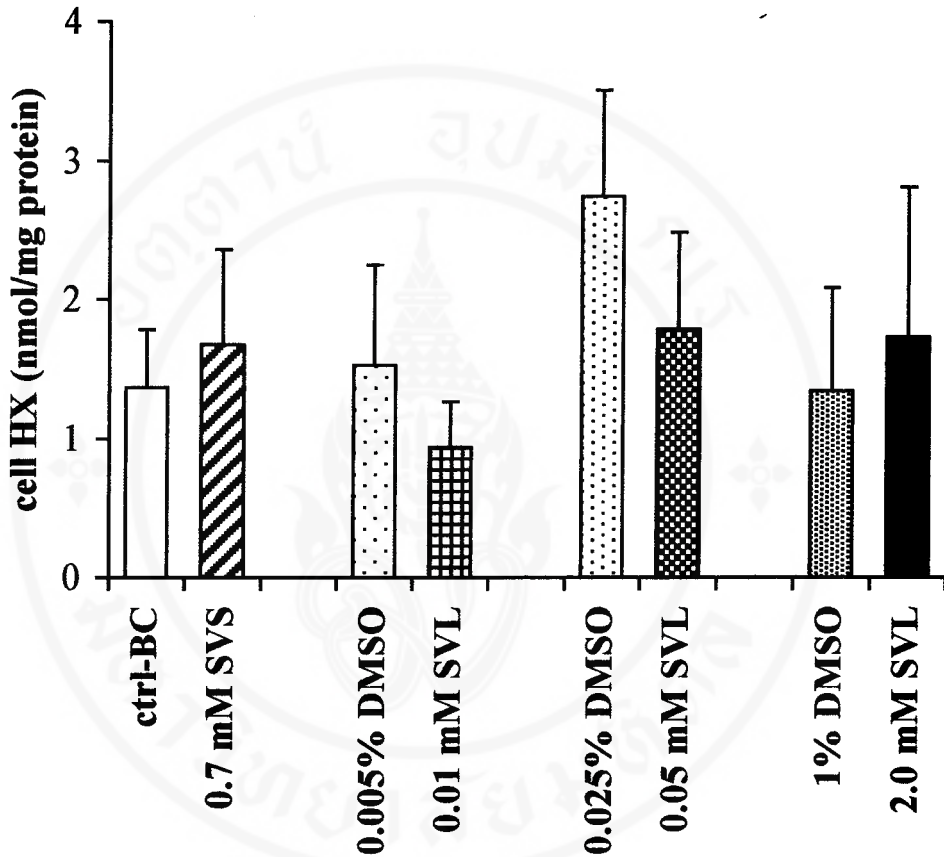


**Figure 20.** The effects of 0.7 mM stevioside and various concentrations (0.01, 0.05 and 2.0 mM) of steviol on cell hypoxanthine (HX) content extracted from rabbit renal proximal tubule suspensions after a 20-minute treatment. The values are shown as nmol of hypoxanthine/mg of tubule protein; n = 4.

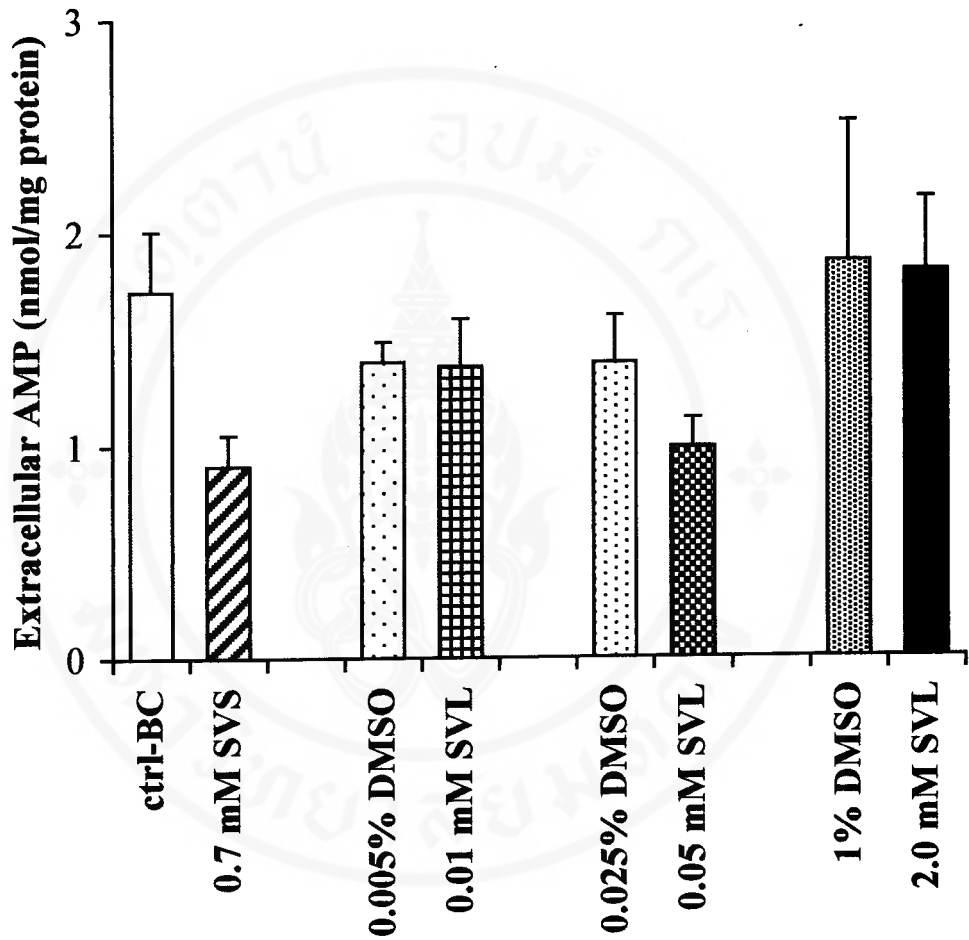


**Figure 21.** The AMP content in the incubation medium of renal proximal tubule suspensions treated with 0.7 mM stevioside and various concentrations (0.01, 0.05 and 2.0 mM) of steviol for 20 minutes. The values are shown as nmol of AMP/mg of tubule protein;  $n = 4$ .

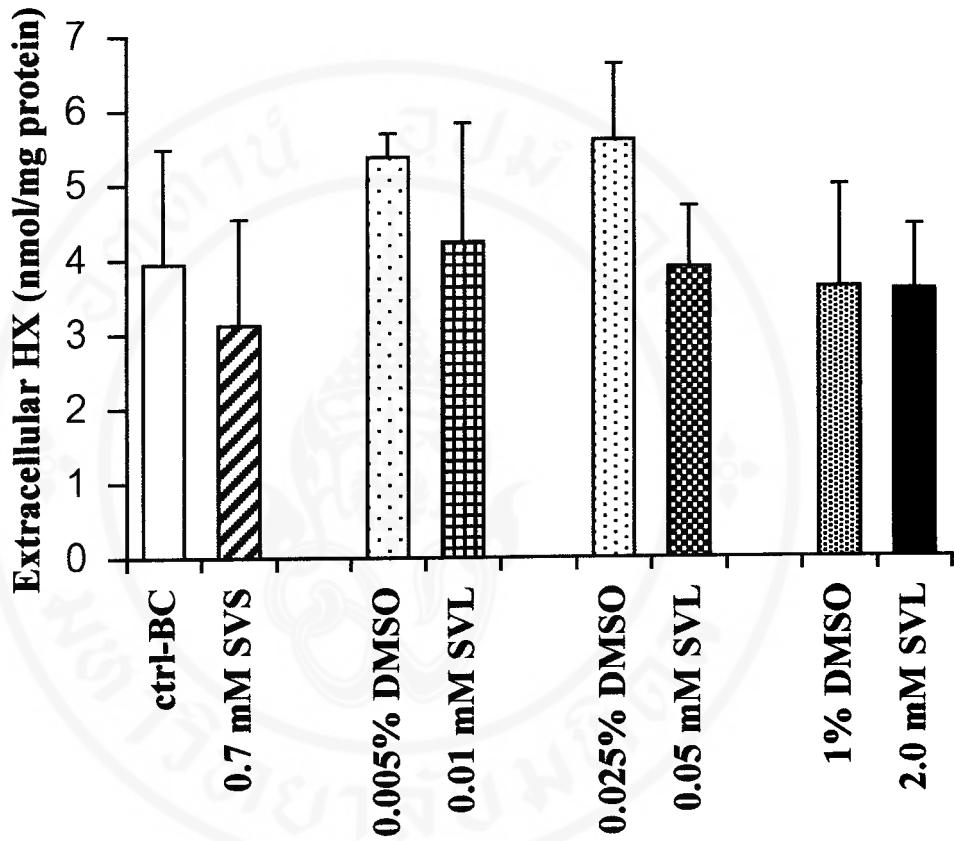


**Figure 22.** The hypoxanthine content in the incubation medium of renal proximal tubule suspensions treated with 0.7 mM stevioside and various concentrations (0.01, 0.05 and 2.0 mM) of steviol for 20 minutes. The values are shown as nmol of hypoxanthine/mg of tubule protein; n = 4.

## 5. KINETIC STUDY OF STEVIOSIDE AND STEVIOL ON PAH UPTAKE IN PROXIMAL TUBULE SUSPENSIONS

To examine whether stevioside and steviol inhibited PAH transport by competing with PAH at the PAH transporter site, we performed a kinetic study.

### 5.1 Determination of the appropriate time for PAH uptake into renal proximal tubule suspensions

For the kinetic study, the initial rate (linear phase) of transport is required when no saturation of the transporters occurred at that period. The proximal tubule suspension was pre-warmed to 37°C prior to the uptake study so that it would be fully functioning during the rapid uptake measurement. The <sup>14</sup>C-PAH concentration used in this experiment was 5 μM, which was far below the level that would saturate the transport systems. The uptake time was varied to be 15, 30, 45 sec, 1, 2 and 5 min (Figure 23). As the linear phase occurred from 0 to 30 sec, we chose to perform the kinetic uptake study using a 30-second uptake for subsequent experiment because it was in the initial phase of PAH uptake as well as allowing us enough time to perform the uptake.

### 5.2 Kinetic study for PAH uptake into renal proximal tubule suspension

The renal proximal tubule suspensions were incubated with a medium containing various concentrations of PAH for 30 seconds, and PAH uptake to the tubules was determined and plotted using a Lineweaver-Burk plot (between 1/PAH uptake and 1/[PAH]) to obtain the  $K_m$  and  $J_{max}$  of PAH uptake (Figure 23). The  $K_m$  of PAH uptake into proximal tubule suspensions was  $282.0 \pm 45.48 \mu\text{M}$  and the  $J_{max}$  was  $5.0 \pm 2.45 \text{ nmol PAH/mg tubule protein/min}$ .

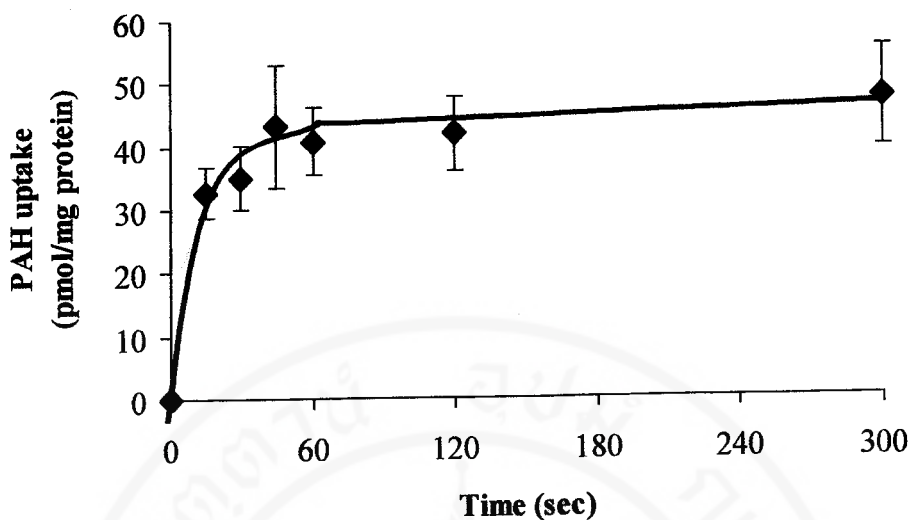


**Figure 23.** The time course of PAH uptake by rabbit renal proximal tubule suspensions. Each point represents mean  $\pm$  SE from three separate experiments. The values of PAH uptake are expressed as pmol/mg protein. The concentration of  $^{14}\text{C}$ -PAH in the incubation medium was 5  $\mu\text{M}$ .

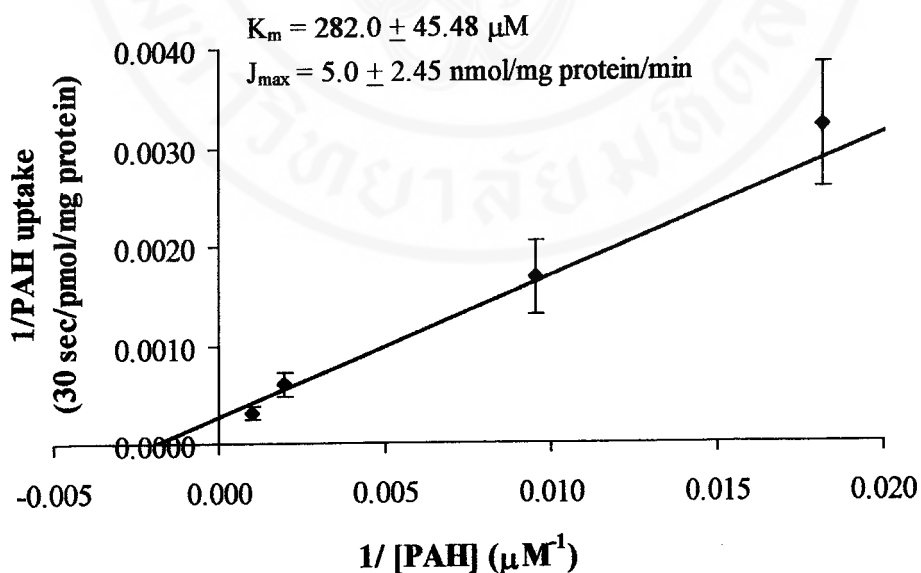


**Figure 24.** The Lineweaver-Burk plot of PAH uptake by rabbit renal proximal tubule suspensions with increasing concentrations of PAH in the medium. Uptakes were determined from 30-second incubations. Data are shown as the reciprocal of PAH uptake on the ordinate versus the reciprocal of PAH concentrations in the medium on the abscissa. Each point represents the mean  $\pm$  SE of 3 separate experiments.

### 5.3 Kinetic study for cis-inhibition of PAH uptake into renal proximal tubule suspensions by stevioside and steviol

To examine the  $K_i$  of stevioside and steviol for PAH uptake, experiments were performed in a paired observation between control and stevioside treatment or control and steviol treatment. As shown in Figure 25, the  $K_m$  for PAH uptake was altered when 0.7 mM stevioside was added to the medium, being 1.5 times higher than that of the control value. The  $J_{max}$  for PAH during the treatment of 0.7 mM stevioside was also slightly changed, but was not significantly different from the control  $J_{max}$  value (without stevioside treatment) [ $4.0 \pm 0$  vs  $5.2 \pm 0.6$  nmol/mg protein/min]. The  $K_i$  of stevioside for PAH uptake was  $1.45 \pm 0.4$  mM.

The effect of steviol can be obtained by using a Lineweaver-Burk plot, as shown in Figure 26. The  $K_m$  of PAH in the presence of 0.01 mM steviol was increased almost 3 times higher than that of the control  $K_m$  (in the absence of steviol). This showed that the affinity of the PAH transporter to PAH was reduced when the tubule was treated with steviol. The  $J_{max}$  of PAH was not significantly changed by the steviol ( $6.0 \pm 2.0$  vs  $6.6 \pm 1.8$  nmol/mg tubule protein/min). This indicated that the inhibition of PAH transport by stevioside and steviol is a competitive type. The  $K_i$  of steviol for PAH uptake in renal proximal tubule suspensions was  $7.4 \mu\text{M}$ . This showed that the affinity of the PAH transporter to steviol was higher than that to stevioside.

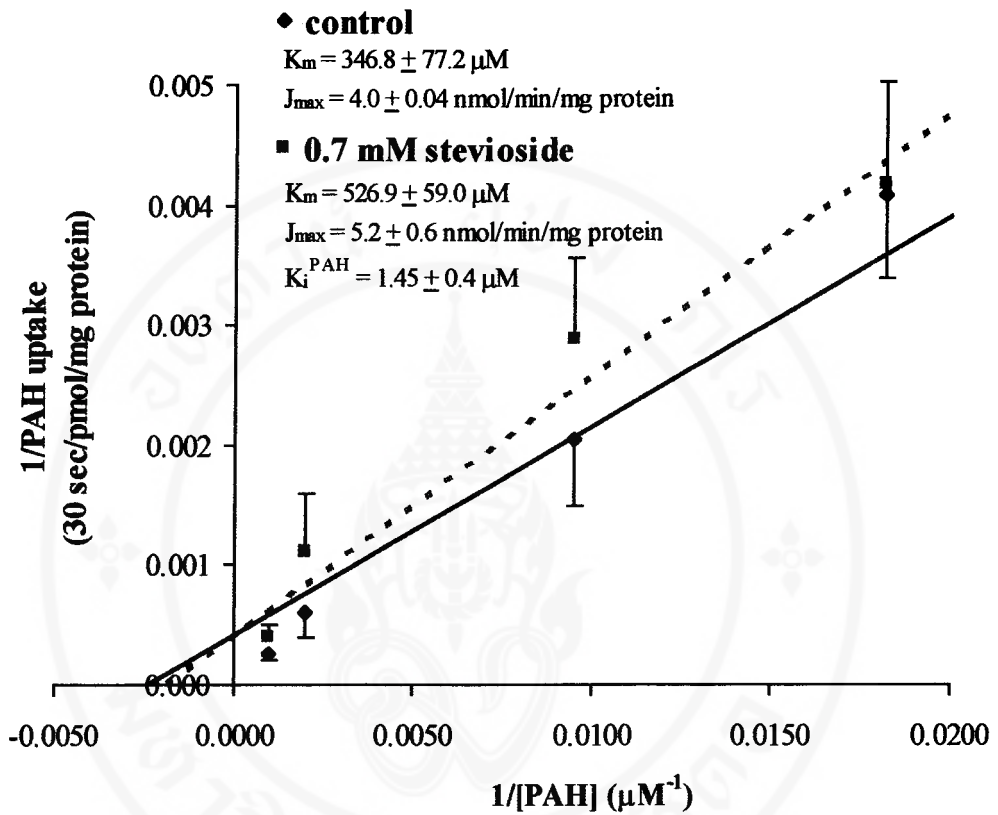


**Figure 25.** The Lineweaver-Burk plot of PAH uptake by rabbit renal proximal tubule suspensions with increasing concentrations of PAH in the medium in the absence (solid diamonds) and presence (solid squares) of stevioside (0.7 mM). Data are shown as the reciprocal of PAH uptake on the ordinate versus the reciprocal of PAH concentrations in the medium on the abscissa. Each point represents the mean  $\pm$  SE of 3 separate experiments.

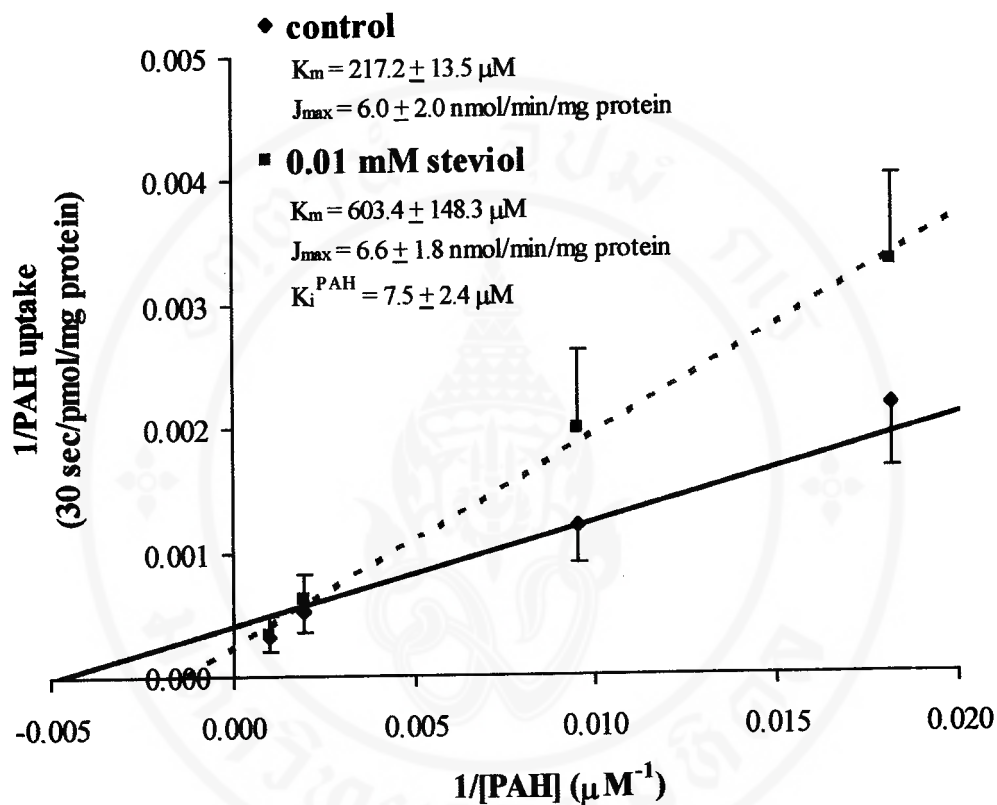


**Figure 26.** The Lineweaver-Burk plot of PAH uptake by rabbit renal proximal tubule suspensions with increasing concentrations of PAH in the medium in the absence (solid diamonds) and presence (solid squares) of steviol (0.01 mM). Data are shown as the reciprocal of PAH uptake on the ordinate versus the reciprocal of PAH concentrations in the medium on the abscissa. Each point represents the mean  $\pm$  SE of 3 separate experiments.

## CHAPTER V

### DISCUSSION

Stevioside, a sweet compound obtained from the *Stevia rebaudiana* plant, has been used commercially as a non-caloric sugar substitute in many countries, especially Japan, for over 20 years. The use of this plant in the form of a crude extract, which contains stevioside as the major component, was also reported to have therapeutic effects, for example, contraceptive, hypotensive, hypoglycemic and diuretic properties (5, 6, 12, 18, 19). This has led many investigators to perform extensive physiological and therapeutic studies including the safety to use in the form of pure compound, especially stevioside. Steviol, the aglycone part of stevioside, is one of the stevioside metabolites during enzymatic hydrolysis (212, 213, 220, 221). The incubation of stevioside with intestinal bacterial microflora obtained from rats *in vitro* showed the complete conversion of stevioside to steviol within an incubation period of 2-4 days. Intracecal and oral administrations of steviol were nearly completely absorbed in the lower bowel of rat (25). Steviol has been reported to be a toxic substance with mutagenic and bactericidal activities in *Salmonella typhimurium* TM 677 (239). However, both stevioside and steviol have also been revealed to have therapeutic value as diuretic drugs by increasing urinary fluid and sodium excretion (10, 17, 28), and as diabetic drugs by stimulating insulin secretion from the pancreas (260). Normally, the safety to use any substance as a drug has been subjected to serious studies. Detailed information concerning the toxicity of stevioside and steviol are

required before their commercial use as a food additive or drug would be granted. The safety of long-term consumption was investigated by Yamada et al. (233) who found that oral consumption of stevioside (75% pure) with an amount as high as 550 mg/kg BW/day for 2 years, showed no toxic or carcinogenic effects in the rat, and did not affect their growth rate. In humans, a likely maximum intake of stevioside was suggested to be only about 2 mg/kg BW/day. This is far below the amount shown earlier to have no toxicity in the rat (234). More recently, Toskulkao and Sutteerawattananon (13) found a significant inhibition of intestinal glucose absorption and a reduction in growth rate in hamsters treated orally with 2.5 g/kg BW/day of stevioside (90% pure) for 12 weeks, whereas lower doses (0.5 and 1.0 g/kg BW/day) had no effect. The different responses observed may be due to the differences in animal species as well as to purity, dose and route of drug administration.

Investigations on the systemic effects of stevioside and steviol were also performed. It was found that the intravenous injection of stevioside (>90% pure) at a dose of 16 mg/kg BW induced a fall in mean arterial blood pressure (mABP) in normal rats (7, 10, 17, 19) and in conscious spontaneously hypertensive rats (SHR) (11). In addition to its systemic effect, studies on rat renal function *in vivo* (9, 10, 17-19) found that both chronic oral intake and acute intravenous administration of stevia extract or stevioside to rats produced increased renal blood flow (RBF), natriuresis and diuresis, whereas the glomerular filtration rate (GFR) did not change. Intravenous infusion of steviol to rats also resulted in diuresis and natriuresis (28). With the intention to differentiate the systemic effect of stevioside from its renal effect,

Thongouppakarn (20) infused stevioside directly into the left renal artery of rats. He found an alteration in rat renal hemodynamics and tubular function and also suggested that the target site of stevioside action on tubular function was the proximal tubule, as indicated by lithium clearance. However, the experimental model used in those previous studies could not differentiate the vascular effects of stevioside and steviol from their renal effects. Thus, the present study was designed to clarify whether stevioside and its metabolite, steviol, have any direct effect on tubular function. The study was performed using intact isolated perfused rabbit renal proximal tubules which has been proven to be a powerful tool to study tubular function (both secretion and reabsorption) (273). With this *in vitro* experimental model, the effects of stevioside and steviol on proximal tubular function can be investigated directly when these substances are present on either the basolateral or the luminal side of the tubule or on both sides at the same time, which mimics the *in vivo* condition. Normally, exogenous compounds that need to be eliminated from the body are present in both the luminal (from glomerular filtration) and peritubular sides of the tubule at the same time. Using this technique, a systemic effect could be eliminated. In addition, this technique is very sensitive and significant changes in transepithelial transport of PAH ( $J_{PAH}$ ) can be detected, even though only small changes in tubular function and metabolism occur (94). In the present study, the mechanisms by which stevioside and steviol altered transepithelial transport of PAH were also examined.

### **The Effect of Stevioside and Its Mechanism of Action on PAH Transport in Rabbit Renal Proximal Tubules**

The present study was initially performed to examine the direct effect of stevioside at a concentration of 0.45 mM, which is equivalent to a dose of 16 mg/kg BW/hr used by Melis's studies (9, 10, 17), and showed the changes in renal function, as mentioned earlier, on the proximal tubular transport of PAH. Neither with the addition of 0.45 mM stevioside into the bathing medium nor the perfusate (luminal fluid), was transepithelial transport of PAH ( $J_{\text{PAH}}$ ) significantly depressed. Higher concentration of stevioside were also examined. A limitation in solubility occurs when stevioside is of high purity. The maximum solubility of stevioside in the buffered medium used in the present study was only 0.7 mM. Stevioside at this concentration (0.7 mM) showed reversible inhibition of transepithelial transport of PAH ( $J_{\text{PAH}}$ ) when stevioside was only present in the bathing medium but not in the perfusate. The lack of effect of stevioside on  $J_{\text{PAH}}$  on the luminal side and its reversible inhibitory effect on the basolateral side indicate that a high dose of stevioside has relatively little effect on renal proximal tubular secretory function.

The cellular mechanism by which stevioside inhibited  $J_{\text{PAH}}$  in isolated perfused renal proximal tubule is not known. Transepithelial secretion of PAH by renal proximal tubules involves transport into the cell against an electrochemical gradient at the basolateral membrane, which is the rate-limiting step, followed by movement down an electrochemical gradient into the lumen across the luminal membrane. The transport process of PAH across the basolateral membrane is termed tertiary active transport in which the final step is transport of PAH (or another organic

anion) into the cell in exchange for a dicarboxylate ion moving out of the cell down its electrochemical gradient (29, 33, 61, 90, 94, 97). The outwardly-directed gradient for dicarboxylate is maintained through the uptake of dicarboxylate coupled with sodium ions into the cell and the intracellular production of dicarboxylate, whereas the sodium gradient that drives sodium-dicarboxylate cotransport is maintained through the hydrolysis of ATP by basolateral  $\text{Na}^+\text{-K}^+$  ATPase. Therefore, interfering with one or more of these entry processes could result in a reduction of  $J_{\text{PAH}}$ . Alternatively, interference with the luminal exit step of PAH, a carrier-mediated process (126), could also result in decreased  $J_{\text{PAH}}$ . Our results indicated that stevioside inhibited  $J_{\text{PAH}}$  only when present in the bathing medium, but not in the lumen, suggesting that only the basolateral membrane is susceptible to stevioside action.

As reported by Toskulkao and coworkers (22), stevioside given orally 2.5 g/kg BW/day for 12 weeks inhibited the intestinal  $\text{Na}^+\text{-K}^+$  ATPase activity of hamsters. It is possible that the inhibitory effect of stevioside on  $\text{Na}^+\text{-K}^+$  ATPase may also occur in other cells. The determination of  $\text{Na}^+\text{-K}^+$  ATPase activity in 0.7 mM stevioside-treated tubules revealed no alteration of this enzyme activity after an incubation for 20 minutes (Figure 16), while  $J_{\text{PAH}}$  was significantly depressed at this incubation time (Figure 10) when the same concentration of stevioside was used. As indicated earlier, due to the indirect link between the active transport of PAH and  $\text{Na}^+\text{-K}^+$  ATPase activity (75), the change in PAH transport may not result from an alteration in  $\text{Na}^+\text{-K}^+$  ATPase activity. Stevioside at the concentration of 0.7 mM used in this experiment (>95% pure) did not show an inhibitory effect on  $\text{Na}^+\text{-K}^+$  ATPase activity of rabbit renal proximal tubule suspensions, whereas the lower purity use

(90% pure) in Limpanichakul's study (21) caused a reduction of  $\text{Na}^+\text{-K}^+$  ATPase activity by about 30 and 45% for stevioside at concentrations of 0.5 and 1 mM, respectively. The discrepancy of the present results and that of the previous study (21) might be due to the purity of stevioside used. In other words, a contaminant might be the cause of the actions observed in the earlier studies. However, the results from the present study indicated that the reduction of  $J_{\text{PAH}}$  by stevioside treatment may not involve  $\text{Na}^+\text{-K}^+$  ATPase activity. Further examination was performed using HPLC to detect the alteration of cell ATP content and the degradation products of adenine nucleotides in the tubules treated with stevioside compared with the ones without stevioside treatment. Stevioside at the concentration of 0.7 mM did not alter the ATP content of the tubular cells compared with control treatment. Although the precise mechanism is not known, a number of statements can be made. It seems likely that stevioside cannot enter the cell due to its large and complex molecular structure (Figure 2). This assumption is supported by the study of Yamamoto and coworkers (253) showing that stevioside had no effect on oxygen uptake and gluconeogenesis in the isolated renal tubules of rat. Additionally, stevioside could inhibit oxidative phosphorylation in isolated rat liver mitochondria (251, 252, 254) but did not affect energy metabolism in intact cells (25). Using HPLC analysis, Podprasart (261) reported that stevioside could not pass into rabbit renal proximal tubule suspensions after incubation with stevioside (1.0 mM) for 60 minutes. These results support the proposal that stevioside affects the transport of PAH from outside the cell. The observations that stevioside did not affect cell ATP content and  $\text{Na}^+\text{-K}^+$  ATPase activity in the present study (Figures 16 and 17) support this assumption as well.

Moreover, the recovery of  $J_{PAH}$  after the removal of stevioside from the bathing medium also suggest that the effect of stevioside on  $J_{PAH}$  was only temporary. In contrast, contradictory results on  $Na^+K^+$  ATPase activity were obtained from stevioside-treated rats *in vivo* (258), wherein inhibition of  $Na^+K^+$  ATPase activity was observed in the kidney of stevioside-treated rats at a dose of 0.2 g/kg BW/hr given intravenously for 1 hour (258). Renal mitochondrial activity was also inhibited in that stevioside treatment. In that study also, stevioside was used at the very high concentration of 0.18 M, which was about 250 times greater than the maximum solubility of stevioside used in the present study, without precipitation. It has been known that the higher the purity of stevioside, the more difficult it is to get it dissolved in an aqueous solution (11). Thus, the effects observed by stevioside treatment in the *in vivo* study mentioned above may be due to the effect of contaminants or to metabolites of stevioside such as steviol (27) or isosteviol, the isomer of steviol which was reported to be more stable than stevioside (212). Steviol and isosteviol could inhibit mitochondrial enzyme activity, oxidative phosphorylation (251, 254), the oxygen uptake and gluconeogenesis in the intact isolated rat renal tubules (253). However, a definitive explanation for this discrepancy is still lacking.

The most likely mechanism responsible for the inhibition of  $J_{PAH}$ , that was seen in the present study, is that stevioside acts directly on the anion transporter system for PAH uptake at the basolateral membrane to inhibit PAH entry into the renal proximal tubular cells. This is consistent with the observations using rat renal cortical slices (23) and rabbit renal proximal tubule suspensions (21) where stevioside inhibits PAH accumulation into the renal cortical slices and proximal tubule

suspensions. A direct correlation between PAH accumulation and the transepithelial transport rate of PAH has been reported (94). In other words, the amount of PAH entry into the renal proximal cell at the basolateral membrane sets the rate at which PAH can be secreted into the lumen. Thus, the present data are compatible with the inhibition of PAH entry at the basolateral membrane, which is the rate-limiting step for the transepithelial transport of PAH.

It needs to be pointed out that the concentration of stevioside used in the present study (0.7 mM) to produce a significant inhibition of transepithelial transport of PAH in isolated perfused rabbit renal proximal tubules is higher than that used in the previous studies (0.1 mM) by Toskulkao et al. (23) and Limpanichakul (21). The difference may be due to the difference in the animal models used, as well as to the purity and sources of stevioside. The purity of stevioside used in the present study (obtained from Sigma Chemical Co., St. Louis, MO) was more than 95%, whereas the stevioside used in the previous studies (21, 23) was about 90%. It is possible that contaminants may be responsible for the effects observed, rather than stevioside itself (2). The major known impurities are rebaudioside A-E (2, 4). However, further study needs to be performed to elucidate the effect of these impurities.

To examine the interaction of stevioside at the basolateral PAH transporter of rabbit renal proximal tubules, a kinetic study of PAH transport was performed to obtain the  $K_m$  value (the concentration of PAH in the bath at which a transporter moves a solute at half its maximal rate) and the  $J_{max}$  value (the rate at which a transporter operates when fully saturated by PAH). The  $K_m$  value for PAH uptake into the rabbit renal proximal tubule suspensions in the present study was about 200-

300  $\mu\text{M}$  and the  $J_{\text{max}}$  was approximately 4-6 nmol/min/mg of tubule protein. The values obtained from this study were close to those reported previously, where the  $K_m$  value was in the range of 100-200  $\mu\text{M}$  (54, 62, 274) and the  $J_{\text{max}}$  value was 5.3 nmol/mg/min (274) for PAH transport in intact renal tubules of rabbits (both in single tubules and in tubule suspension). The results obtained from the kinetic study of this study showed that stevioside exhibited a competitive inhibition with PAH uptake across the basolateral membrane. Thus, it is possible that stevioside at a concentration of 0.7 mM inhibited the transepithelial transport of PAH by interfering with the binding of PAH with the PAH transporter at the basolateral membrane. It needs to be pointed out that the  $K_i$  value of stevioside for PAH uptake is 1.45 mM, which is higher than the concentration that significantly inhibited transepithelial transport of PAH (0.7 mM) in the present study. That would indicate that a 50% inhibition of  $J_{\text{PAH}}$  would be observed with a concentration of stevioside equal to  $K_i$  for the PAH uptake, if we could use stevioside at that concentration (1.45 mM). If this occurs, it will support the direct inhibition or interference of stevioside with PAH at the basolateral entry step, the rate-limiting step for the transepithelial transport of PAH.

It has been reported that only a small amount of stevioside taken orally is absorbed into the plasma (224). Thus, it is unlikely that at the normal human daily consumption rate of approximately 2 mg/kg BW (234), stevioside concentrations in the plasma or in the kidney would rise to levels that would severely impair renal function. Therefore, stevioside may be capable of therapeutic use in the future. However, further investigations should focus on the purity of stevioside to be used and on the effects of the metabolites from its degradation in the body.

### **The Effect of Steviol and Its Mechanism of Action on PAH Transport in Rabbit Renal Proximal Tubules**

It is known that dimethylsulfoxide (DMSO) is a good solvent that promotes the solubility of hydrophobic substances. Although it is used extensively for this purpose, it was reported to have certain biological effects, such as growth inhibition of Hela cells in culture (275), lowering of blood pressure (199) and producing diuresis in newborn rabbits (276). Treatment with 4.5 ml of 100% DMSO/kg BW, i.p., 5 days per week for 3 weeks in mice caused cardiotoxicity (277). In addition, DMSO at a concentration of 10% (v/v) or higher caused inhibition of  $\text{Na}^+\text{-K}^+$  ATPase activity by about 30% (199, 200, 278). Since the steviol used in the present study was dissolved in DMSO, the effect of the DMSO used in the medium on  $J_{\text{PAH}}$  was also examined. The effect of 0.125% (v/v) of DMSO, the maximum concentration used in the perfusion study, on  $J_{\text{PAH}}$  was determined throughout the period of experiment (65 minutes) as shown in Figure 12. The results showed that DMSO used at this low amount did not affect proximal tubular function. That helps to conclude with certainty that the reduction in  $J_{\text{PAH}}$  observed after steviol treatment resulted from the effect of steviol itself, and the DMSO used was not involved. Moreover, a control solution containing DMSO with the same concentration used to dissolve steviol at each concentration was used to bathe and perfuse the tubule during the control and recovery periods as their own control. Steviol in the bathing medium displayed an inhibitory effect on  $J_{\text{PAH}}$  in a concentration-dependent manner (Figure 13). The maximum inhibition was about 90% with steviol treatment at concentrations of 0.05 mM or higher. These results indicated that steviol depressed the transepithelial

transport of PAH of rabbit renal proximal tubules almost completely. It was found that the basolateral membrane was more susceptible to steviol's action, since steviol given in the bathing medium depressed  $J_{PAH}$  to a greater extent than when given in the luminal perfusate. Steviol at a concentration of 0.01 mM, when it was present in the bathing medium, reduced  $J_{PAH}$  by about 50-60%, whereas no significant effect on  $J_{PAH}$  was observed during its presence in the perfusate. The higher concentration (0.05 mM) of steviol also showed a different degree of inhibition on  $J_{PAH}$  between its presence in the bathing medium and in the perfusate. The presence of 0.05 mM steviol in the bathing medium depressed  $J_{PAH}$  by about 90%, but when it was present in the perfusate it depressed  $J_{PAH}$  by only approximately 70% (Figures 13 and 15). From these data, it seems likely that steviol was more effective in depressing the transepithelial transport of PAH from the basolateral side than from luminal side. The explanation for this observation is not known. It is probable that luminal steviol can pass through the luminal membrane of the proximal tubule, reaching the basolateral side and inhibiting PAH transport at the PAH transporter. Due to its long journey to the target site, some of the steviol might lose its potency. This is why its effect observed from the luminal side is less than that on the basolateral side. In contrast, steviol that was presented on the basolateral side might get to the target site faster, leading to the higher potency observed. The most likely target site is the PAH transporter on the basolateral membrane. However, steviol might affect other factors that involve the transepithelial transport of PAH, for example, energy metabolism within the proximal tubule and the activity of the  $Na^+K^+$  ATPase enzyme that participates in the transepithelial transport of PAH. It should be noted that the

addition of 0.05 mM steviol to the perfusate depressed  $J_{PAH}$  to a similar degree as that observed when steviol at concentrations between 0.015 and 0.025 mM was added to the bathing medium. This indicates that only half or less of the luminal steviol reached its site of action to depress  $J_{PAH}$ . Thus, with a concentration of steviol at 0.01 mM in the lumen, only 0.005 mM of it might get to the target site, so that no effect on  $J_{PAH}$  was observed. As mentioned earlier, transepithelial secretion of PAH by renal proximal tubules involves transport into the cell against an electrochemical gradient at the basolateral membrane, which is the rate-limiting step, followed by movement down an electrochemical gradient into the lumen across the luminal membrane. The net transport of PAH involves ATP and  $Na^+K^+$  ATPase activity. The results from the present study indicate that steviol depressed  $J_{PAH}$  mainly when it was present in the bathing medium. This suggests that the basolateral membrane is more susceptible to steviol's action than the luminal membrane, and is consistent with the previous observation using rat renal cortical slices (23) in which steviol (>90% pure) inhibited PAH accumulation into rat renal cortical slices *in vitro*. Steviol at concentrations between 1.56-100  $\mu$ M significantly reduced PAH accumulation by about 26-76%, the maximum inhibition of PAH accumulation in renal cortical slices being observed with 50  $\mu$ M steviol treatment. The present study also found that steviol at a concentration of 50  $\mu$ M produced the maximum inhibitory effect on  $J_{PAH}$ , although the degree of inhibition in isolated perfused proximal tubules of rabbit kidney was greater than that in rat renal cortical slices. However, the mechanisms by which steviol exerted its effects have not exactly been identified. The possibility that steviol may affect the exit step of PAH at the luminal membrane can not be ruled-out. We propose that the

mechanisms responsible for steviol action in the reduction of  $J_{PAH}$  might number 4 possibilities, these being:

**Firstly:** steviol may act as an inhibitor of  $Na^+ - K^+$  ATPase activity at the basolateral membrane of the proximal tubule, like ouabain, a potent inhibitor of  $Na^+ - K^+$  ATPase.

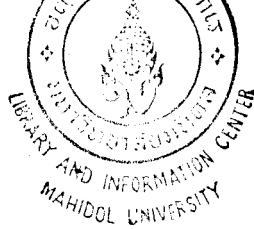
**Secondly:** steviol may enter the renal cells and then inhibit metabolic energy production within the cells, either by itself or by its degradation products.

**Thirdly:** steviol may act directly on the PAH transporter at the basolateral membrane, resulting in the reduction of PAH entry into the cell, which leads to the reduction of  $J_{PAH}$ .

**Fourthly:** steviol may affect the exit step of PAH at the luminal membrane.

To discriminate between these possibilities, further experiments were performed to study the effect of steviol on  $Na^+ - K^+$  ATPase activity. Steviol at various concentrations (0.01 and 0.05 mM) as used in the perfusion studies were used to examine their effects on  $Na^+ - K^+$  ATPase activity in rabbit renal proximal tubule suspensions. The results from the present study showed no significant alteration in this enzyme activity of rabbit renal proximal tubule suspension, either compared with its own control value obtained from the DMSO-containing solution or the control value obtained from a solution without DMSO addition (Figure 16). Moreover, the higher concentration of steviol (2 mM) had no inhibitory effect on  $Na^+ - K^+$  ATPase activity of rabbit renal proximal tubule suspension either. This high concentration (2 mM) of steviol was reported earlier to inhibit glucose absorption in the inverted gut sac and in the intestinal ring tissue of hamsters by about 85% and 46%, respectively,

after a 60-minute incubation (14, 256). In agreement with our results, steviol (2 mM) also showed no significant change in the  $\text{Na}^+\text{-K}^+$  ATPase activity of the hamster intestine (256). However, a previous study (261) found a significant reduction of  $\text{Na}^+\text{-K}^+$  ATPase activity in rabbit renal proximal tubule suspensions with steviol (0.5-2.0 mM) treatment of about 10-17%. This discrepancy in results obtained by the same method as the study and the same animal species used might be due to the difference in age and body weight of rabbits used. The previous study used young rabbits (BW only 1.0 – 1.5 kg) whereas the present study used mature rabbits (BW 1.5 – 2.5 kg, age 3-4 months). It was noticed that the control value of  $\text{Na}^+\text{-K}^+$  ATPase activity obtained in the present study was higher than that of Podprasart's study ( 8-10 vs 4-5  $\mu\text{mol Pi/mg}$  of tubule protein/hr). These values were similar to those of previous reports in both rabbits and rats (75, 174, 186), where the value of  $\text{Na}^+\text{-K}^+$  ATPase activity was also reported to be higher in adults than in young animals (174, 186). This might help to explain the discrepancy mentioned above. In addition, it is possible that young rabbits might be susceptible to toxic substances more than adults. However, the depression of  $J_{\text{PAH}}$  by steviol treatment at concentrations of 0.01 and 0.05 mM, as observed in the present study, showed no correlation with alteration in  $\text{Na}^+\text{-K}^+$  ATPase activity, because no change in the enzyme activity was observed, while  $J_{\text{PAH}}$  was inhibited. After removal of steviol from the bathing medium, a slight increase in  $J_{\text{PAH}}$  was detected, but the depression of  $J_{\text{PAH}}$  did not recover within the experimental period examined in this study. It is likely that steviol may pass the membrane and exert its effect within the proximal tubular cell, thus steviol may remain in the proximal tubule after the removal of stevioside from the media, leading to either a



permanent or prolonged depression of tubular function after steviol removal. The molecular structure of steviol is about 2.5 times smaller than stevioside, and is analogous to that of atractiligenin, the aglycone of atractyloside, which demonstrated an inhibition of oxidative phosphorylation and translocation of adenine nucleotides in mitochondria. Steviol is also more hydrophobic than stevioside, which makes it easily pass across the lipid membrane into the cell. Moreover, steviol was reported to inhibit glucose absorption in hamster intestine and also to decrease the intestinal mucosal ATP content (256), which was accompanied by a reduction in mitochondrial NADH cytochrom C reductase and cytochrome oxidase activities. The rabbit renal proximal tubule suspensions treated with 0.01 and 0.05 mM steviol *in vitro* in the present study did not exhibit a reduction in intracellular ATP content, in spite of a marked inhibition of  $J_{PAH}$ . A high concentration of steviol (2.0 mM) was found to inhibit NADH cytochrom C reductase and cytochrome oxidase activities in hamster jejunum (256), which would affect ATP production. The cell ATP content in rabbit renal proximal tubules was also markedly inhibited after 20 minutes of 2 mM steviol treatment in the present study (Figure 17). In contrast, cell AMP content was markedly high (Figure 19), while cell ADP and hypoxanthine, which is the main breakdown products of AMP, were not significantly changed from control values (Figures 18 and 20). These results are consistent with the lowered glucose production and inhibition of oxygen uptake in rat renal cortical tubules treated with 0.5 to 3.0 mM steviol (253). It was reported that steviol, like atractyligenin, induced a reduction in oxidative phosphorylation and prevented ADP/ATP translocation in rat liver mitochondria (254). This mechanism may explain the results observed in renal proximal tubules,

that the intracellular ATP content was reduced, leading to an accumulation of AMP in the cell. This is because, when ADP cannot enter the inner mitochondrial membrane, no ATP is produced from mitochondria, resulting in the dephosphorylation of ADP to AMP. Moreover, due to the lack of ATP, high concentrations of AMP will occur because the interconversion of ATP and AMP to ADP is eliminated (279). Therefore, if steviol inhibits ATP/ADP translocation, mitochondrial ATP production would also be inhibited. Normally, AMP acts as an indicator for the energy status of the cell. When ATP is used in energy-requiring processes, this causes the formation of ADP, leading to an increase in the concentration of AMP (279). Previous studies in ischemic kidney found a rapid reduction in cortical ATP content (283-285). Decreased ATP appeared, along with an accumulation of AMP (283-286). Moreover, it was reported that the AMP, which was markedly high in the tissues under hypoxic or ischemic conditions, was further hydrolyzed slowly to mainly hypoxanthine in the rabbit kidney (285, 286) and to a mixture of hypoxanthine and xanthine in the rat kidney (283, 284). Thus, there is a progressive degradation of adenine nucleotides in the cells during hypoxic conditions. No accumulation of ADP was detected in the renal cortex, probably as a result of continued activity of adenylate kinase (287). Most of the decrease in cell ATP content was initially accounted for by increased cell AMP content (288). The main breakdown product of AMP was hypoxanthine, which was found mostly in the extracellular medium (272). It might be due to the exit of hypoxanthine from the proximal tubular cells. In a study by Mandel et al. in 1990, neither the ADP nor the AMP contents in the rabbit proximal tubular cells seemed to change much under 4-minute anoxic conditions *in vitro*, but significant increases in

the extracellular AMP and hypoxanthine content occurred during the significant reduction of cell ATP content in this condition. It was also reported that the remaining cell ADP and AMP, as well as extracellular AMP contents, were readily used for resynthesis of ATP during reoxygenation of the proximal tubules *in vitro* (272), the cell ATP content was recovered, and the extracellular AMP content reduced to control levels, whereas extracellular hypoxanthine was still high in the proximal tubules under reoxygenation. The present study with 2 mM steviol treatment in proximal tubules suspensions showed an increase in cell AMP content, but no significant alteration of hypoxanthine content, either in the cell or in the extracellular medium, was observed. This might be explained by the shorter duration of observation and the slower rate of hydrolyzation of AMP to hypoxanthine in this study. However, the condition used in this study was oxygenation of the proximal tubule suspensions, the AMP and hypoxanthine content in the cells and extracellular medium were not high in the control group and stevioside and steviol at lower concentration treatment groups. This indicates that the proximal tubule suspensions used in the present study were not in a hypoxic condition. The high concentration of steviol (2 mM) might inhibit some processes to produce ATP, resulting in a lowered ATP content in the proximal cells, as mentioned above, and then causing an accumulation of AMP in the cells, as found in the present experiment. Evidence that steviol can enter the proximal tubule cells, as reported by Podprasart (261) from RP-HPLC analysis, supports this responsibility of steviol's action, but the pathway by which steviol passes across the cell membrane is not known. Moreover, a deterioration in renal function was observed in rats after intravenous administration

of steviol at doses of 1.0 and 3.0 mg/kg BW/hr (28). In addition, intragastric administration of steviol 5 g/kg BW in hamsters also resulted in an increase in BUN and creatinine concentrations after 36 hours of treatment. Histopathological investigation of hamster kidneys revealed a marked degeneration of proximal tubular cells (227). This nephrotoxicity observed after steviol treatment may be associated with the conversion of steviol to an active metabolite, oxosteviol, which is a major product of the oxidation of steviol by a microsomal enzyme (280). Oxosteviol was also reported to inhibit oxidative phosphorylation in rat renal tubules (253). This is in good agreement with the reduction of cell ATP content in tubules treated with 2 mM steviol, as observed in the present study. The decreased energy production in the cell is able to reduce the  $\text{Na}^+\text{-K}^+$  ATPase activity, and subsequently produces a reduction in the transepithelial transport of PAH across the renal proximal tubules. It is interesting that 2 mM steviol in the present study induced a reduction of cell ATP, but did not alter the  $\text{Na}^+\text{-K}^+$  ATPase activity of the proximal tubule cells (Figures 16 and 17). This is probably due to the fact that steviol does not directly inhibit the function of  $\text{Na}^+\text{-K}^+$  ATPase. During the time when cell ATP is reduced, the  $\text{Na}^+\text{-K}^+$  ATPase activity should also be reduced, but may not be permanently defected. Moreover, the procedure used for the  $\text{Na}^+\text{-K}^+$  ATPase activity determination may not be able to detect any change because many substrates used during assay procedures are given maximally, including ATP, so the activity of an enzyme would be at a maximum level if its function is still normal or there is no structural change of this enzyme. Nevertheless, the results from the present study showed a decrease in  $J_{\text{PAH}}$  with 0.01 and 0.05 mM steviol treatment, whereas the activity of  $\text{Na}^+\text{-K}^+$  ATPase and cell ATP

content were not significantly changed at the concentrations of steviol used. Therefore, the changes in the transepithelial transport of PAH observed in this study cannot be fully explained by the alterations of these two factors. These results raised the possibility that there have to be other mechanisms involving steviol action to result in reduced  $J_{\text{PAH}}$ . A further experiment was performed to investigate whether steviol acts on the PAH transporter to inhibit transport of PAH across the basolateral membrane. The type of inhibition was examined using a kinetic study of PAH uptake into the isolated renal proximal tubules of rabbits in both the absence and presence of steviol in the bathing medium. It has been known that the substance or inhibitor that acts on the binding site of an enzyme or on the transporter of the interested substrate would cause changes in the affinity of the transporter to the substrate (alter  $K_m$ ), whereas the maximum rate of transport ( $J_{\text{max}}$ ) does not change, this type of inhibition being called competitive inhibition. The values of  $K_m$  and  $J_{\text{max}}$  for peritubular PAH uptake in the present study (217  $\mu\text{M}$  and 6 nmol/min/mg protein) are consistent with those obtained from previous reports (54, 62, 274). The present study (Figure 26) showed that the presence of steviol in the bathing medium reduced the affinity ( $K_m$ ) of the transporter to PAH, but had no effect on the maximal transport rate ( $J_{\text{max}}$ ). Therefore, the inhibition of  $J_{\text{PAH}}$  by steviol was found to be competitive with PAH. The  $K_i$  value indicated the high specificity of steviol to the PAH transporter, as seen in Figure 26. The results from the present study are not capable of demonstrating whether steviol enters the proximal tubule cells via the PAH transporter or only interferes with the entry of PAH at the binding site. Based on the knowledge of substrate specificity to PAH binding site (35), steviol seems to have the appropriate

molecular structure for binding to the PAH transporter. The hydrophobic ring and one negative charge from the carboxylic group in its chemical structure might explain the higher specificity of steviol than stevioside. It needs to be pointed out that the  $K_i$  value of steviol for PAH transport was only 7.5  $\mu\text{M}$ , this value being near the concentration of steviol (10  $\mu\text{M}$ ) used in the perfusion studies that exhibited a half-inhibition of the transepithelial transport of PAH from the basolateral side to the proximal tubular lumen. These data further confirm that the transport of PAH across the basolateral membrane is the rate-limiting step for the transepithelial secretion of PAH. Therefore, inhibition of PAH entry across the basolateral membrane will depress the transepithelial transport of PAH. Although the exact mechanisms by which steviol reduced the  $J_{\text{PAH}}$  in the proximal tubules was not clear, it seems likely that steviol at low concentrations acted mainly on the basolateral PAH transporter to depress  $J_{\text{PAH}}$ . However, higher concentrations of steviol may involve reduction of the cell ATP content and  $\text{Na}^+\text{-K}^+$  ATPase activity that work in concert with the interference with the basal entry step of PAH, leading to the depression of  $J_{\text{PAH}}$ . It was not possible to examine the fourth possibility for steviol's effect on  $J_{\text{PAH}}$  proposed earlier, due to the fact that the mechanisms by which PAH exits the cell via the luminal member is not exactly known (126). This makes it difficult to find an approach to use in order to examine this possibility. However, this possibility cannot be excluded. In conclusion, the current study indicates that steviol has a harmful effect on renal proximal tubular secretory function. This effect was more prominent when steviol was presented on the basolateral side than on the luminal side.

The possible mechanisms by which stevioside and steviol reduced  $J_{PAH}$  were suggested and are summarized in Figure 27.



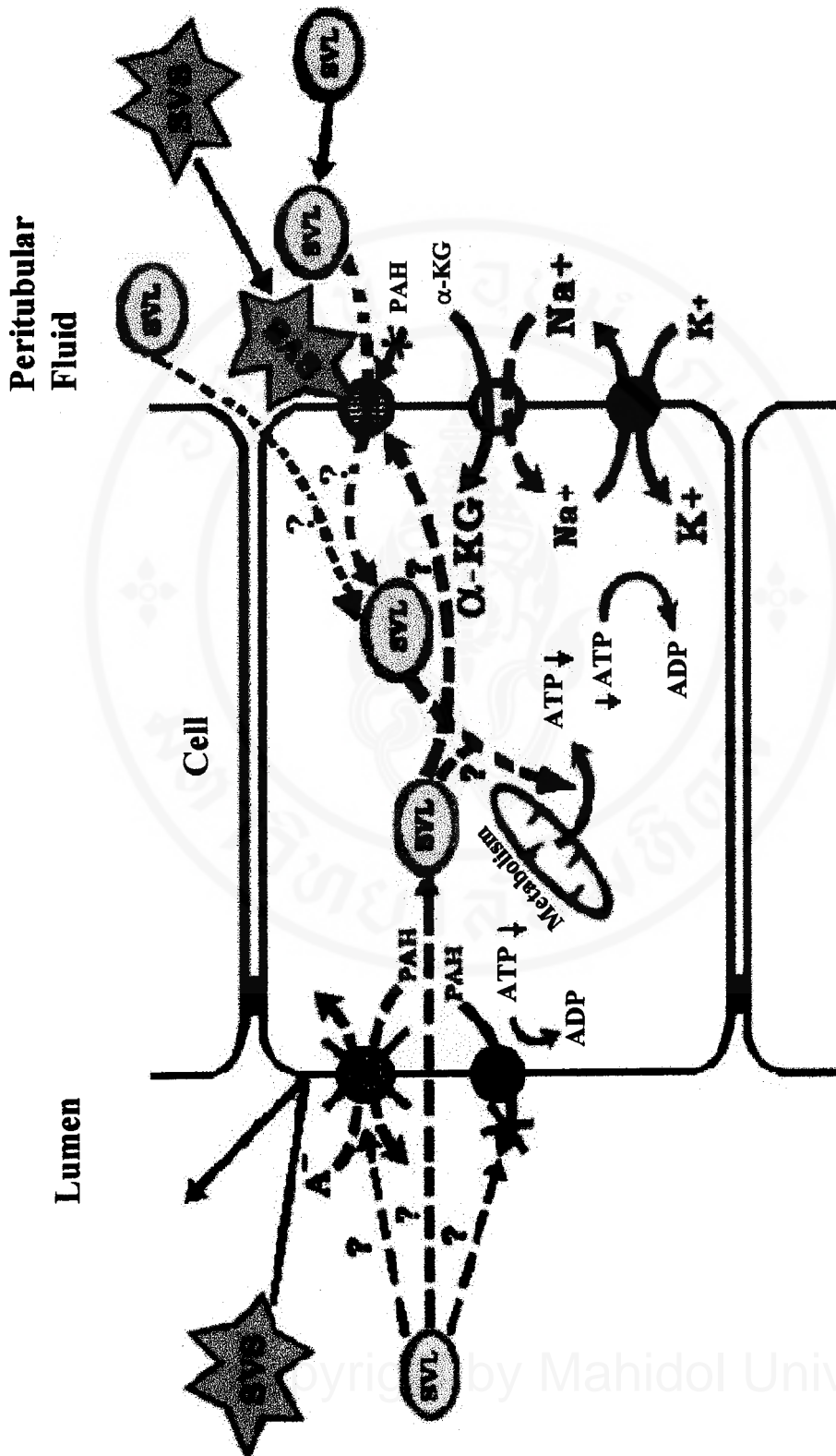


**Figure 27.** A schematic picture illustrating the possible mechanisms by which stevioside and steviol depress the transepithelial transport of p-aminohippurate (PAH) in rabbit renal proximal tubules.  
 SVS : stevioside; SVL : steviol; α-KG : alpha-ketoglutarate.

## CHAPTER VI

### CONCLUSION

The perfusion technique is an advantage in examining the direct effect of stevioside and steviol on renal proximal tubular function and in distinguishing between luminal and basolateral effects of stevioside and steviol. The results obtained from this study can be summarized as follows:

1. Addition of stevioside at a concentration of 0.45 mM to either the tubular lumen and the bathing medium or to both at the same time had no effect on the transepithelial transport of PAH. A higher concentration of stevioside (0.7 mM, maximum solubility in the buffer medium) inhibited PAH transport only when present in the bathing solution, but not in the perfusate.

2. Stevioside at a concentration of 0.7 mM depressed the transepithelial transport of PAH by interfering with the basolateral entry step, the rate-limiting step for transepithelial transport. It interacted with the basolateral PAH transporter as a competitive inhibitor. No alterations of Na<sup>+</sup>-K<sup>+</sup> ATPase activity or intracellular ATP content were observed in the proximal tubules treated with stevioside.

3. The lack of a stevioside effect on the transepithelial transport of PAH on the luminal side and its reversible inhibitory effect on the basolateral side indicate that stevioside does not permanently change PAH transport. Thus, it does not harm proximal tubular function.

4. Addition of steviol to the bathing medium significantly depressed the transepithelial transport of PAH in a dose-dependent manner which reached a maximum at a concentration of 0.05 mM.

5. Steviol at a low concentration (0.01 mM) inhibited the net transepithelial secretion of PAH when it was present on the basolateral side of the proximal tubule, but not in the tubular lumen. Steviol at a higher concentration (0.05 mM), when present in the tubular lumen, significantly inhibited the transepithelial PAH transport. This indicates that steviol produces a toxic effect on proximal tubular function.

6. No alterations in  $\text{Na}^+\text{-K}^+$  ATPase activity or intracellular ATP content were observed with steviol treatment at the doses of 0.01 and 0.05 mM that showed a depression of  $J_{\text{PAH}}$ . The action of steviol in reducing  $J_{\text{PAH}}$  seems to be its interference with the PAH transporter at the basolateral membrane.

7. A very high concentration of steviol (2 mM) has a more toxic effect on energy metabolism within the cell, therefore, it is probable that steviol enters the proximal tubular cells and induces a toxic effect on tubular function.

## REFERENCES

1. Bridel M, Lavieille R. The sweet principle of Kaa-he-e (*Stevia rebaudiana*). J Pharm Clin 1931; 14: 99-154.
2. Crammer B, Ikan R. Sweet glycosides from the stevia plant. Chem Brit 1986; 22: 915-7.
3. Fujita H, Edahiro T. Safety and utilization of stevia sweetener. The Food Industry 1979; 22: 1-8.
4. Kinghorn AD, Soejarto DD. Stevioside. In: Alternative sweeteners Vol 2. Edited by O'Brien NL, Gelardi RC. New York, Dekker, 1991: 122-144.
5. Planas GM, Kuc J. Contraceptive properties of *Stevia rebaudiana*. Science 1968; 162: 1007.
6. Boeckh EMA, Humboldt G. Efeitos cardiocirculatorios do extrato aquoso total em individuos normais e do esteviosideo em ratos. Cienc Cult 1981; 32: 208-10.
7. Melis MS, Sainati AR. Participation of prostaglandins in the effect of stevioside on renal function and arterial pressure in rats. Braz J Med Biol Res 1991; 24: 1269-76.
8. Melis MS, Sainati AR. Effect of calcium and verapamil on renal function of rats during treatment of stevioside. J Ethnopharmacol 1991; 33: 257-62.
9. Melis MS. Influence of calcium on the blood pressure and renal effects of stevioside. Braz J Med Biol Res 1992; 25: 943-9.

10. Melis MS. Stevioside effect on renal function of normal and hypertensive rats. *J Ethnopharmacol* 1992; 36: 213-7.
11. Chan P, Xu DY, Liu JC, Chen YJ, Tomlinson B, Huang WP, Cheng JT. The effect of stevioside on blood pressure and plasma catecholamines in spontaneously hypertensive rats. *Life Sci* 1998; 63: 1697-84.
12. Curi R, Alvarez M, Bazotte RB, Botion LM, Godoy JL, Bracht A. Effect of *Stevia rebaudiana* on glucose tolerance in normal adult man. *Braz J Med Biol Res* 1986; 19: 771-4.
13. Toskulkao C, Sutheerawattananon M. Effects of stevioside, a natural sweetener, on intestinal glucose absorption in hamsters. *Nutr Res* 1994; 14: 1711-20.
14. Toskulkao C, Sutheerawattananon M, Wanichanon C, Saitongdee P, Suttajit M. Effects of stevioside and steviol on intestinal glucose absorption in hamster. *J Nutr Sci Vitaminol* 1995; 41: 105-13.
15. Ishii EL, Schwab AJ, Bracht A. Inhibition of monosaccharide transport in the intact rat liver by stevioside. *Biochem Pharmacol* 1987; 36: 1417-33.
16. Suanarunsawat T, Chaiyabutr N. The effect of stevioside on glucose metabolism in rat. *Can J Physiol Pharmacol* 1997; 75: 976-82.
17. Melis MS. Renal excretion of stevioside in rats. *J Nat Prod* 1992; 55: 688-90.
18. Melis MS. Chronic administration of aqueous extract of *Stevia rebaudiana* in rats- Renal effects. *J Ethnopharmacol* 1995; 47: 129-34.
19. Melis MS. A crude extract of *Stevia rebaudiana* increased the renal plasma flow of normal and hypertensive rats. *Braz J Med Biol Res* 1996; 29: 669-75.

20. Thongouppakarn P. Effect of stevioside on renal functions in rat [M.S. Thesis in Physiology]. Bangkok: Faculty of Graduate Studies, Mahidol University; 1994.
21. Limpanichakul Y. Effect of stevioside on Na<sup>+</sup>-K<sup>+</sup> ATPase in renal proximal tubules of rabbit [M.S. Thesis in Physiology]. Bangkok: Faculty of Graduate Studies, Mahidol University; 1995.
22. Toskulkao C, Deechakawan W, Leardkamolkarn V, Glinsukon T, Buddhasukh D. The low calorie natural sweetener stevioside: Nephrotoxicity and its relationship to urinary enzyme excretion in the rat. *Phytother Res* 1994; 8: 281-6.
23. Toskulkao C, Deechakawan W, Temcharoen P, Buddhasukh D, Glinsukon T. Nephrotoxic effects of stevioside and steviol in rat renal cortical slices. *J Clin Biochem Nutr* 1994; 16: 123-31.
24. Panichkul T, Glinsukon T, Buddhasukh D, Cheuychit P, Pimolsri U. The plasma levels of urea nitrogen, creatinine and uric acid and urine volume in rats and hamsters treated with stevioside. *Thai J Toxicol* 1988; 4: 47-52.
25. Wingard RE. Jr, Brown JP, Enderlin FE, Dale JA, Hale RL, Seitz CT. Intestinal degradation and absorption of the glycosidic sweeteners stevioside and rebaudioside A. *Experientia* 1980; 36: 519-20.
26. Hutapae AM, Toskulakao C, Buddhasukh D, Wilairat P, Glinsukon T. Digestion of stevioside, a natural sweetener by various digestive enzymes. *J Clin Biochem Nutr* 1997; 23: 177-86.

27. Cardoso VN, Barbosa MF, Muramoto E, Mesquita CH, Almeida MA. Pharmacokinetic studies of  $^{131}\text{I}$ -stevioside and its metabolites. *Nucl Med Biol* 1996; 23: 97-100.
28. Melis MS. Effects of steviol on renal function and mean arterial pressure in rats. *Phytomedicine* 1996/97; 3: 349-52.
29. Pritchard JB, Miller DS. Mechanisms mediating renal secretion of organic anions and cations. *Physiol Rev* 1993; 73: 765-96.
30. Lohr JW, Willsky GR and Acara MA. Renal drug metabolism. *Pharmacol Rev* 1998; 50: 107-41.
31. Rozman KK, Klaasen CD. Absorption, distribution and excretion of toxicants. In: Klaasen CD, editor. *Casarett and Doull's Toxicology*. New York: McGraw-Hill, 1996: 91-112.
32. Vander AJ, Sherman JG, Luciano DS. *The Mechanisms of body function*. New York: McGraw-Hill, 1995.
33. Pritchard JB, Miller DS. Renal secretion of organic anions and cations. *Kidney Int* 1996; 49: 1649-54.
34. Miller DS, Pritchard JB. Dual pathways for organic anion secretion in renal proximal tubule. *J Exp Zool* 1997; 279: 462-70.
35. Ullrich KJ. Renal transporters for organic anions and organic cations. Structural requirements for substrates. *J Membrane Biol* 1997; 158: 95-107.
36. Sekine T, Watanabe N, Hosoyamada M, Kanai Y, Endou H. Expression cloning and characterization of a novel multispecific organic anion transporter. *J Biol Chem* 1997; 272: 18526-9.

37. Sweet DH, Wolff NA, Pritchard JB. Expression cloning and characterization of ROAT1. The basolateral organic anion transporter in rat kidney. *J Biol Chem* 1997; 272: 30088-95.
38. Markovich D, Bissig M, Sorribas V, Hagenbuch B, Meier PJ, Murer H. Expression of rat renal sulfate transport systems in *Xenopus leavis* oocytes. *J Biol Chem* 1994; 269: 3022-6.
39. Ullrich KJ, Rumrich G. Luminal transport step of para-aminohippurate (PAH): transport from PAH-loaded proximal tubular cells into the tubular lumen of the rat kidney *in vivo*. *Pflügers Arch* 1997; 433: 735-43.
40. Pajor AM. Sequence and functional characterization of a renal sodium/dicarboxylate cotransporter. *J Biol Chem* 1995; 270: 5779-85.
41. Sekine T, Cha SH, Hosoyamada M, Kanai Y, Watanabe N, Furuta Y, Fukuda K, Igarashi T, Endou H. Cloning, functional characterization and localization of a rat renal Na<sup>+</sup>-dicarboxylate transporter. *Am J Physiol* 1998; 275: F298-305.
42. Masuda S, Saito H, Nonoguchi H, Tomita K, Inui K. mRNA distribution and membrane localization of the OAT-K1 organic anion transporter in rat renal tubules. *FEBS Letters* 1997; 407: 127-31.
43. Shaub TP, Kartenbeck J, König J, Vogel O, Witzgall R, Kriz W, Keppler D. Expression of the conjugate export pump encoded by the *mrp2* gene in the apical membrane of kidney proximal tubule. *J Am Soc Nephrol* 1997; 8: 1213-21.

44. Shaub TP, Kartenbeck J, Konig J, Spring H, Dorsam J, Staehler G, Storkel S, Thon WF, Keppler D. Expression of the MRP2 gene-encoded conjugate export pump in human kidney proximal tubules and in renal cell carcinoma. *J Am Soc Nephrol* 1999; 10: 1159-69.
45. Grundemann D, Gorboulev V, Gambaryan S, Veyhl M, Koepsell H. Drug excretion by a new prototype of polyspecific transporter. *Nature* 1994; 372: 549-52.
46. Okuda M, Saito H, Urakami Y, Takano M, Inui KI. CDNA cloning and functional expression of a novel rat kidney organic cation transporter, OCT2. *Biochem Biophys Res Comm* 1996; 224: 500-7.
47. Gottesman MM, Pastan I. Biochemistry of multidrug resistance mediated by the multidrug transporter. *Annu Rev Biochem* 1993; 62: 385-427.
48. Horio M, Pastan I, Gottesman MM, Handler JS. Transepithelial transport of vinblastine by kidney derived cell lines. Application of a new kinetic model to estimate *in situ*  $K_m$  of the pump. *Biochim Biophys Acta* 1990; 1027: 116-22.
49. Cross RJ, Taggart JV. Renal tubular transport: accumulation of p-aminohippurate by rabbit kidney slices. *Am J Physiol* 1950; 161: 181-90.
50. Tune BM, Burg MB, Patlak CS. Characteristics of p-aminohippurate transport in proximal renal tubules. *Am J Physiol* 1969; 217: 1057-63.
51. Maunsbach AB. Observations on the segmentation of the proximal tubule in the rat kidney. Comparison of results from phase contrast, fluorescence and electron microscopy. *J Ultrastruct Res* 1966; 16: 239-58.

52. Tisher CC, Rosen S, Osborne GB. Ultrastructure of the proximal tubule of the rhesus monkey kidney. *Am J Pathol* 1969; 56: 469-517.
53. Woodhall PB, Tisher CC, Simonton CA, Robinson RR. Relationship between para-aminohippurate secretion and cellular morphology in rabbit proximal tubules. *J Clin Invest* 1978; 61: 1320-9.
54. Shimomura A, Chonko AM, Grantham JJ. Basis for heterogeneity of para-aminohippurate secretion in rabbit proximal tubules. *Am J Physiol* 1981; 240: F430-6.
55. Grantham JJ. Studies of organic anion and cation transport in isolated segments of proximal tubules. *Kidney Int* 1982; 22: 519-25.
56. Roch-Ramel F, White F, Vowles L, Simmonds HA, Cameron JS. Micropuncture study of tubular transport of urate and PAH in the pig kidney. *Am J Physiol* 1980; 239: F107-12.
57. Tanner GA, Isenberg MT. Secretion of p-aminohippurate by rat kidney proximal tubule. *Am J Physiol* 1970; 219: 889-92.
58. Brokl OH, Braun EJ, Dantzler WH. Transport of PAH, urate, TEA and fluid by isolated perfused and nonperfused avian renal proximal tubules. *Am J Physiol* 1994; 266: R1085-94.
59. Dantzler WH. PAH transport by snake proximal renal tubules: difference from urate transport. *Am J Physiol* 1974; 226: 634-41.
60. Irish JM, Dantzler WH. PAH transport and fluid absorption by isolated perfused frog proximal renal tubules. *Am J Physiol* 1976; 230: 1509-16.

61. Dantzler WH, Wright SH. Renal tubular secretion of organic anions. *Adv Drug Del Rev* 1997; 25: 217-30.
62. Dantzler WH and Evans KK, Wright SH. Kinetics of interactions of para-aminohippurate, probenecid, cysteine conjugates and N-acetyl cysteine conjugates with basolateral organic anion transporter in isolated rabbit proximal renal tubules. *J Pharmacol Exp Ther* 1995; 272: 663-72.
63. Shpun S, Evans KK, Dantzler WH. Interaction of  $\alpha$ -KG with basolateral organic anion transporter in isolated rabbit renal S<sub>3</sub> proximal tubules. *Am J Physiol* 1995; 268: F1109-16.
64. Dantzler WH. K<sup>+</sup> effect on PAH transport and membrane permeabilities in isolated snake renal tubules. *Am J Physiol* 1974; 227: 1361-70.
65. Dantzler WH, Bentley SK. Bath and lumen effects of SITS on PAH transport by isolated perfused renal tubules. *Am J Physiol* 1980; 238: F16-25.
66. Shimada H, Moewes B, Burckhardt G. Indirect coupling to Na<sup>+</sup> of p-aminohippuric acid uptake into rat renal basolateral membrane vesicles. *Am J Physiol* 1987; 253: F795-801.
67. Pritchard JB. Rat renal cortical slices demonstrate p-aminohippurate/glutarate exchange and sodium/glutarate coupled p-aminohippurate transport. *J Pharmacol Exp Ther* 1990; 255: 969-75.
68. Maxild J. Effect of externally added ATP and related compounds on active transport of p-aminohippurate and metabolism in cortical slices of the rabbit kidney. *Arch Int Physiol Biochem* 1978; 86: 509-30.

69. Podevin RA, Boumendil-Podevin EF. Inhibition by cyclic AMP and dibutyryl cyclic AMP of transport of organic acids in kidney cortex. *Biochim Biophys Acta* 1975; 375: 106-14.
70. Ross CR, Weiner IM. Adenine nucleotides and PAH transport in slices of renal cortex: effects of DNA and CN. *Am J Physiol* 1972; 222: 356-9.
71. Sheikh MI, Maxild J, Moller JV. Effect of vanadate on the renal accumulation of p-aminohippurate in the rabbit kidney tubules *in vitro*. *Biochem Pharmacol* 1981; 30: 2141-6.
72. Kikuta Y, Hoshi T. Role of sodium ions in p-aminohippurate transport by newt kidney. *Biochim. Biophys Acta* 1979; 553: 404-16.
73. Dantzler WH. Effects of  $K^+$ ,  $Na^+$ , and ouabain on urate and PAH uptake by snake and chicken kidney slices. *Am J Physiol* 1969; 217: 1510-9.
74. Burg MB, Orloff J. Effect of strophanthidin on electrolyte content and PAH accumulation of rabbit kidney slices. *Am J Physiol* 1962; 202: 565-71.
75. Spencer AM, Sack J, Hong SK. Relationship between PAH transport and Na-K-ATPase activity in the rabbit kidney. *Am J Physiol* 1979; 236: F126-30.
76. Podevin RA, Boumendil-Podevin EF, Priol C. Concentrative PAH transport by rabbit kidney slices in the absence of metabolic energy. *Am J Physiol* 1978; 235: F278-85.
77. Sheikh MI, Moller JV.  $Na^+$ -gradient dependent stimulation of renal transport of p-aminohippurate. *Biochem J.* 1982; 208: 243-6.
78. Berner W, Kinne R. Transport of p-aminohippuric acid by plasma membrane vesicles isolated from rat kidney cortex. *Pflügers Arch* 1976; 361: 269-77.

79. Eveloff J, Kinne R, Kinter WB. p-Aminohippuric acid transport into brush border vesicles isolated from flounder kidney. *Am J Physiol* 1979; 237: F291-8.
80. Kasher JS, Holohan PD, Ross CR. Na<sup>+</sup> gradient-dependent p-aminohippurate (PAH) transport in rat basolateral membrane vesicles. *J Pharmacol Exp Ther* 1983; 227: 122-9.
81. Ullrich KJ, Rumrich G, Fritzsich G, Kloss S. Contraluminal para-aminohippurate (PAH) transport in the proximal tubules of the rat kidney. I. Kinetics, influence of cations, anions, and capillary preperfusion. *Pflügers Arch* 1987; 409: 229-35.
82. Kikuta Y, Hayashi H, Saito Y. Effects of changes in sodium electrochemical potential gradient on p-aminohippurate transport in newt kidney. *Biochim Biophys Acta* 1979; 556: 354-65.
83. Eveloff J. p-Aminohippurate transport in basal-lateral membrane vesicles from rabbit renal cortex: stimulation by pH and sodium gradients. *Biochim Biophys Acta* 1987; 474-80.
84. Ullrich KJ, Rumrich G, Fritzsich G, Kloss S. Contraluminal para-aminohippurate (PAH) transport in the proximal tubule of the rat kidney. II. Specificity: aliphatic dicarboxylic acid. *Pflügers Arch* 1987; 408: 38-45.
85. Ullrich KJ, Rumrich G, Kloss S. Contraluminal para-aminohippurate transport in the proximal tubule of the rat. III. Specificity: monocarboxylic acids. *Pflügers Arch* 1987; 409: 547-54.

86. Sheikh MI, Moller JV. Nature of Na<sup>+</sup>-independent stimulation of renal transport of p-aminohippurate by exogenous metabolites. *Biochem Pharmacol* 1983; 32: 2745-9.
87. Moller JV, Sheikh MI. Renal organic anion transport system: pharmacological, physiological, and biochemical aspects. *Pharmacol Rev* 1983; 34: 315-58.
88. Pritchard JB. Luminal and peritubular steps in renal transport of p-aminohippurate. *Biochim Biophys Acta* 1987; 906: 295-308.
89. Pritchard JB. Coupled transport of p-aminohippurate by rat basolateral membrane vesicles. *Am J Physiol* 1988; 255: F597-604.
90. Chatsudthipong V, Dantzler WH. PAH/ $\alpha$ -KG countertransport stimulates PAH uptake and net secretion in isolated rabbit renal tubules. *Am J Physiol* 1992; 263: F384-91.
91. Burckhardt G, Ullrich KJ. Organic anion transport across the contraluminal membrane-dependence on sodium. *Kidney Int* 1989; 36: 370-7.
92. Pritchard JB, Miller DS. Comparative insights into the mechanisms of renal organic anion and cation secretion. *Am J Physiol* 1991; 261: R1329-40.
93. Schmitt C, Burckhardt G. p-Aminohippurate/2-oxoglutarate exchange in bovine renal brush-border and basolateral membrane vesicles. *Pflügers Arch* 1993; 423: 280-90.
94. Chatsudthipong V, Dantzler WH. PAH- $\alpha$ -KG countertransport stimulates PAH uptake and net secretion in isolated snake renal tubules. *Am J Physiol* 1991; 261: F858-67.

95. Shuprisha A, Lynch RM, Wright SH, Dantzler WH. Real-time assessment of  $\alpha$ -ketoglutarate effect on organic anion secretion in perfused rabbit proximal tubules. *Am J Physiol* 1999; 277: F513-23.
96. Welborn JR, Shpun S, Dantzler WH. Effect of  $\alpha$ -ketoglutarate on organic anion transport in single rabbit renal proximal tubules. *Am J Physiol* 1998; 274: F165-74.
97. Pritchard JB. Intracellular  $\alpha$ -ketoglutarate controls the efficacy of renal organic anion transport. *J Pharmacol Exp Ther* 1995; 274: 1278-84.
98. Nagai J, Yano I, Hashimoto Y, Takano M, Inui K. Efflux of intracellular alpha-ketoglutarate via p-aminohippurate/dicarboxylate exchange in OK kidney epithelial cells. *J Pharmacol Exp Ther* 1998; 285: 422-7.
99. Dantzler WH and Evans KK. Effect of  $\alpha$ -KG in lumen on PAH transport by isolated perfused rabbit renal proximal tubules. *Am J Physiol* 1996; 271: F521-6.
100. Dickman KG, Mandel LJ. Relationship between  $\text{HCO}_3^-$  transport and oxidative metabolism in rabbit proximal tubule. *Am J Physiol* 1992; 263: F342-51.
101. Reyes JL, Melendez E, Alegria A, Jaramillo-Juarez F. Influence of sex differences on renal secretion of organic anions. *Endocrinology* 1998; 139: 1581-7.
102. Stark U, Vanden Bergh H, Rover N, Greven J. Effect of activation of protein kinase A and of protein kinase C on the kinetics of the renal basolateral PAH transporter. *Fundam Clin Pharmacol* 1998; 12: 44-9.

103. Hohage H, Lohr M, Querl U, Greven J. The renal basolateral transport system for organic anions: properties of the regulation mechanism. *J Pharmacol Exp Ther* 1994; 269: 659-64.
104. Rover N, Kramer C, Stark U, Gabriels G, Graven J. Basolateral transport of glutarate in proximal S<sub>2</sub> segments of rabbit kidney: kinetics of the uptake process and effect of activators of protein kinase A and C. *Pflügers Arch* 1998; 436: 423-8.
105. Kutzer M, Meer S, Haller S, Greven J. Basolateral glutarate transport by isolated S<sub>2</sub> segments of rabbit kidney proximal tubules. *J Pharmacol Exp Ther* 1996; 277: 316-20.
106. Takano M, Nagai J, Yasuhara M, Inui K-I. Regulation of p-aminohippurate transport by protein kinase C in OK kidney epithelial cells. *Am J Physiol* 1996; 271: F469-75.
107. Nagai J, Yano I, Hashimoto Y, Takano M, Inui K-I. Inhibition of PAH transport by parathyroid hormone in OK cells: involvement of protein kinase C pathway. *Am J Physiol* 1997; 273: F674-9.
108. Masereeuw R, Russel FGM, Miller DS. Multiple pathways of organic anion secretion in renal proximal tubule reveal by confocal microscopy. *Am J Physiol* 1996; 271: F1173-82.
109. Ullrich KJ, Rumrich G. Contraluminal transport systems in the proximal renal tubule involved in secretion of organic anions. *Am J Physiol* 1988; 254: F453-62.

110. Ullrich KJ, Rumrich G, Gloss S. Contraluminal para-aminohippurate (PAH) transport in the proximal tubule of the rat kidney. IV. Specificity: mono- and polysubstituted benzene analogs. *Pflügers Arch* 1988; 413: 134-46.
111. Ullrich KJ, Rumrich G, Wieland TH, Dekant W. Contraluminal para-aminohippurate (PAH) transport in the proximal tubule of the rat kidney. VI. Specificity: amino acids, their N-methyl-, N-acetyl- and N-benzoyl derivatives; glutathione and cysteine conjugates, di- and oligopeptides. *Pflügers Arch* 1989; 415: 342-50.
112. Ullrich KJ. Specificity of transporters for organic anions and organic cations in the kidney. *Biochim Biophys Acta* 1994; 1197: 45-62.
113. Fritsch G, Rumrich G, Ullrich KJ. Anion transport through the contraluminal cell membrane of renal proximal tubule. The influence of hydrophobicity and molecular charge distribution on the inhibitory activity of organic anions. *Biochim Biophys Acta* 1989; 978: 249-56.
114. Eveloff J, Morishige WK, Hong SK. The binding of phenol red to rabbit renal cortex. *Biochim Biophys Acta* 1976; 448: 167-80.
115. Holohan PD, Pessah NI, Ross CR. Binding of N-methylnicotinamide and p-aminohippuric acid to a particulate fraction from dog kidney. *J Pharmacol Exp Ther* 1975; 195: 22-33.
116. Sheikh MI. Renal handling of phenol red. I. A comparative study on the accumulation of phenol red and p-aminohippurate in rabbit kidney tubule *in vitro*. *J Physiol* 1972; 277: 565-90.

117. Berndt WO. Probenecid binding by renal cortical slices and homogenates. *Proc Soc Exp Biol Med* 1967; 126: 123-6.
118. Miller DS, Stewart DE, Pritchard JB. Intracellular compartmentation of organic anions within renal cells. *Am J Physiol* 1993; 264: R882-90.
119. Miller DS, Barners DM, Pritchard JB. Confocal microscopic analysis of fluorescein compartment within crab urinary bladder cells. *Am J Physiol* 1994; 267: R16-25.
120. Miller DS, Pritchard JB. Nocodazole inhibition of organic anion secretion in teleost proximal tubules. *Am J Physiol* 1994; 267: R695-704.
121. Dantzler WH, Bentley SK. Effects of inhibitors in lumen on PAH and urate transport by isolated renal tubules. *Am J Physiol* 1979; 236: F379-86.
122. Dantzler WH, Bentley SK. Effects of chloride substitutes on PAH transport by isolated perfused renal tubules. *Am J Physiol* 1981; 241: F632-44.
123. Benyajati S, Dantzler WH. Enzymatic and transport characteristics of isolated snake renal brush border membranes. *Am J Physiol* 1988; 255: R52-60.
124. Dantzler WH, Bentley SK. Low Na<sup>+</sup> effects on PAH transport and permeabilities in isolated snake renal tubules. *Am J Physiol* 1976; 230: 256-62.
125. Dantzler WH. Organic acid (or anion) and organic base (or cation) transport by renal tubules of nonmammalian vertebrates. *J Exp Zool* 1989; 249: 247-57.
126. Chatsudthipong V, Jutabha P, Evans KK, Dantzler WH. Effects of inhibitors and substitutes for chloride in lumen on p-aminohippurate transport by isolated perfused rabbit renal proximal tubules. *J Pharmacol Exp Ther* 1999; 288: 993-1001.

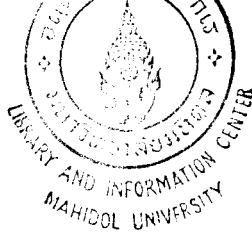
127. Dantzler WH, Brokl OH. Effects of low  $[Ca^{2+}]$  and  $La^{3+}$  on PAH transport by isolated perfused renal tubules. *Am J Physiol* 1984; 246: F175-87.
128. Dantzler WH, Brokl OH. Verapamil and quinidine effects on PAH transport by isolated perfused renal tubules. *Am J Physiol* 1984; 246: F188-200.
129. Blomstedt JW, Aronson PS. pH-Gradient-stimulated transport of urate and p-aminohippurate in dog renal microvilles membrane vesicles. *J Clin Invest* 1980; 65: 931-4.
130. Guggino SE, Martin GJ, Aronson PS. Specificity and modes of the anion exchanger in dog microvillus membranes. *Am J Physiol* 1983; 244: F612-21.
131. Kahn AM, Aronson PS. Urate transport via anion exchange in dog renal microvillus membrane vesicles. *Am J Physiol* 1983; 244: F56-63.
132. Kahn AM, Branham S, Weinman EJ. Mechanism of urate and p-aminohippurate transport in rat microvillus membrane vesicles. *Am J Physiol* 1983; 245: F151-8.
133. Karniski LP, Aronson PS. Anion exchange pathways for  $Cl^-$  transport in rabbit microvillus membranes. *Am J Physiol* 1987; 253: F513-21.
134. Martinez F, Manganel M, Montrose-Fafizadeh C, Werner D, Roch-Ramel F. Transport of urate and p-aminohippurate in rabbit renal brush-border membrane. *Am J Physiol* 1990; 258: F1145-53.
135. Steffens TG, Holohan PD, Ross CR. Operational modes of the organic anion exchanger in canine renal brush-border membrane vesicles. *Am J Physiol* 1989; 256: F596-609.

136. Werner D, Martinez F, Roch-Ramel F. Urate and p-aminohippurate transport in the brush-border membrane of pig kidney. *J Pharmacol Exp Ther* 1990; 252: 792-9.
137. Miller DS, Letcher S, Barnes DM. Fluorescence imaging study of organic anion transport from renal proximal tubule cell to lumen. *Am J Physiol* 1996; 271: F508-20.
138. Masereeuw R, Moons MM, Toomey BH, Russel FGM, Miller DS. Active lucifer yellow secretion in renal proximal tubule: evidence for organic anion transport system crossover. *J Pharmacol Exp Ther* 1999; 289: 1104-11.
139. Leier I, Hummel-Eisenbeiss J, Cui Y, Keppler D. ATP-dependent para-aminohippurate transport by apical multidrug resistance protein MRP2. *Kidney Int* 2000; 57: 1636-42.
140. Uchino H, Tamai I, Yamashita K, Minemoto Y, Sai Y, Yabuuchi H, Miyamoto K, Takeda E, Tsuji A. *Biochem Biophys Res Commun* 2000; 270: 254-9.
141. Bakos E, Evers R, Sinko E, Varadi A, Borst P, Sarkadi B. Interactions of the human multidrug resistance proteins MRP1 and MRP2 with organic anions. *Mol Pharmacol* 2000; 57: 760-8.
142. Balshaw DM, Millette LA, Wallick ET. The Sodium Pump. In: Sperelakis N, editor. *Cell physiology*. 2<sup>nd</sup> ed. San Diego: Academic Press; 1998. p.216-24.
143. Lane LK, Copenhaver GH, Lindenmayer GE, Schwartz A. Purification and characterization of an [<sup>3</sup>H] ouabain binding to the transport adenosine triphosphatase from outer medulla of canine kidney. *J Biol Chem* 1973; 248: 7197-200.

144. Kyte J. Properties of the two polypeptides of Na, K-ATPase. *J Biol Chem* 1972; 247: 7642-9.
145. Esmann M, Skou JC, Christiansen C. Solubilization and molecular weight determinations of the Na, K-ATPase from rectal glands of *Squalus acanthias*. *Biochim Biophys Acta* 1979; 567: 410-20.
146. Perrone JR, Hackney JF, Dixon JF, Hokin LE. Molecular properties of purified Na, K-ATPase and their subunits from the rectal gland of *Squalus acanthias* and the electric organ of *Electrophorus electricus*. *J Biol Chem* 1975; 250: 4178-84.
147. Hastings DF, Reynolds IA. Molecular weight of Na, K-ATPase from shark rectal gland. *Biochemistry* 1979; 18: 817-21.
148. Shull GE, Greeb J, Lingrel JB. Molecular cloning of three distinct forms of the Na, K-ATPase alpha subunit from rat brain. *Biochemistry* 1986; 25: 8129-32.
149. Sweadner KJ, Goldin SM. Active transport of sodium and potassium ions: Mechanism, Function and Regulation. *N Eng J Med* 1980; 302: 777-83.
150. Shull GE, Lane LK, Lingrel JB. Amino acid sequence of the  $\beta$ -subunit of the (Na<sup>+</sup>, K<sup>+</sup>)-ATPase deduced from a cDNA. *Nature* 1986; 321: 429-31.
151. Blanco G, Mercer RW. Isozymes of the Na-K-ATPase: heterogeneity in structure, diversity in function. *Am J Physiol* 1998; 275: F633-50.
152. Munzer JS, Daly SE, Jewell-Motz EA, Lingrel JB, Blostein R. Tissue- and isoform-specific kinetic behavior of the Na, K-ATPase. *J Biol Chem* 1994; 269: 16668-76.

153. Shamraj OI, Lingrel JB. A putative fourth Na<sup>+</sup>,K<sup>+</sup>-ATPase alpha-subunit gene is expressed in testis. *Proc Natl Acad Sci USA* 1994; 91: 12952-6.
154. Palasis M, Kuntzweiler TA, Arguello JM, Lingrel JB. Ouabain interactions with the H5-H6 hair pin of the Na, K-ATPase reveal a possible inhibition mechanism via the cation binding domain. *J Biol Chem* 1996; 271: 14176-82.
155. Horowitz B, Eakle KA, Scheiner-Bobis G, Randolph GR, Chen CY, Hitzeman RA, Farley RA. Synthesis and assembly of functional mammalian Na, K-ATPase in yeast. *J Biol chem.* 1990; 265: 4189-92.
156. Sweadner KJ. Isozymes of the Na<sup>+</sup>, K<sup>+</sup>-ATPase. *Biochim Biophys Acta* 1989; 988: 185-220.
157. McDonough AA, Geering K, Farley RA. The sodium pump needs its  $\beta$  subunit. *FASEB J* 1990; 4: 1598-605.
158. Lutsenko S, Kaplan JH. An essential role for the extracellular domain of the Na, K-ATPase  $\beta$ -subunit in cation occlusion. *Biochemistry* 1993; 32: 6737-43.
159. Chow DC, Forte JG. Functional significance of the beta-subunit for heterodimeric P-type ATPase. *J Exp Biol* 1995; 198: 1-17.
160. Glynn IM, Karlisch SJD. The sodium pump. *Annu Rev Physiol* 1975; 37: 13-55.
161. Post RL, Jolly PC. The linkage of sodium, potassium, and ammonium active transport across the human erythrocyte membrane. *Biochim Biophys Acta* 1957; 25: 118-28.

162. Thomas RC. Membrane current and intracellular sodium changes in a snail neurone during extrusion of injected sodium. *J Physiol* 1969; 201: 495-514.
163. Tepperman K, Millette LA, Johnson CL, Jewell-Motz EA, Lingrel JB, Wallick ET. Mutational analysis of Glu-327 of Na<sup>+</sup>, K<sup>+</sup>-ATPase reveals stimulation of <sup>86</sup>Rb<sup>+</sup> uptake by external K<sup>+</sup>. *Am J Physiol* 1997; 273: C2065-79.
164. Glynn IM. Annual review prize lecture. All Hands to the sodium pump? *J Physiol (Lond)* 1993; 462: 1-30.
165. Jørgensen PL. Purification and characterization of (Na<sup>+</sup>-K<sup>+</sup>)-ATPase. V. conformational changes in the enzyme: transitions between the Na- form and the K-form studied with tryptic digestion as a tool. *Biochim Biophys Acta* 1975; 401: 399-415.
166. Jørgensen PL. Mechanism of the Na<sup>+</sup>, K<sup>+</sup> pump: protein structure and conformations of the pure (Na<sup>+</sup>-K<sup>+</sup>)-ATPase. *Biochim Biophys Acta* 1982; 694: 27-68.
167. Ewart HS, Klip A. Hormonal regulation of the Na<sup>+</sup>-K<sup>+</sup> ATPase: mechanisms underlying rapid and sustained change in pump activity. *Am J Physiol* 1995; 269: C295-311.
168. Schwartz A, Lindenmayer GE, Allen JC. The sodium-potassium adenosine triphosphatase: Pharmacological, physiological and biochemical aspects. *Pharmacol Rev* 1975; 27: 3-134.
169. Jørgensen PL. Sodium and potassium ion pump in kidney tubules. *Physiol Rev* 1980; 60: 864-917.



170. Torreti J, Hendler E, Weinstein E, Longnecker RE, Epstein FH. Functional significance of Na-K-ATPase in the kidney: effects of ouabain inhibition. *Am J Physiol* 1972; 222: 1398-405.
171. Charney AN, Silva P, Epstein FH. An *in vitro* inhibitor of Na, K-ATPase present in an ATP preparation. *J Appl Physiol* 1975; 39: 156-8.
172. Cantley LC, Cantley LG, Josephson L. A characterization of vanadate interaction with Na, K-ATPase. *J Biol Chem* 1978; 253: 7361-8.
173. Kinne R, schmitz JE, Kinne-saffran E. The localization of the Na<sup>+</sup>-K<sup>+</sup>-ATPase in the cells of rat kidney cortex. A study on isolated plasma membranes. *Pflügers Arch* 1971; 321: 191-206.
174. Schmidt U, Dubach UC. Na-K stimulated adenosine-triphosphatase: intracellular localization within the proximal tubule of rat nephron. *Pflügers Arch* 1971; 330: 265-70.
175. Shaver JLF, Stirling C. Ouabain binding to renal tubule of the rabbit. *J Cell Biol* 1978; 76: 278-92.
176. Kyte J. Immunoferritin determination of the distribution of (Na<sup>+</sup>+K<sup>+</sup>) ATPase over the plasma membranes of renal convoluted tubule. I. distal segment. *J Cell Biol* 1976; 68: 287-303.
177. Kyte J. Immunoferritin determination of the distribution of (Na<sup>+</sup>+K<sup>+</sup>) ATPase over the plasma membranes of renal convoluted tubule. II. proximal segment. *J Cell Biol* 1976; 68: 304-18.

178. Kasturi R, Yuan J, McLean LR, Margolies MN, Ball WJ, Jr. Identification of a model cardiac glycoside receptor: comparison with Na<sup>+</sup>-K<sup>+</sup>-ATPase. *Biochemistry* 1998; 37: 6658-66.
179. Hendler ED, Torretti J, Epstein FH. The distribution of sodium-potassium-activated adenosine triphosphatase in medulla and cortex of the kidney. *J Clin Invest* 1971; 1329-37.
180. Doucet A, Katz AI, Morel F. Determination of Na-K-ATPase activity in single segments of the mammalian nephron. *Am J Physiol* 1979; 237: F105-13.
181. Katz AI, Doucet A, Morel F. Na-K-ATPase activity along the rabbit, rat and mouse nephron. *Am J Physiol* 1979; 237: F114-20.
182. Schmidt U, Horster M. Na-K-activated ATPase: Activity maturation in rabbit nephron segments dissected *in vitro*. *Am J Physiol* 1977; 233: F55-60.
183. EL Mernissi G, Doucet A. Quantitation of [<sup>3</sup>H] ouabain binding and turnover of Na-K-ATPase along the rabbit nephron. *Am J Physiol* 1984; 247: F158-67.
184. Garg LC, Knepper MA, Burg MB. Mineralocorticoid effects on Na-K-ATPase in individual nephron segments. *Am J Physiol* 1981; 240: F536-44.
185. Aperia A, Larsson L, Zetterstrom R. Hormonal induction of Na-K-ATPase in developing proximal tubular cells. *Am J Physiol* 1981; 241: F356-60.
186. Aperia A, Larsson L. Induced development of proximal tubular Na-K ATPase basolateral cell membranes and fluid reabsorption. *Acta Physiol Scand* 1984; 121: 133-41.
187. Celsi G, Larsson L, Aperia A. Proximal tubule reabsorption and Na<sup>+</sup>-K<sup>+</sup> ATPase activity in remnant kidney of young rats. *Am J Physiol* 1986; 251: F588-93.

188. Celsi G, Nishi A, Akusjarvi G, Aperia A, Abundance of  $\text{Na}^+\text{-K}^+\text{-ATPase}$  mRNA is regulated by glucocorticoid hormones in infant rat kidneys. *Am J Physiol* 1991; 260: F192-7.
189. Larsson SH, Rane S, Fukada Y, Aperia A, Lechene C. Changes in Na influx precede post-natal increase in Na, K-ATPase activity in rat renal proximal tubular cells. *Acta Physiol Scand* 1990; 138: 99-100.
190. Rane S, Aperia A. Ontogeny of Na-K-ATPase activity in thick ascending limb and of concentrating capacity. *Am J Physiol* 1985; 249: F723-8.
191. Schwartz GJ, Evan AP. Development of solute transport in rabbit proximal tubule. III. Na-K-ATPase activity. *Am J Physiol* 1984; 246: F845-52.
192. Aperia A, Larsson L. Correlation between fluid reabsorption and proximal tubule ultrastructure during development of the rat kidney. *Acta Physiol Scand* 1979; 105: 11-22.
193. Larsson L, Aperia A, Elinder G. Structural and functional development of the nephron. *Acta Paediatr Scand Suppl* 1983; 305: 56-60.
194. Welling LW, Welling DJ. Surface areas of brush border and lateral cell walls in the rabbit proximal nephron. *Kidney Int* 1975; 8: 343-8.
195. Welling LW, Evan AP, Gattone VH, Rollins S, Saunders R, Spitzer A. Correlation of structure and function in developing proximal tubule of guinea pig. *Am J Physiol* 1989; 256: F13-7.
196. Klein LE, Lo CS. Regulation of rat renal ( $\text{Na}^+\text{+K}^+$ )-adenosine triphosphatase mRNA levels by corticosterone. *Experientia* 1992; 48: 768-73.

197. Lo CS, Edelman IS. Effect of triiodothyronine on the synthesis and degradation of renal cortical ( $\text{Na}^+\text{+K}^+$ )-adenosine triphosphatase. *J Biol Chem* 1976; 251: 7834-40.
198. Lo CS, August TR, Liberman UA, Edelman IS. Dependence of renal ( $\text{Na}^+\text{+K}^+$ )-adenosine triphosphatase activity on thyroid status. *J Biol Chem* 1976; 251: 7826-33.
199. Chiou S, Vesely DL. Dimethyl sulfoxide inhibits renal  $\text{Na}^+\text{-K}^+$ -ATPase at a site different from ouabain and atrial peptides. *Life Sci* 1995; 57(10): 945-55.
200. McConnell EJ, Wagoner MJ, Keenan CE, Raess BU. Inhibition of Calmodulin-stimulated ( $\text{Ca}^{2+}\text{+Mg}^{2+}$ )-ATPase activity by dimethyl sulfoxide. *Biochem Pharmacol* 1999; 57: 39-44.
201. Maxild J, Moller JV, Sheikh MI. Involvement of  $\text{Na}^+\text{-K}^+$  ATPase in p-aminohippurate transport by rabbit renal tissue. *J Physiol* 1981; 315: 189-201.
202. Hanson JR, De Oliveira BH. Stevioside and related sweet diterpenoid glycosides. *Nat Prod Rep* 1993; 10: 301-9.
203. Mowrey D. Life with stevia: How sweet it is! [Online] 1992; [13 screens]. Available from: <http://www.healthfree.com/stev/ifc.htm> [Accessed 1999 August 5].
204. Wood HB, Jr., Allerton R, Diehl HW, Fletcher HG. Jr. Stevioside I. The structure of the glucose moieties. *J Org Chem* 1955; 20: 875-83.
205. Johnson RE, Jr. Stevioside, "Naturally". A special presentation to the Calorie Control Council 23<sup>rd</sup> Annual Meeting Tucson, Arizona, November 4-7,

- 1990; [4 screens] Available from: [http://www.holisticmed.com/sweet/stv\\_ej.txt](http://www.holisticmed.com/sweet/stv_ej.txt) [Accessed 1999 August 5].
206. Brandle JE, Starratt AN, Gijzen M. *Stevia rebaudiana*: Its biological, chemical and agricultural properties. [Online] June 16, 2000; [18 screens]. Available from: [http://res2.agr.ca/london/pmrc/faq/stevia\\_rev.html](http://res2.agr.ca/london/pmrc/faq/stevia_rev.html) [Accessed 2000 June 28].
207. Kinghorn AD, Soejarto DD. Current status of stevioside as a sweetening agent for human use. In: Wagner H, Hikino H, Farnsworth NR, editors. Economic and medical plant research. London: Academic Press; 1985.
208. Brandle JE, Rosa N. Heritability for yield, leaf: stem ratio and stevioside content estimated from a landrace cultivar of *Stevia rebaudiana*. [Online] 1998; [5 screens]. Available from: <http://res2.agr.ca/london/pmrc/faq/cjps-ste.html> [Accessed 2000 June 28].
209. Tamura Y, Nakamura S, Fujui H, Tabata M. Comparison of stevia plants grown from seeds, cuttings and stem tip cultures for growth and sweet diterpene glycosides. *Plan Cell Rep* 1984; 3: 180-2.
210. Metivier J, Viana AM. The effect of long and short day length upon the growth of whole plants and the level of soluble proteins, sugars and stevioside in leaves of *Stevia rebaudiana* Bert. *J Exp Bot* 1979; 30: 1211-22.
211. Sutteerawattananon M, Toskulkao C. Stevioside: the low calorie natural sweetener. *Thai J Toxicol* 1994; 10: 24-33.
212. Mosettig E, Nes WR. Stevioside II. The structure of the aglucon. *J Org Chem* 1955; 20: 884-99.

213. Glinsukon T, Pimbau J, Panichkul T. Minireview article: stevioside, a natural sweetener from *Stevia rebaudiana* Bertoni: Toxicological evaluation. Thai J Toxicol 1988; 4: 1-22.
214. Salvatore G, Paganuzzi AS, Silano V, Aurli AD. Stevioside: occurrence, uses, chemical and biological properties. Chim Oggi 1983; 8: 31-7.
215. Wood HB, Jr, Fletcher HG. Stevioside III. The anomeric 2,3,4,6-tetra-O-acetyl-1-O-mesitoyl-D-Glucopyranoses and their behavior with alkali. J Am Chem Soc 1956; 78: 207-10.
216. Tama Biochemical Co., Ltd. Safety of Stevia. 7-1 Nishishinjuku, 2-Chome, Shinjuku-KU. Japan: Tokyo 160, 1981; pp. 1-20.
217. Masaaki Y, Moriko T, Kyoji T, Kayoko T, Aiki Y, Yoshifumi J. Studies on stevioside, natural sweetener: effect on the growth of some oral microorganisms. Hiroshima Diagaku Shigaku Zasshi 1977; 9: 12-7.
218. Tomita T, Sato N, Arai T, Shiraishi H, Sato M, Takeuchi M, Kamio Y. Bactericidal activity of a fermented hot-water extract from *Stevia rebaudiana* Bertoni towards enterohemorrhagic *Escherichia coli* O157: H7 and other food-borne pathogenic bacteria. Microbiol Immunol 1997; 41: 1005-9.
219. Ogawa T, Nozaki M, Matzui M. Total synthesis of stevioside. Tetrahedron 1980; 36: 2641-8.
220. Raddat M, Heftmann E, Lang A. Biosynthesis of steviol. Arch Biochem Biophys 1965; 110: 496-9.

221. Kensuke N, Kenji I, Hiroshi S. Acid hydrolysis of stevioside. *Nippon Nogei Kagaku Kaishi* 1977; 51: 179-81.
222. Nakayama K, Kasahara D, Yamamoto F. Absorption, distribution, metabolism and excretion of stevioside in rats. *J Food Hyg Soc Japan* 1986; 27: 1-8.
223. Ishii-Iwamoto EL, Bracht A. Stevioside is not metabolized in the isolated perfused rat liver. *Res Commun Mol Patho Pharmacol* 1995; 87: 167-75.
224. Hutapae AM, Toskulkao C, Wilairat P, Buddhasukh D. High-performance liquid chromatographic separation and quantitation of stevioside and its metabolites. *J Liq Chrom & Rel Technol* 1999; 22: 1161-70.
225. Hutapae AM. Digestion, disposition and metabolism of stevioside [Ph.D. Thesis in Physiology]. Bangkok: Faculty of Graduate Studies, Mahidol University, 1998.
226. Pendergast WR. Hand-delivery. [Online] 1991; [10 screens]. Available from: <http://www.holisticmed.com/sweet/stv-petition.txt> [Accessed 2000 March 28].
227. Toskulkao C, Chaturat L, Temcharoen P, Glinsukon T. Acute toxicity of stevioside, a natural sweetener, and its metabolite, steviol, in several animal species. *Drug Chem Toxicol* 1997; 20: 31-44.
228. Krejci ME, Koechel DA. Acute effects of carboxyatractyloside and stevioside, inhibitors of mitochondrial ADP/ATP translocation, on renal function and ultrastructure in pentobarbital-anesthetized dogs. *Toxicology* 1992; 72: 299-313.

229. Jitrawang P. Effect of stevioside and steviol on reproductive capability and micronucleus formation in hamsters [M.S. Thesis in Toxicology] Bangkok: Faculty of Graduate Studies, Mahidol University, 1998.
230. Chairoungdua A. Dominant lethal study of stevioside and steviol in male hamster [M.S. Thesis in Toxicology]. Bangkok: Faculty of Graduate Studies, Mahidol University, 1998.
231. Tama Biochemical Co., Ltd. Stevix and steviosin-newly developed natural sweetening agents, 7-1 Nishishinjuku, 2-Chome, Shinjuku-Ku, Tokyo, 160, Japan 1981; 14: 99-154.
232. Akashi H, Yokoyama Y. Dried-leaf extracts of stevia. Toxicological test. *Shokuhin Kogyo* 1975; 18: 34-43.
233. Yamada A, Ohgaki S, Noda T, Shimizu M. Chronic Toxicity study of dietary stevia extracts in F344 rats. *J Food Hyg Soc Japan* 1985; 26: 169-83.
234. Xili L, Chengjiany B, Eryi X, Reining S, Yeungming W, Haodong S, Zhiyian H. Chronic oral toxicity and carcinogenicity study of stevioside in rats. *Food Chem Toxicol* 1992; 30: 957-65.
235. Toyoda K, Matsui H, Shoda T, Uneyama C, Takada K, Takahashi M. Assessment of the carcinogenicity of stevioside in F344 rats. *Food Chem Toxicol* 1997; 35: 597-603.
236. Yodyinguard V, Bunyawong S. Effect of stevioside on growth and reproduction. *Hum Reprod* 1991; 6: 158-65.
237. Mori N, Sakanoue M, Takeuchi M, Shimpo K, Tanabet S. Effects of stevioside on fertility in rats. *Shokuhin Eiseigaku Zasshi* 1981; 22: 409.

238. Usami M, Sakemi K, Kawashima K, Tsuda M, Ohno Y. Teratogenicity study of stevioside in rats. *Eisei Shikenjo Hokoku* 1995; 113: 31-5.
239. Pezzuto JM, Compadre CM, Swanson SM, Nanayakkara, NPD, Kinghorn AD. Metabolically activated steviol, the aglycone of stevioside, is mutagenic. *Proc Natl Acad Sci* 1985; 82: 2478-82.
240. Matsui M, Sofuni T, Nohmi T. Regionally-targeted mutagenesis by metabolically-activated steviol: DNA sequence analysis of steviol-induced mutants of guanine phosphoribosyl transferase (gpt) gene of *Salmonella typhimurium* TM 677. *Mutagenesis* 1996; 11: 565-72.
241. Wasuntarawat C, Temcharoen P, Toskulkao C, Mungkornkarn P, Suttajit M, Glinsukon T. Developmental toxicity of steviol, a metabolite of stevioside, in the hamster. *Drug Chem Toxicol* 1998; 21: 207-22.
242. Kurahashi H, Yamaguchi Y, Tsuzuki S, Maechashi H. Pharmacological studies of stevioside. *Matsumoto Shigaku* 1982; 8: 56-62.
243. Melis MS, Sainati AR, Maciel RE. Effects of two concentrations of stevioside on renal function and mean arterial pressure in rats. *IRCS Med Sci* 1986; 14: 973.
244. Portella-Nunes BA, Pereira NA. Efeito do Caá-Heê (*Stevia rebaudiana*) (Bert) Bertoni sobre a fertilidade de animais experimentais. *Rev Bras Farm* 1988; 69: 46-50.
245. Dorfman RJ, Nes WR. Anti-androgenic activity of dihydroisosteviol. *Endocrinology* 1960; 67: 282-5.

246. Uehara OA, Utino VH, Miyata I, Valle LBS, Oliveira-Filho RM. Stevioside androgen interactions. In: 7<sup>th</sup> Symp. Natural Products and Pharmacology. Sao Paulo, vol 1, p. 74.
247. Oliveira-Filho RM, Uehara OA, Minetti CASA, Valle LBS. Chronic administration of aqueous extract of *Stevia rebaudiana* (Bert.) Bertoni in rats: endocrine effects. Gen Pharmacol 1989; 2: 187-91.
248. Melis MS. Effects of chronic administration of *Stevia rebaudiana* on fertility in rats. J Ethnopharmacol 1999; 167: 157-61.
249. Susuki H, Kasai T, Sumihara M, Sugisawa H. Effects of oral administration of stevioside on levels of blood glucose and liver glycogen of intact rats. Nippon Nogei Kagaku Kaishi 1977; 51: 171-3.
250. Lee SJ, Lee KR, Park IR, Kimm KS, Tachai BS. A Study of the safety of stevioside as a new sweetening source. Hanguk Sikipum Kwahakhoe Khi 1979; 11: 224-31.
251. Bracht AK, Alvarez M, Bracht A. Effects of *Stevia rebaudiana* natural products on rat liver mitochondria. Biochem Pharmacol 1985; 34: 873-82.
252. Kelmer-Bracht AM, Kimmelmeier FS, Ishii EL, Alvarez M, Bracht A. Effect of *Stevia rebaudiana* natural products on cellular and sub-cellular metabolism. Arq Biol Tecnol 1985; 28: 431-55.
253. Yamamoto NS, Kelmer-Bracht AM, Ishii EL, Kimmelmeier FS, Alvarez M, Bracht A. Effect of steviol and its structural analogues on glucose production and oxygen uptake in rat renal tubules. Experientia 1985; 41: 55-7.

254. Vignais PV, Duce ED, Vignais PM, Huet J. Effects of atractyligenin and its structural analogues on oxidative phosphorylation and on the translocation of adenine nucleotides in mitochondria. *Biochim Biophys Acta* 1966; 118: 465-83.
255. Hubler MO, Bracht A, Kelmer-Bracht AM. Influence of stevioside on hepatic glycogen levels in fasted rats. *Res Commun Chem Pathol Pharmacol* 1994; 84: 111-8.
256. Toskulkao C, Sutheerawattananon M, Piyachaturawat P. Inhibitory effect of steviol, a metabolite of stevioside, on glucose absorption in everted hamster intestine *in vitro*. *Toxicol Lett* 1995; 80: 153-9.
257. Usami M, Seino Y, Takai J, Nakahara H, Seino S, Ikeda M, Imura H. Effect of cyclamate sodium, saccharin sodium and stevioside on arginine-induced insulin and glucagon secretion in isolated perfused rat. *Horm Metab Res* 1980; 12: 705-6.
258. Suanarunsawat T, Chaiyabutr N. The effect of intravenous infusion of stevioside on the urinary sodium excretion. *J Anim Physiol a Anim Nutr* 1996; 76: 141-50.
259. Malaisse WJ, Vanonderbergen A, Louchami K, Jijakli H, Malaisse-Lagae F. Effects of artificial sweeteners on insulin release and cationic fluxes in rat pancreatic islets. *Cell Signal* 1998; 10: 727-33.
260. Jeppesen PB, Gregersen S, Poulsen CR, Hermansen K. Stevioside acts directly on pancreatic  $\beta$  cells to secrete insulin: actions independent of cyclic

- adenosine monophosphate and adenosine triphosphate-sensitive  $K^+$ -channel activity. *Metabolism* 2000; 49: 208-14.
261. Podprasart V. Stevioside and steviol: The effect on  $Na^+K^+$  ATPase activity and the correlation with distribution in intracellular and extracellular compartments of rabbit renal proximal tubule [M.S. Thesis in Toxicology]. Bangkok: Faculty of Graduate Studies, Mahidol University; 1998.
262. Das S, Das AK, Murphy RA, Punwani IC, Nasution MP, Kinghorn AD. Evaluation of the cariogenic potential of the intense natural sweeteners stevioside and rebaudioside A. *Caries Res* 1992; 26(5): 363-6.
263. Kinghorn AD, Kaneda N, Baek NI, Kennelly EJ, Soejarto DD. Noncariogenic intense natural sweeteners. *Med Res Rev* 1998; 18(5): 347-60.
264. Railey K. Stevia- an alternative for sugar? [Online]. Available: <http://www.chetday.com/stevia.html> [2000, June 28].
265. DeMuylder E, Naudts P, Geuns J, Simoens S, Vanhoudt L. Utilization of stevioside, a new natural, non-caloric feed sweetener, in feeds for dogs. [Online], 9 screens. Available: <http://users.skynet.be/sky39544/stepadog.htm> [2000, June 28].
266. Igarashi Y, Aperia A, Larsson L, Zetterstrom R, Effect of betamethasone on  $Na^+K^+$ -ATPase activity and basal and lateral cell membranes in proximal tubular cells during early development. *Am J Physiol* 1983; 245: F232-7.
267. Burg M, Grantham J, Abramow M, Orloff J. Preparation and study of fragments of single rabbit nephrons. *Am J Physiol* 1966; 210: 1293-8.

268. Dantzler WH. Characteristics of urate transport by isolated perfused snake proximal renal tubules. *Am J Physiol* 1973; 244: 445-53.
269. Vinay P, Gougoux A, Lemieux G. Isolation of a pure suspension of rat proximal tubules. *Am J Physiol* 1981; 241: F403-11.
270. Groves CE, Evans KK, Dantzler WH, Wright SH. Peritubular organic cation transport in isolated rabbit proximal tubules. *Am J Physiol* 1994; 266: F450-8.
271. Hull-Ryde EA, Cummings RG, Lowe JE. Improved method for high energy nucleotide analysis of canine cardiac muscle using reversed-phase high-performance liquid chromatography. *J Chromatogr* 1983; 275: 411-7.
272. Mandel LJ, Schnellmann RG, Jacobs WR. Intracellular glutathione in the protection from anoxic injury in renal proximal tubules. *J Clin Invest* 1990; 85: 316-24.
273. Dantzler WH, Wright SH, Chatsudthipong V, Brokl OH. Basolateral tetraethylammonium transport in intact tubules: specificity and trans-stimulation. *Am J Physiol* 1991; 261: F386-92.
274. Groves CE, Morales M, Wright SH. Peritubular transport of ochratoxin A in rabbit renal proximal tubules. *J Pharmacol Exp Ther* 1998; 284: 943-8.
275. Trivedi AB, Kitabatake N, Doi E. Toxicity of DMSO as a solvent in bioassay system with Hela cells evaluated colorimetrically with 3-(4,5-dimethylthiazol-2-yl)-2,5-diphenyl-tetrazolium bromide. *Agric Biol Chem* 1990; 54: 2961-6.

276. Rijtema M, Mosig D, Drukker A, Guignard JP. The effects of dimethyl sulfoxide on renal function of the newborn rabbit. *Biol Neonate* 1999; 76(6): 355-61.
277. Kramer K, Van Acker SA, Grimbergen JA, Van den Berg DJ, Van der Vijgh WJ, Bast A. Effect of dimethyl sulfoxide (DMSO) in the electrocardiogram (ECG) in freely moving male Balb/c mice. *Gen Pharmacol* 1995; 26: 1403-7.
278. Fontes CFL, Scofano HM, Barrabin H, Norby JG. The effect of dimethylsulfoxide on the substrate site of  $\text{Na}^+/\text{K}^+$  ATPase studied through phosphorylation by inorganic phosphate and ouabain binding. *Biochim Biophys Acta* 1995; 1235: 43-51.
279. Mayes PA. Bioenergetics: The role of ATP. In: Murray RK, Granner DK, Mayes PA, Rodwell VW, editors. *Harper's Biochemistry*. 23<sup>rd</sup> ed. USA: Appleton & Lange; 1993; p.105-11.
280. Comprade CM, Hussain RA, Nanayakkara NPD, Pezzuto JM, Kinghorn AD. Mass spectral analysis of some derivatives and *in vitro* metabolites of steviol, the aglycone of the natural sweeteners, stevioside, rebaudioside and rubusoside. *Biomed Environm Mass Spectro* 1988; 15: 211-22.
281. Podevin RA, Boumendil-Podevin EF. Monovalent cation and ouabain effects on PAH uptake by rabbit kidney slices. *Am J Physiol* 1977; 232: F239-47.
282. Glinsukon T. Physiological properties of stevioside. In Suttajit M, Apisariyakul A, Buddhasukh D, editors. *Steval research* Chiang Mai: Star Press; 1991. p. 41-55.

283. Thorn W, Liemann F. Metabolitkonzentrationen in der Niere und Paraaminohippursaureclearance nach acuter Ischämie und in der Erholung nach Ischämie. *Pflügers Arch* 1961; 273: 528-42.
284. Gerlach E, Deuticke B, Dreisbach RH. Zum Verhalten von Nucleotiden und ihren Dephosphorylierten Abbauprodukten in der Niere bei Ischämie und kurzzeitiger Postischämischer Wiederdurchblutung. *Pflügers Arch* 1963; 278: 296-315.
285. Buhl R. Purine metabolism in ischaemic kidney tissue. *Dan Med Bull* 1982; 29: 1-26.
286. Busch EW, Von Borcke IM, Martinez B. Abbauege und Abbaumuster der Purinnucleotide in Herz-, Leber-, und Nierengewebe von Kaninchen nach Kreislauf-stillstand. *Biochim Biophys Acta* 1968; 166: 546-56.
287. Cunarro JA, Schultz SE, Johnson WA, Weiner MW. Effects of ischemia on metabolite concentration in dog renal cortex. *Renal Physiol* 1982; 5: 143-55.
288. Weinberg JM, Humes HD. Increases of cell ATP produced by exogenous adenine nucleotides in isolated rabbit kidney tubules. *Am J Physiol* 1986; 250: F720-33.

**APPENDIX I****SUCROSE-HEPES BUFFERED MEDIUM**

<b>Final concentrations</b>	<b>MW</b>	<b>for 1 L of medium</b>
250 mM sucrose	342.3	85.575 g
10 mM HEPES	238.3	2.383 g

Sucrose and HEPES were dissolved in approximately 950 ml distilled water and then gassed with pure O<sub>2</sub> for at least 20 minutes. The pH was adjusted to 7.4 with 1 M Trizma-base [tris (hydroxymethyl) amino methane base] (the addition of trizma-base was stopped when the pH reached 6.8, then was slowly adjusted to pH 7.4). Distilled water was then added until a volume of 1L was obtained.

**APPENDIX II****BICARBONATE BUFFERED MEDIUM**

<b>Final concentrations</b>	<b>MW</b>	<b>Stock concentrations</b>	<b>Volume for 500 ml buffer</b>
110 mM NaCl	58.443	1.1 M (32.1436 g/500 ml)	50 ml
5 mM KCl	74.56	0.5 M (3.728 g/100 ml)	5 ml
2 mM NaH <sub>2</sub> PO <sub>4</sub> .H <sub>2</sub> O	137.99	0.2 M (2.7598 g/100 ml)	5 ml
1 mM MgSO <sub>4</sub> .7H <sub>2</sub> O	246.48	0.1 M (2.4648 g/100 ml)	5 ml
10 mM CH <sub>3</sub> COONa.3H <sub>2</sub> O	136.08	1 M (6.8040 g/50 ml)	5 ml
1.8 mM CaCl <sub>2</sub> .2H <sub>2</sub> O	147.02	0.18 M (2.6464 g/100 ml)	5 ml
8.3 mM D-glucose	180.16	0.83 M (7.4766 g/50 ml)	5 ml
5 mM L-alanine	89.09	0.5 M (2.22725 g/50 ml)	5 ml
1 mM Na-citrate	210.14	0.1 M (1.0507 g/50 ml)	5 ml
1.5 mM Na-lactate	112.1	0.15 M (0.8408 g/50 ml)	5 ml
1 mM Na-Malate	160.0	0.1 M (0.8000 g/50 ml)	5 ml
0.9 mM glycine	75.07	0.09 M (0.6756/100 ml)	5 ml

25 mM NaHCO<sub>3</sub> ⇒ Weighed this out and added to the mixture of the above solution

(1.05 g/500 ml of medium)

The above compounds were mixed and then distilled water was added until the volume was near 500 ml, then it was bubbled with 5% CO<sub>2</sub> and 95% O<sub>2</sub> for at

least 20 min. The pH of buffer was then adjusted to 7.4 and the final volume was adjusted to 500 ml with distilled water.

The bathing medium for the microperfusion experiment contained 3 g of dextran per 100 ml of bicarbonate-buffered medium.



**APPENDIX III****BICARBONATE-HEPES BUFFERED MEDIUM**

<b>Final concentrations</b>	<b>MW</b>	<b>Stock solutions</b>	<b>Volume of stock for 500 ml buffer</b>
115 mM NaCl	58.443	1.15 M (16.8024 g/250 ml)	50 ml
10 mM HEPES	238.3	0.1 M (5.9575 g/250 ml)	50 ml
1 mM L-alanine	89.09	0.1 M (0.4455 g/50 ml)	5 ml
5 mM Glucose	180.16	0.5 M (4.504 g/50 ml)	5 ml
2 mM Heptanoic acid	130.2	-	0.13 ml
4 mM Na-lactate	112.1	0.4 M (2.242 g/50 ml)	5 ml
5 mM Maleic acid	160.0	0.5 M (4 g/50 ml)	5 ml
5 mM KCl	74.56	0.5 M (3.728 g/100 ml)	5 ml
2 mM NaH <sub>2</sub> PO <sub>4</sub> ·H <sub>2</sub> O	137.99	0.2 M (2.7598 g/100 ml)	5 ml
1 mM MgSO <sub>4</sub> ·7H <sub>2</sub> O	246.48	0.1 M (2.4648 g/100 ml)	5 ml
1 mM CaCl <sub>2</sub> ·2H <sub>2</sub> O	147.02	0.1 M (1.4702 g/100 ml)	5 ml

NaHCO<sub>3</sub> 0.12 g/100 ml (w/v) was weighed and added to the buffered solution and gassed with 5% CO<sub>2</sub> and 95% O<sub>2</sub>. The pH of medium was then adjusted to 7.4 with 1 N NaOH.

## APPENDIX IV

### ENZYMATIC DIGESTION SOLUTION

The digestion solution was prepared from 150 units/ml collagenase type IV, 0.2% (w/v) bovine serum albumin and 10 mM deferoxamine mesylate. The volume was made up to 25 ml with bicarbonate-HEPES-buffered medium, then kept on ice and gassed with 95% O<sub>2</sub> and 5% CO<sub>2</sub> until used.

## APPENDIX V

### PERCOLL GRADIENT SOLUTION

The solution used for the separation of proximal tubules from other contaminants such as distal tubules, glomeruli and cell debris, contained 40% (v/v) percoll (Pharmacia Biotech AB) in a bicarbonate-buffered medium. This solution was prepared by mixing 14 ml of percoll with 14 ml of 2 x concentration of bicarbonate-buffered medium and 7 ml of bicarbonate-buffered medium. The pH was adjusted to 7.4 at 4°C with 1 N HCl. The percoll solution will precipitate if NaOH is added to the solution. Thus, it was important not to let the pH drop to below 7.4 when adjusting the pH.

## APPENDIX VI

### PROTEIN DETERMINATION

The method used for determination of protein content in the proximal tubules was modified from Lowry's method using Folin Phenol reagent (Lowry et al. 1951).

#### REAGENTS

##### 1. Solution A (alkaline tartrate reagent)

This solution contained the following substances:

$\text{Na}_2\text{CO}_3$	10.0	g
$\text{Na}_2\text{C}_4\text{H}_4\text{O}_6 \cdot 2\text{H}_2\text{O}$	0.1	g
NaOH	1.2	g

These substances were dissolved in distilled water to make a 500 ml solution.

##### 2. Solution B (0.5% (w/v) copper sulfate)

This solution contained 0.5 g of  $\text{CuSO}_4 \cdot 5\text{H}_2\text{O}$  dissolved in distilled water to a final volume of 100 ml.

3. Solution C was freshly prepared before assay time. It contained a mixture of solutions A and B in a ratio of 50:1.

##### 4. Solution D (1 N Folin phenol reagent)

This solution was prepared from 2 N Folin Ciocalteu Phenol reagent diluted with distilled water in a ratio of 1:1. This solution was used immediately after its preparation.

## 5. Standard protein solution

Various concentrations (25, 50, 100, 150 and 200 mg%) of bovine serum albumin were used to construct the standard curve.

## ASSAY PROCEDURES

1. 2 ml of solution C was added into each tube.
2. 40  $\mu$ l of distilled water (blank) or standard protein or sample (unknown) was subsequently added and mixed well with a vortex mixer and then left at room temperature for 10 min.
3. 0.2 ml of solution D was added and mixed thoroughly, then let stand for 60 min at room temperature.
4. Optical density at 650 nm was read by a spectrophotometer (Jasco model 7850, Japan Spectroscopic Co., Ltd.)
5. The concentration of protein in samples was determined from the linear equation of the standard curve.

## APPENDIX VII

### DETERMINATION OF Na<sup>+</sup>-K<sup>+</sup>ATPase ACTIVITY

This assay consisted of 2 stages of reaction, namely, the generation of inorganic phosphate (P<sub>i</sub>) during ATP hydrolysis (ATP  $\xrightarrow{\text{ATPase}}$  ADP + P<sub>i</sub>), and the color development of P<sub>i</sub> using the modified method of Fiske & Subbarow.

Since Na<sup>+</sup>-K<sup>+</sup> ATPase activity is ouabain-sensitive ATPase activity, its magnitude can be determined from the difference between total ATPase activity and ouabain-insensitive ATPase activity, which is the remaining ATPase activity after the addition of ouabain to the assay solution.

### REAGENTS

#### 1. 2 x-concentrated buffer:

This buffer consisted of 200 mM NaCl, 20 mM KCl, 10 mM MgCl<sub>2</sub> and 167 mM Tris base. It was prepared as follows:

	MW	g/0.5 L of buffer
NaCl	58.44	5.844
MgCl <sub>2</sub>	203.33	1.017
KCl	74.56	0.746
Tris base	121.10	10.112

The pH of the buffer solution was adjusted to 7.4 with HCl and kept in the refrigerator.

**2. 30 mM ATP (disodium salt, MW 551.1)**

This was prepared by dissolving 165.33 mg of ATP in 10 ml of distilled water. It was kept in aliquots at  $-70^{\circ}\text{C}$ .

**3. 100 mM EDTA (disodium salt, MW 372.24)**

This solution was prepared by dissolving 3.7224 g of EDTA in distilled water to the volume of 100 ml. The pH was adjusted to 7.4 with NaOH, and kept in the refrigerator.

**4. Assay mixture**

This solution was made freshly daily before use. It consisted of 5 parts of 2x buffer, 1 part of 30 mM ATP, 0.3 parts of 100 mM EDTA and 4 parts of distilled water.

**5. Assay mixture containing 2.5 mM ouabain (MW = 728.79)**

1.8220 mg of ouabain octahydrate was added to each ml of assay mixture. The pH of this solution was maintained at 7.4. This solution was also freshly prepared daily before the assay.

**6. 5% (w/v) trichloroacetic acid (TCA, MW = 163.39)**

5 g of TCA was dissolved in distilled water to a final volume of 100 ml. It was kept in the refrigerator until used.

**7. Phosphate standards**

$\text{KH}_2\text{PO}_4$  (MW 136.09) of the highest quality available was used to prepare the standard stock at a concentration of 100 mM and kept in aliquots at  $-70^{\circ}\text{C}$ . The concentrations of standards, 5, 10, 20 and 30 mM, were prepared from dilutions of the standard stock.

### 8. Reducing reagent: Fiske & Subbarow reducer (Sigma, #661-8)

This reagent was freshly prepared daily by dissolving 25 mg of Fiske & Subbarow reducer in 1 ml of distilled water. After the preparation, the solution was kept in a dark or an aluminum foil-covered container.

### 9. Sulfate-Molybdate reagent

This solution contained 1 part of 2.5% (w/v) ammonium molybdate, 1 part of 5N sulfuric acid ( $\text{H}_2\text{SO}_4$ ), and 6 parts of distilled water. After preparation, it was stored at room temperature.

## ASSAY PROCEDURES

Each sample assay was made in quadruplicate; two for total ATPase assay using the assay mixture, and the other two for an ouabain-insensitive ATPase assay using ouabain to inhibit  $\text{Na}^+\text{-K}^+$  ATPase activity. An assay mixture containing 2.5 mM ouabain was used for the latter.

### Reaction I: generation of $\text{P}_i$

1. 0.5 ml of assay mixture was placed in 2 tubes for each sample and the other 2 tubes were filled with 0.5 ml assay mixture containing ouabain. These tubes were placed on ice.
2. 25  $\mu\text{l}$  of sample was added to each tube mentioned above. For blank tubes, 25  $\mu\text{l}$  of distilled water was used instead of sample. They were mixed well with a vortex mixer.
3. The reaction was initiated by incubation at 37°C for 1 hour.

4. At the end of the incubation period, the reaction was quenched by the addition of 0.5 ml of 5% TCA to the mixture.

**Reaction II: color development of  $P_i$  using Fiske & Subbarow**

1. 3 ml of sulfate-molybdate reagent was added to each of the above reaction tubes and mixed well with a vortex mixer.

2. 50  $\mu$ l of reducing agent was then added and mixed again. Subsequently, the tubes were allowed to sit at room temperature for 30 min.

3. The denatured protein was removed from each assay tube by centrifugation at a speed of approximately 2,000 rpm for 5 min to prevent interference with absorbance reading from protein.

4. The optical density was measured at 660 nm using a spectrophotometer (Jasco Model 7850, Japan Spectronic Co., Ltd.)

The concentration of  $P_i$  liberated from the ATPase activity of each sample was obtained from the graph plotted between absorbance VS concentration of standard phosphate. The amount of  $P_i$  generated from  $Na^+-K^+$  ATPase activity was calculated from the  $P_i$  generated by total ATPase activity minus that of ouabain-insensitive ATPase activity. The unit of ATPase activity was expressed as  $\mu$ mol  $P_i$ /mg protein/hr.

## APPENDIX VIII

### DETERMINATION OF $^{14}\text{C}$ -PAH

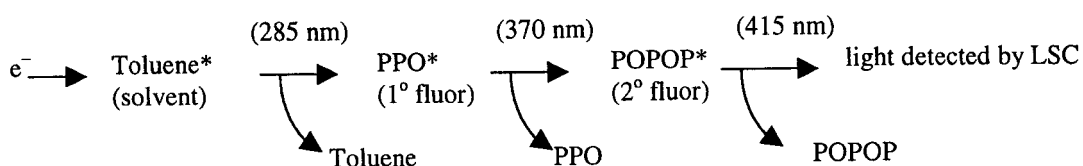
Carbon-14 ( $^{14}\text{C}$ ) is a radioisotope which dissipates low-energy beta-particles, with a half life of more than 5,000 years. Determination of the radioactivity in the sample was performed by diluting the sample containing  $^{14}\text{C}$  with a liquid scintillation fluid. The solvent molecules in the scintillation fluid function to absorb energy from the electrons and raise its energy level to the excited state. Emission of a photon of light happens when its energy level returns back to ground state. One or more fluorescent compounds (fluors) in a scintillation fluid will shift the emitted wavelength to a longer range that is more readily detected by the liquid scintillation counter (LSC). The radioactivity was presented as disintegration per minute (dpm).

Scintillation fluid or cocktail contained:

- 5.0 g of 2,5-diphenyloxazole (PPO) as primary fluor
- 0.3 g of 1,4 bis 5-phenyl-2-oxalzoyl benzene (POPOP) as secondary fluor
- 500 ml of toluene as a solvent
- 500 ml of Triton X-100 (p-isooctylphenoxyethanol) as a detergent.

Fluors are not readily solubilized and it may be necessary to stir them overnight in a fume hood or let them sit at least 2-3 days to get them into solution.

The process of radioactivity counting is shown below



## PROCEDURES

1. 0.1 ml of distilled water was added to a vial followed by the addition of collected sample (80-120 nl).
2. 1 ml of cocktail was filled and mixed well by using a vortex mixer.
3. The above vial was placed into the scintillation glass vial and the radioactivity counted by a  $\beta$ -counter for 10 minutes.
4. Background value was subtracted from the count before being converted to the amount of  $^{14}\text{C}$ -PAH.

In order to determine  $^{14}\text{C}$ -PAH in proximal tubules during kinetic study, the proximal tubular cells were overlaid on a glass microfiber filter. The filter was placed in a glass scintillation vial and the tubules on the filter were solubilized with 1 N NaOH for at least 3 hours or until no tissue was observed on the filter. This solution was neutralized with 1 N HCl (using an equal volume to 1 N NaOH). 5 ml of scintillation fluid was added to the vial, mixed well by using vortex mixer and then the radioactivity was counted for 10 minutes.

## APPENDIX IX

### MAKING PIPETTES FOR PERFUSION STUDY

#### 1. Left hand set

##### 1.1 Holding pipette

This pipette was made of a glass tube (O.D. 3 mm). After using the general vertical puller to make one end of the tube small and sharp, this end of the tube was then made to have 2 constrictions, as shown in figure 28, using a microforge. The tip of the pipette was 35-40  $\mu\text{m}$  in diameter, which fitted properly with the rabbit renal proximal tubule.

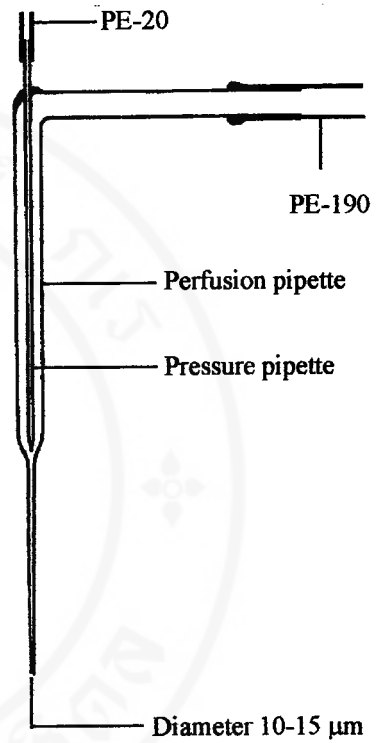
##### 1.2 Perfusion pipette

This pipette was made of a glass tube with a 1.2-1.5 mm O.D. The tube was bent to 90° with a Bunsen Burner after pulling its end with the vertical puller. The pulled pressure pipette, which was made of a glass tube (O.D. 0.018" and I.D. 0.012"), was inserted into the perfusion pipette at the created opening on the bending site, as shown in figure 28, and these two glass tubes were sealed in the appropriate position with epoxy glue. The PE-20 (5-6 cm long) was connected to the end of the pressure pipette and a PE-190 (6-7 cm long) was attached to the end of the perfusion pipette. The tip of the perfusion pipette was sharpened with a microforge to obtain a final diameter of 10-15  $\mu\text{m}$ , which could be inserted into the lumen of the renal proximal tubule.

**(a) Holding pipette**



**(b) Perfusion pipette**



**(c) Collecting pipette**

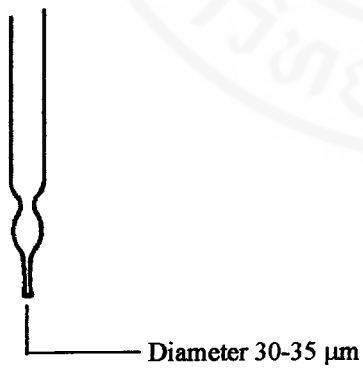


**Figure 28.** The illustrations of a holding pipette (a); a perfusion pipette (b); and a collecting pipette (c).

## 2. Right hand set

### 2.1 Collecting pipette

This pipette was made of a glass tube with an outer diameter of 1.2-1.5 mm. The shape of the reservoir was made by heating the glass tube with a microforge to obtain a reservoir neck with a diameter of 300-350  $\mu\text{m}$  (this size was large enough to allow the sampling pipette to freely pass through). The end of the tip was 30-35  $\mu\text{m}$  in diameter, as shown in figure 28.

### 3. Sampling pipette (use for collecting samples from collection side)

This was made of a thin glass tube with a thick wall. Its outer diameter was around 200  $\mu\text{m}$  and the length was 18-20 cm. The end of the tube was made to a round tip with a thin wall using a microforge. A 2 cm long PE-10 tube was attached to the end of the sampling pipette and then inserted to a 35-40 cm long the PE-50 tube. The other end of PE-50 was connected to a needle (No. 23 gauge, 1" long).

### Calibration of sampling pipette

- Scintillation vials were prepared; each was added with 0.1 ml  $\text{H}_2\text{O}$  (at least 3 vials for 1 sampling pipette).
- $^3\text{H}_2\text{O}$  solution of known activity (dpm/nl) was prepared.
- A syringe was connected to the needle at the end of the sampling pipette, the syringe was drawn to partially fill the sampling pipette with  $^3\text{H}_2\text{O}$  solution, then the syringe was disconnected from the needle.
- The length of the solution in the pipette was measured using a special steel ruler.

- The solution was blown out into the vial containing 0.1 ml H<sub>2</sub>O, and pulled in and out 2 or 3 times to wash out <sup>3</sup>H<sub>2</sub>O into the vial.
- The sampling pipette was rinsed several times with distilled water and dried with acetone.
- At least triple determination was done for each pipette.
- Scintillation fluid was added to each vial containing H<sub>2</sub>O and <sup>3</sup>H<sub>2</sub>O solution (sample); It was then shaken well.
- <sup>3</sup>H in each vial was counted for 20 min using a β-counter.
- The conversion factor for each pipette was calculated using the following equation:

$$\frac{\text{DPM of sample}}{\text{mm length of solution in sampling pipette}} \times \frac{1}{\text{DPM/nl of H}_3\text{O solution}} = \frac{\text{nl of solution}}{\text{mm length in sampling pipette}}$$

- The values of triple determination for each pipette were averaged and used as a conversion factor for each time of sample collection.

### System set up

#### 1. Right hand set

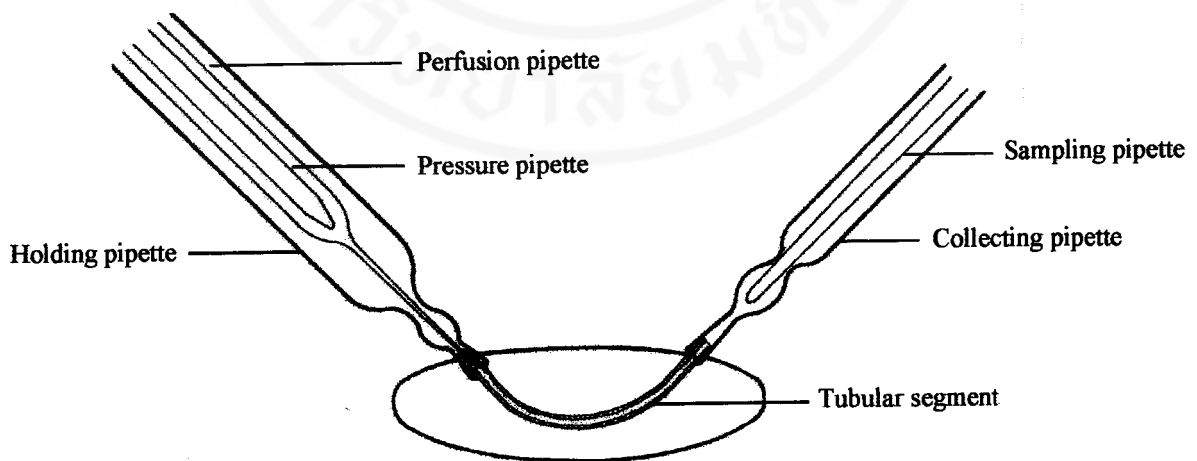
- Tape was attached around the collecting pipette at the site that would be inserted for fixing on the manipulator.
- The end of collecting pipette (cylindrical end) was inserted into the fitting on the right hand manipulator, and gently screwed in for fixing.

## 2. Left hand set

- The perfusion pipette set was introduced into the left hand manipulator using a 1.2-1.5 mm open glass tube to guide the tip of the pipette through the system fittings.

- The perfusion pipette set was fixed on the manipulator with epoxy glue, with the fine tip of the pipette being allowed to protrude from the system fitting of the holding pipette.

- The left hand holding pipette was fitted over the perfusion pipette and centered under the microscope while rotating the holding pipette, its tip being filled with distilled water.



Copyright by Mahidol University

**Figure 29.** An illustration of the system for perfusing the tubular segment using the *in vitro* microperfusion technique.

## APPENDIX X

### PERFUSION & COLLECTION OF SAMPLES

The isolated proximal tubules were transferred to a bathing chamber containing a bicarbonate-buffered medium with 3 g/100 ml dextran. Before hooking the tubule on the holding pipette, the perfusion set was filled with a bicarbonate-buffered medium filtered through a 0.22  $\mu\text{m}$  Millipore filter (type GS). One end of the isolated tubule was hooked on the holding pipette by gentle suction using a syringe connected to the line from the fitting part of the holding pipette. The tip of the perfusion pipette was introduced into the tubular lumen so that the perfusate could flow from this end to the other end of the tubule. The collecting pipette was fixed to the other end of the tubule using a PE-tube-attached syringe connecting to the collecting pipette, and the other end of the tubule was gently sucked into the tip of the collecting pipette. During suction, a glass needle was used to guide the end of the tubule near the opening of the tip of the pipette. The fluid (perfusate) flowed from the perfusion set through the tubular lumen and accumulated in the reservoir of the collecting pipette. This luminal fluid was collected by gently introducing the sampling pipette into the reservoir of the collecting pipette and slight suction applied with the syringe connected to the sampling pipette in order to empty the reservoir. The length of collected fluid in the sampling pipette was measured and recorded.

**BIOGRAPHY**

<b>NAME</b>	<b>Miss Promsuk Jutabha</b>
<b>DATE OF BIRTH</b>	<b>September 12, 1968</b>
<b>PLACE OF BIRTH</b>	<b>Chonburi, Thailand</b>
<b>INSTITUTIONS ATTENDED</b>	<b>Mahidol University, 1986-1990:</b> <b>Bachelor of Science (Nursing and Midwifery), First class honor</b> <b>Chulalongkorn University, 1991-1994:</b> <b>Master of Science (Physiology)</b> <b>Mahidol University, 1995-2000:</b> <b>Doctor of Philosophy (Physiology)</b>
<b>RESEARCH GRANT</b>	<b>Institutional strengthening program of Faculty of Science, Mahidol University and National Science and Technology Development Agency (NSTDA) Scholarship, Thailand.</b>

**PUBLICATIONS:**

1. Jutabha P, Chomdej B. Effect of *Cymbopogon citratus* stapf. on renal function in dogs. Chula Med J 1995; 39(6): 425-35.

2. Chatsudthipong V, Jutabha P, Evan KK, Dantzer WH. Effects of inhibitors and substitutes for chloride in lumen on p-aminohippurate transport by isolated perfused rabbit renal proximal tubules. *J Pharmacol Exp Ther* 1999; 281: 993-1001.
3. Chatsudthipong V, Jutabha P. Effect of stevioside on PAH transport by isolated perfused rabbit renal proximal tubule. *FASEB J* 1999; 13: A61.
4. Jutabha P, Chatsudthipong V. Toxic effect of steviol on PAH transport by isolated perfused rabbit renal proximal tubule. *FASEB J* 2000; 14: A353.
5. Jutabha P, Toskulkaeo C, Chatsudthipong V. Effect of stevioside on PAH transport by isolated perfused rabbit renal proximal tubule. *Can J Physiol Pharmacol* 2000; 78(9): 737-44.